Mon. Not. R. astr. Soc. (1984) **209**, 765–824

Photographic photometry of RR Lyrae variables in the globular cluster M15

Elizabeth A. Bingham *Royal Greenwich Observatory, Herstmonceux Castle, Hailsham, East Sussex BN27 1RP, UK*

Carla Cacciari★ *Osservatorio Astronomico Universitario, 40100 Bologna, Italy* and *ESTEC, Astronomy Division Villafranca Satellite Tracking Station, Madrid, Spain*

R. J. Dickens† *Royal Greenwich Observatory, Herstmonceux Castle, Hailsham, East Sussex BN27 1RP, UK*

F. Fusi Pecci *Osservatorio Astronomico Universitario, 40100 Bologna, Italy*

Accepted 1984 January 22. Received 1983 December 19; in original form 1983 July 29

Summary. Light curves in B and V are presented for 56 RR Lyrae variables in the Oosterhoff Group II globular cluster M15. Our measures are combined with original measures published by Sandage, Katem & Sandage (SKS) to yield data of improved precision for a total of 62 RR Lyraes. Correlations between the various light curve parameters are obtained, and their significance is discussed. In particular, the new period–colour relation shows less scatter than that published by SKS, and less overlap in colour between *c*- and *ab*-types. The multimode variables now occur close to the (ab/c) transition colour, as expected from their periods. An accurate assessment of the sources of error in the period-colour relation enables the prediction of a range in mass amongst the variables, with a (1σ) dispersion of $\sim 0.025\,M_\odot$. The theoretical period–colour relation is used to derive a mass-to-light ratio (solar units), $\log\,(M^{0.81}/L) = -1.92 \pm 0.03$ which, with a mean mass of $0.65 \pm 0.05\,M_\odot$ obtained by Cox, Hodson & Clancy for the multimode variables gives $\log\,L = 1.77 \pm 0.06\,L_\odot$ or $M_{\rm bol} = +0.34 \pm 0.15$. This luminosity implies an age a few billion years less than current estimates, but there are still many uncertainties attached to such a derivation.

From a number of independent estimates of the helium abundance (see Section 3.2) a value of $Y = 0.25 \pm 0.03$ seems to be the most appropriate for M15. The observed distribution of stars in the $\log L/\log T_e$ diagram of M15 agrees satisfactorily with what could be expected from the appropriate evolutionary tracks of Sweigart & Gross (SG). However, the mass-to-light ratios of

★ Present address: Space Telescope Science Institute, Homewood Campus, Baltimore MD 21218, USA.

† Present address: Space and Astrophysics Division, Rutherford Appleton Laboratory, Chilton, Didcot, Oxfordshire OX11 0QX, UK.

these 'standard' models can only be reconciled with those derived pulsationally, within the quoted uncertainties, if the helium abundance, $Y, \gtrsim 0.30$. If $Y \lesssim 0.25$ as also might be expected from external evidence, the evolutionary models predict a lower luminosity ($\Delta \log L \sim 0.1$) than obtained from pulsation theory. This discrepancy can be removed on the basis of the expected behaviour of non-standard models, as shown by Caputo, Castellani & Gregorio.

The observations are compared in detail with those of RR Lyraes in the Oosterhoff I cluster M3 in a discussion of the Oosterhoff problem. It is shown that the Oosterhoff effect, as manifest between M15 and M3 cannot be simply described in terms of a period shift, since the distribution of amplitude and number with period and temperature differ in detail, in particular a unique amplitude–temperature relation over both pulsation modes is not possible. We confirm Sandage's result, though with somewhat different arguments, that the correlation of period shift with heavy element abundance [Fe/H] over many clusters requires an anticorrelation of [Fe/H] with Y within the standard frame of evolution models.

Finally, the morphology of the SG tracks appropriate to account for the difference in overall horizontal branch morphology between M15 and M3 leads to a natural explanation of the great excess of *c*-type variables in the neighbourhood of the transition temperature found in Oosterhoff II clusters like M15 (an effect which contributes significantly to the difference in mean period between the Oosterhoff groups). The tracks indicate that many of the RR Lyraes in M15 begin their horizontal branch evolution within the instability strip, spending much longer in the centre of the strip than variables in M3-like clusters which evolve more rapidly bluewards across the strip. The distribution in M15 peaks just bluewards of the transition temperature giving rise to the many *c*-type variables found there. The multimode variables occur precisely at the transition temperature (the same in M15 and M3) and appear to be a 'stable' mode of pulsation. However, further work is still needed to determine precisely the luminosity and/or mass differences that produce the observed period shift between the Oosterhoff groups.

1 Introduction

Observations in more than one waveband of RR Lyrae variables in globular clusters provide important data for the study of the evolution of horizontal branch stars. The light curve parameters provide information about the distribution of the variables with temperature, and show correlations between period, amplitude, luminosity and temperature. These relationships and the use of pulsation theory allow the determination of fundamental parameters such as the mass of the evolving stars and their helium content. Observations show variations in RR Lyrae properties from cluster to cluster but explanations of the differences are still uncertain. The determination of physical differences between clusters is important for understanding the morphology of the horizontal branch, and relating such differences to stellar evolution and to estimating ages among galactic globular clusters. One major systematic difference discovered by Oosterhoff (1939, 1944) is the division of clusters into two distinct groups according to the mean periods of the RR Lyrae variables, $\langle P_{ab} \rangle = 0.55$ days for group I and $\langle P_{ab} \rangle = 0.65$ days for group II. In fact a complete understanding of horizontal branch morphology in globular clusters requires a solution to the Oosterhoff dichotomy and cannot be achieved without a detailed analysis and comparison of the data for RR Lyraes in clusters representative of the two Oosterhoff groups.

After the early studies of a large sample of RR Lyraes in the most variable-rich Oosterhoff I cluster M3 by Roberts & Sandage (1955), Baker & Baker (1956) and Sandage (1959), several other group I clusters have been observed in at least two wavebands in order to obtain colour data on their RR Lyraes (NGC 6712 by Sandage, Smith & Norton 1965; NGC 6171 by Dickens 1970; NGC 6981 by Dickens & Flinn 1972; M14 by Wehlau & Potts 1973; NGC 6723 by Menzies 1974; M4 by Sturch 1977; Cacciari 1979; NGC 3201 by Cacciari 1983). M13 (Pike & Meston 1977) has too few RR Lyraes to assign to a group. In order to select an Oosterhoff II cluster for comparison we note that by far the most variable-rich clusters of this type are ω Cen and M15. However, ω Cen is peculiar in many respects, showing a considerable spread in [Fe/H] among its RR Lyrae stars and with both Oosterhoff groups apparently present, evidenced by some 'metal-rich' RR Lyraes with periods close to those of Oosterhoff I clusters (Butler, Dickens & Epps 1978, hereafter BDE), so it cannot be taken as representative of the Oosterhoff group II clusters. Observations of the group II cluster NGC 4833 by Demers & Wehlau (1977) are available for 11 variables and for NGC 4590 = M68 by Andrews (1980) for 24 variables. Therefore a detailed study of the variables in M15, unambiguously classified as Oosterhoff group II, is very important.

Photometric observations of the globular cluster M15 = NGC 7078 (RA = $21^h 27^m.6$, Dec = $+11° 57'$ 1950, $l = 65.0$, $b = -27.3$, Shapley & Sawyer (1935) concentration class IV, spectral type F3, Kukarkin (1974) richness index = 0.74) on the International System have been published by Brown (1951), Johnson & Schwarzschild (1951) and Arp (1955). Photoelectric and photographic observations in the *UBV* system have been made by Sandage, Katem & Kristian (1968), Sandage (1969, 1970), Sandage & Katem (1977), Aurière & Cordoni (1981) and Buonanno *et al.* (1983a). The colour–magnitude diagram shows many properties of the 'typical' metal-poor clusters: $\Delta V = 3.2$ at $(B-V)_0 = 1.4$ (Sandage & Wallerstein 1960), $(B-V)_{0,g} = 0.68$ (Sandage & Smith 1966) and $S = 6.9$ (Hartwick 1968). Previous determinations of metal abundance by Sandage (1970), Butler (1975), Hesser, Hartwick & McClure (1977), Harris & Canterna (1977), Cohen (1978), Searle & Zinn (1978) and Zinn (1980), suggest a mean value of [Fe/H] ~ -2.15. However, Pilachowski, Sneden & Wallerstein (1983) find [Fe/H] $= -1.76$ and Bica & Pastoriza (1983) a value of -1.71. Clearly the metal abundance of M15 is still controversial; we adopt [Fe/H] $= -2.0 \pm 0.15$ in this paper. The Dickens (1972) type 3 horizontal branch is populated on both sides of the RR Lyrae gap although with a rather sparse red horizontal branch (Buonanno *et al.* 1983a); the horizontal branch includes 112 variables, among which 65 are RR Lyraes with known period (Sawyer Hogg 1973).

UBV photographic photometry of these variables was begun at Mount Wilson and Palomar Observatories (Sandage 1959, 1970). We undertook a detailed study of RR Lyrae variables in M15 using *B* and *V* plates taken with the Loiano and Asiago telescopes between 1974 and 1979. The results of the Mount Wilson study were announced by Sandage, Katem and Sandage (1981, hereafter SKS), in the first of a series of papers on the Oosterhoff period groups and the ages of globular clusters (Sandage 1981b, 1982a, 1982b). A comparison of our independent data with theirs revealed differences in mean photometric parameters which significantly affect the final correlations and consequent interpretation. We found differences in $B-V$ colours, in the amount of scatter among both *ab*- and *c*-type variables and the amount of colour overlap between them. In order to consider all the available data for the most meaningful discussion we decided to re-reduce the Mount Wilson observations in the same way as the Bologna observations and combine both data sets. We believe this to be worthwhile in order to enable the most comprehensive analysis of the colour data for the

M15 RR Lyraes, being the best example of a globular cluster of Oosterhoff group II, including detailed comparison with similar data for M3 (group I).

We give full details of our reduction of all the data in the second section of the paper. Our new independent data are presented in Sections 2.1 to 2.4 together with our new reduction of SKS data in Sections 2.2. to 2.4. We have analysed photometric errors in the final combined data (Section 2.5) and present the period–colour relation at various stages in the reductions (Section 2.6) to show that the final combined data is of improved precision. In the third part of the paper we discuss the correlations between observed light curve parameters such as amplitude and mean colour index (Section 3.1), and make a detailed discussion of the derivation of physical parameters of the RR Lyrae variables, their effective temperatures, bolometric magnitudes, mass-luminosity ratio and helium abundance (Section 3.2). Using pulsational data and the mass for double-mode RR Lyrae variable stars given by Cox, Hodson & Clancy (1983) we find the absolute magnitude of the RR Lyraes and discuss the implication of this result for the cluster age (Section 3.3). In Section 3.4 we discuss the Oosterhoff dichotomy as manifest by the observed properties and pulsation parameters of M15 and M3 RR Lyraes. A comparison with stellar evolution models is made in Section 3.5. We discuss how the pulsation results can be explained by current evolutionary horizontal branch models in fitting M15 data alone (Section 3.5.1) and by a comparison of M15 and M3 (Section 3.5.2). In Section 3.5.3 we use the predictions of stellar evolution models to discuss the observed horizontal branch morphology and in Section 3.5.4 discuss the Oosterhoff effect between M15 and M3 in terms of current evolutionary models and pulsation theory.

Table 1. List of Bologna plates of M15 from Loiano or Asiago (A).

Plate no.	Hel. J.D. 2440000+	Col.	Exp. min	Plate no.	Hel. J.D. 2440000+	Col.	Exp. min	Plate no.	Hel. J.D. 2440000+	Col.	Exp. min
A147	1981.275	V	15	433	3395.461	V	15	918	3787.443	V	20
A571	2274.485	V	10	440	3399.324	B	8	920	3788.265	B	5
A572	2274.506	B	5	443	3399.388	B	15	926	3789.285	B	5
A584	2276.486	B	10	444	3399.432	V	15	946	3793.295	V	5
A585	2276.494	V	10	445	3399.466	B	12	1120	4117.345	B	7
A586	2276.502	B	10	446	3399.482	V	16	1129	4118.377	V	10
A587	2276.510	V	10	447	3399.531	B	12	1130	4118.409	B	4
A593	2277.563	B	10	452	3401.340	B	16	1131	4118.418	V	8
A594	2277.572	V	10	453	3401.368	V	30	1132	4118.444	B	4
A602	2281.447	B	15	454	3401.408	B	40	1133	4118.449	V	8
A603	2281.461	V	15	A1619	3401.513	V	15	1137	4144.331	B	7
A616	2296.411	V	5	A1712	3459.304	V	15	1138	4144.342	V	12
A619	2298.379	V	5	A1714	3459.321	V	15	1139	4144.377	B	7
A620	2298.383	B	5	852	3722.495	V	25	1140	4144.388	V	14
A621	2298.388	V	5	854	3722.556	V	25	1142	4144.424	V	14
A658	2305.476	B	5	858	3723.484	V	20	1147	4145.318	B	8
A669	2306.468	V	5	865	3756.401	V	27	1148	4145.327	V	15
A670	2306.477	B	10	866	3756.438	B	35	1152	4156.270	V	8
A678	2307.444	V	10	871	3759.352	V	20	1153	4156.277	B	5
A688	2309.379	B	5	876	3761.319	B	20	1154	4156.303	V	8
A690	2309.432	V	10	877	3761.336	V	20	1155	4156.310	B	20
A712	2338.337	V	5	881	3774.314	V	17	1156	4156.344	V	11
A1077	2715.332	B	10	882	3775.280	V	20	1157	4156.353	B	8
A1078	2715.342	B	10	883	3775.310	B	20	1158	4156.368	V	8
A1084	2716.267	B	15	884	3775.336	V	18	1159	4156.375	B	6
A1106	2752.269	B	10	885	3775.358	B	20	1160	4156.405	V	9
A1107	2752.278	V	15	886	3775.381	V	20	1161	4156.414	B	8
A1109	2752.296	V	15	887	3775.413	B	20	1162	4156.432	V	10
407	3392.328	B	15	888	3775.438	V	24	1163	4156.441	B	8
408	3392.358	V	16	889	3775.454	B	20	1166	4168.378	B	6
416	3393.367	V	15	890	3775.472	V	22	1168	4168.410	B	8
418	3393.439	B	15	892	3776.286	V	20	1169	4168.421	V	14
426	3394.376	B	15	916	3787.280	V	20				

2 Observations and reductions

2.1 BOLOGNA PHOTOGRAPHIC PHOTOMETRY

Our photographic observations were obtained with the 152 cm F/8 Ritchey-Chretien telescope of Loiano (plate scale 17″/mm) from 1977 September to 1979 October, and with the 182 cm F/9 telescope of Asiago (12″/mm) from 1973 October to 1977 November. 44 *B* and 54 *V* plates were measured with the Sartorius iris-diaphragm photometer at the Royal Green-

Table 2. Photographic differences resulting from measuring photoelectric standard stars in M15 (Sandage 1970, tables 5 and 6) on Bologna plates. Δ gives Sandage photoelectric value minus mean Bologna photographic value. L: Loiano plates (36 V, 31 B), A: Asiago plates (18 V, 13 B). Stars are identified in Sandage (1970) plates 9 and 10.

No.	$V_{p.e.}$	$(B-V)_{p.e.}$	ΔV_L	s.d.	ΔV_A	s.d.	ΔB_L	s.d.	ΔB_A	s.d.
S5	12.87	0.78	-.01	.02	-.02	.03	0	.02	-.01	.03
S6	13.40	1.19	0	.04	0	.04	+.02	.04	-.06	.07
X7	13.50	0.76	+.03	.03	+.05	.04	-.03	.04	+.02	.04
X5	13.72	1.02	+.01	.03	+.04	.03	+.04	.05	+.04	.04
P5	14.02	0.73	-.01	.02	-.04	.03	+.02	.04	+.02	.05
X6	14.11	1.01	-.08	.03	-.06	.03	-.07	.04	0	.05
P13	14.32	0.97	+.01	.03	-.01	.03	-.01	.03	+.01	.04
S36	14.39	0.91	-.03	.04	-.05	.05	-.04	.06	-.04	.06
P8'	14.47	1.00	+.02	.03	+.01	.01	0	.04	+.01	.04
S11	14.68	0.88	+.02	.04	+.01	.03	-.01	.07	+.01	.03
P14	14.82	0.82	+.03	.04	+.03	.03	+.04	.06	+.04	.03
B	14.84	1.15	+.04	.04	+.05	.02	+.06	.10	0	.06
P6	14.93	0.90	-.04	.03	-.03	.03	-.01	.04	0	.04
A	15.05	0.76	+.04	.03	+.04	.02	+.05	.05	+.04	.07
S37	15.33	0.82	+.04	.05	+.07	.03	+.08	.08	+.11	.04
P11	15.41	0.83	-.02	.04	-.01	.03	-.02	.05	+.01	.05
P15	15.42	1.34	+.03	.04	+.05	.03	+.03	.10	-.01	.06
P7	15.62	0.82	-.03	.03	0	.02	+.03	.04	+.04	.06
P1	15.71	0.79	-.06	.04	-.01	.03	+.02	.05	+.01	.06
D	15.73	0.74	+.01	.06	-.03	.04	-.01	.09	-.06	.06
IV-108K	15.87	0.22	-.04	.05	-.06	.04	-.06	.05	-.05	.05
I-135K	15.91	0.18	-.11	.04	-.13	.03	-.09	.05	-.09	.04
IV-19K	15.93	0.17	-.02	.04	-.05	.04	-.05	.06	-.07	.06
IV-68K	15.95	0.23	+.03	.05	-.01	.03	+.01	.06	0	.05
P4	15.98	0.17	-.03	.03	-.02	.04	-.04	.05	-.02	.03
I-50K	16.05	0.12	+.09	.04	+.07	.03	+.07	.05	+.07	.07
IV-25K	16.06	0.10	+.03	.03	0	.03	-.03	.06	+.03	.06
IV-17K	16.06	0.11	+.03	.03	+.02	.03	-.01	.06	0	.05
I-20K	16.08	0.17	+.03	.04	+.04	.03	-.02	.08	-.05	.04
P3	16.09	0.79	-.22	.04	-.16	.04	-.14	.07	-.14	.08
IV-4K	16.11	0.12	+.06	.05	+.06	.02	+.02	.06	+.03	.06
P10	16.26	0.84	+.02	.05	+.04	.04	+.06	.07	+.05	.05
F	16.27	0.85	+.02	.08	-.07	.06	-.03	.10	-.11	.10
III-156K	16.28	0.09	-.08	.06	-.11	.06	-.07	.10	-.03	.09
P8	16.38	0.74	0	.03	+.02	.03	-.01	.08	-.01	.04
P2	16.47	0.96	+.01	.05	+.05	.04	+.05	.07	+.06	.06
AB	16.50	0.76	0	.05	+.05	.04	+.03	.08	+.06	.04
Y	16.54	0.78	0	.04	+.01	.03	+.04	.08	+.01	.06
AI	16.56	0.76	-.01	.04	+.02	.02	+.01	.07	-.02	.07
I-95K	16.59	0.00	-.04	.06	-.05	.04	-.05	.06	-.03	.03
AH	16.61	0.90	+.06	.05	+.07	.08	+.06	.09	+.01	.03
I-198K	16.64	-0.01	+.13	.07	+.08	.06	+.12	.08	+.14	.06
III-W2-3	16.67	0.01	+.02	.05	-.05	.03	0	.06	0	.05
K	16.69	1.12	+.02	.07	-.01	.07	+.05	.07	-.01	.05
AC	16.69	0.75	-.04	.04	+.02	.06	-.01	.11	+.05	.06
X	16.72	1.12	+.06	.04	+.09	.04	+.06	.08	+.04	.05
P12	16.76	0.80	-.01	.06	0	.03	+.04	.07	+.05	.06
I-73K	16.76	-0.04	-.05	.07	-.07	.04	-.06	.06	-.05	.03
P9	16.84	-0.01	+.02	.06	-.03	.05	+.01	.06	-.03	.07
W	16.92	0.71	-.02	.06	+.01	.05	-.01	.08	-.01	.03
I	16.95	1.03	+.02	.07	-.02	.10	+.01	.08	-.02	.05
I-W5-4	17.21	-0.04	-.05	.06	-.09	.05	-.08	.09	-.09	.11
I-112K	17.24	-0.05	+.08	.09	+.10	.05	+.04	.08	+.06	.06
AD	17.46	-0.08	+.03	.06	+.09	.05	-.05	.11	+.03	.06

wich Observatory. The best quality plates were selected out of a larger number available, the plate-filter combinations being: 103a-O (or IIa-O) + GG13 for *B* and 103a-D (or IIa-D) + GG14 for *V*. The list of all plates used is given in Table 1.

On each plate 56 variables (33 *c*-type and 23 *ab*-type), 55 photoelectric standard stars and 68 photographic secondary standards were measured (Sandage 1970, tables 5, 6 and 8). Calibration curves were obtained by fitting a fifth order polynomial to the photoelectric standards and then photographic magnitudes were derived for both variables and standard stars. For photoelectric standards, residuals with respect to Sandage's photoelectric values and relative rms deviations are given in Table 2. For photographic standards, mean magnitudes with relative rms deviations and residuals with respect to Sandage's values are given in Table 3. The agreement is generally good, and the larger rms deviations found for the stars S4 and IV-66 suggest possible variability. This has been confirmed for S4 (and also for II-64) by the results of a search for variability in red giants in globular clusters made by Mosley & White (1975). Comparisons of the residuals versus $(B-V)$ for the photoelectric standard stars in the magnitude ranges of the RR Lyrae variations are shown in Figs 1(a) and 1(b) for Loiano and Asiago plates respectively. These show no significant correlations with colour that would justify correction between the photoelectric and photographic magnitude systems. Fig. 1(c) shows the same comparison for the Mount Wilson plates. The colour equations derived by Dickens (1970) for the Mount Wilson 2.5-m system in 1965–67 are indicated; there is only one blue point, which does not justify application of these colour equations, although they are not inconsistent with the M15 data. However, a comparison of

Table 3. Comparison between photographic photometry for M15 stars measured in the RR Lyrae programme from Bologna plates and Mount Wilson plates (Sandage 1970, table 8). Bologna values are means from 54 *V* plates and 44 *B* plates. Stars are identified in Sandage (1970, plate 9).

No.	V	s.d.	ΔV	B	s.d.	ΔB	No.	V	s.d.	ΔV	B	s.d.	ΔB
	Bologna		MtW-B	Bologna		MtW-B		Bologna		MtW-B	Bologna		MtW-B
S1	12.97	.10	+.05	14.19	.08	+.03							
S2	15.82	.05	+.04	16.02	.05	+.02	I-42	16.42	.07	+.10	16.47	.07	+.01
S3	13.42	.05	+.03	14.52	.06	+.02	43	13.82	.07	+.01	14.83	.11	+.03
S4	12.58	.18	+.11	14.03	.13	+.03	51	15.88	.12	-.08	16.08	.09	-.01
S7	13.60	.06	-.06	14.69	.09	-.07	54	15.85	.05	+.01	16.06	.07	+.02
S8	13.50	.08	-.09	14.57	.12	-.07	58	15.87	.06	+.01	16.07	.07	+.01
S9	15.72	.04	-.05	16.47	.05	0	61	15.80	.06	-.04	16.50	.08	+.08
S10	15.93	.04	-.01	16.10	.05	-.01	72	15.18	.05	+.01	15.90	.06	+.04
S12	15.93	.05	-.04	16.65	.05	+.03							
S13	16.50	.05	+.01	17.23	.07	+.02	II-11	15.78	.07	+.03	15.94	.08	+.07
S16	15.93	.05	+.03	16.06	.07	+.04	23	15.73	.08	+.05	15.90	.10	+.10
S17	16.36	.09	0	17.11	.11	+.02	24	15.60	.09	+.02	16.08	.13	+.11
S18	16.82	.07	+.02	16.75	.07	0	36	15.93	.05	+.02	16.03	.06	+.05
S19	14.79	.05	-.03	15.69	.05	+.03	53	16.43	.06	+.03	17.13	.10	+.05
S20	15.43	.05	-.02	16.34	.06	+.02	54	15.82	.05	+.01	16.02	.07	+.04
S21	16.05	.05	+.06	16.22	.06	+.01	59	15.87	.04	0	16.10	.04	-.02
S22	15.47	.04	-.05	16.28	.07	0	64	13.48	.04	0	14.61	.07	-.01
S23	14.07	.09	-.06	15.12	.12	-.07	73	15.88	.05	+.01	16.03	.08	+.05
S24	15.42	.05	-.02	16.22	.06	+.04	74	15.93	.05	+.02	16.06	.06	+.04
S27	15.45	.05	-.03	16.24	.06	+.01	76	15.61	.04	-.06	16.37	.05	0
S28	16.43	.07	-.01	17.19	.12	+.02							
S29	16.46	.08	-.01	17.19	.12	+.03	III-15	15.83	.06	+.04	15.97	.10	+.07
S30	14.90	.06	-.06	15.77	.06	-.01	28	15.71	.05	-.03	16.25	.09	+.01
S31	16.11	.09	0	16.21	.08	-.03	43	15.82	.05	+.01	16.02	.07	+.02
S32	16.55	.08	+.04	17.27	.12	+.05	52	15.81	.05	+.01	16.04	.08	0
S33	16.84	.09	0	17.58	.14	+.01	67	15.93	.04	0	16.10	.08	0
S34	17.07	.15	-.08	17.79	.15	-.04	71	15.50	.08	+.01	16.12	.09	+.04
S35	16.78	.08	+.02	17.52	.12	+.06							
S38	16.97	.10	-.05	17.67	.14	+.02	IV- 2	15.79	.08	+.05	15.97	.12	+.08
							31	14.85	.06	-.01	15.72	.08	+.05
I- 1	15.90	.10	+.07	15.97	.11	+.11	44	15.79	.05	0	16.03	.08	+.01
4	15.84	.06	+.03	16.01	.09	+.07	45	15.66	.05	-.02	16.23	.08	+.04
7	15.63	.09	+.02	16.12	.10	+.08	46	15.53	.06	-.01	16.29	.09	+.07
9	15.88	.07	+.05	15.99	.09	+.10	63	16.02	.04	+.04	16.14	.07	0
11	15.84	.08	+.05	15.96	.10	+.10	66	15.84	.14	+.11	16.00	.13	+.10
14	15.98	.06	+.04	16.06	.09	+.08	68	15.71	.09	+.06	15.88	.14	+.13

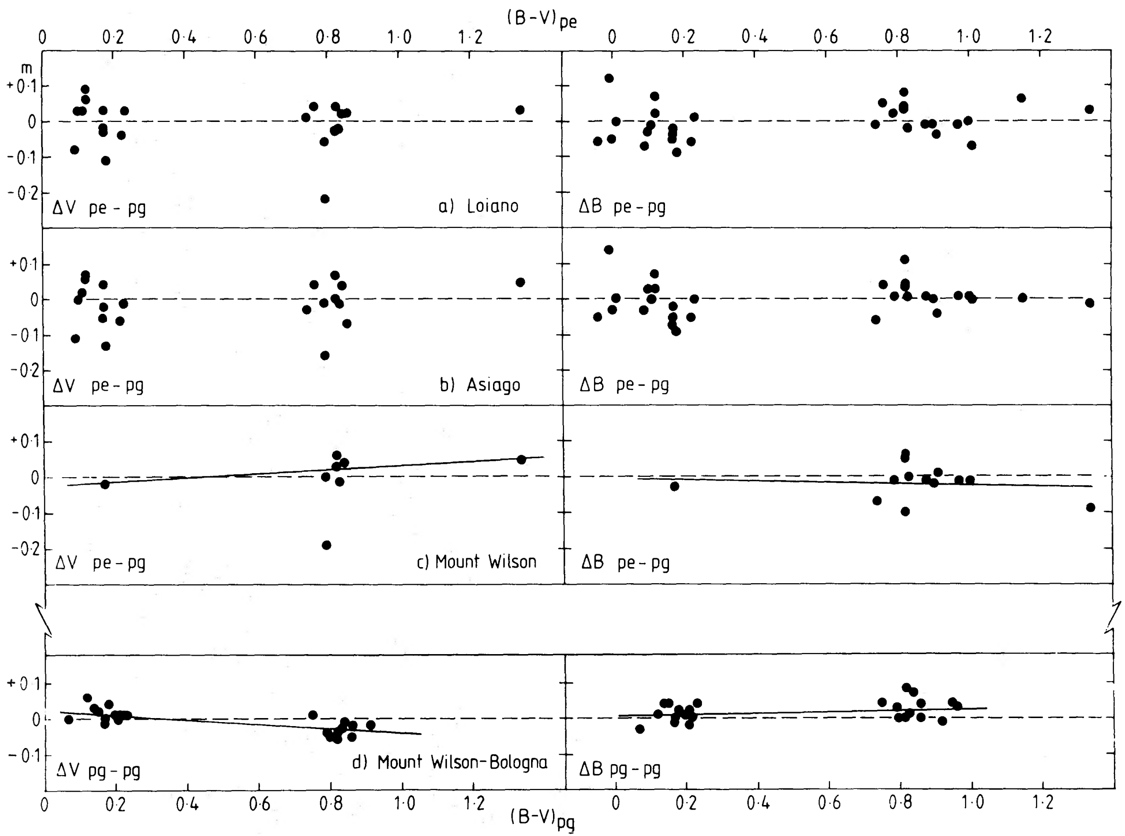

Figure 1. Colour equations between photographic and photoelectric measures of the standard stars (in the ranges $15.0 < V < 16.3$, $15.1 < B 16.8$) where ΔV and ΔB, the differences (photoelectric–photographic) for the Bologna–Loiano plates (a), the Bologna–Asiago plates (b) and the Mount Wilson plates (c) are plotted against colour. Panel (d) shows the differences between Mount Wilson and Bologna photographic values of non-variable stars with $r > 120$ arcsec and $15.0 < V < 16.3$ plotted against colour. Solid lines indicate the effects of colour equations for the Mount Wilson System by Dickens (1970). No corrections have been applied to the photographic measures (see text).

the magnitudes obtained for the photographic secondary standards in the magnitude range of the RR Lyraes ($15.0 < V < 16.3$) and essentially unaffected by background ($r > 120$ arcsec) does show colour effects, as illustrated in Fig. 1(d) (left and right panels). Since there is adequate spatial coverage by the stars in these diagrams (see later discussion) this implies that at least one set of observations are influenced by a colour equation. The colour equation for the later Mount Wilson system (using different filters of the same specification) would give rise to the effect shown by solid lines in Fig. 1(d) and agree quite well with the data. Although these effects are understandable, the differential effects are small over the colour range of the RR Lyraes and since they cannot be considered well established in each individual data set, no colour equations have been finally applied to the measures. We shall further discuss relative colour and magnitude effects between the two series in Section 2.5.

The results of the Bologna measurements of V and B magnitudes for 56 variables (identified by the numbers given in Sawyer Hogg's Catalogue 1973; hereafter SH) are listed in Table 4a, b. The standard deviation of a single measurement, estimated from the magnitude residuals of the photoelectric standard stars, is of the order of ± 0.05 in V and ± 0.08 in B. In some cases, however, the measures of the variables are affected by problems of crowding and/or background which causes larger then normal scatter in the light curves and makes precise period determinations more difficult. A few variables, for which this problem was particularly serious, have been excluded from the present analysis.

Table 4. M15 RR Lyraes.

V MAGNITUDE X 100

HEL.J.D. 2440000+	2	3	4	5	6	7	8	9	10	11	12	13	14	15	16	17	18	19	20	22	23	24	25	26	28	29	30	31
1981.275	1562	1567	1557	1548	1504	1532	1606	1561	1579	1586	1577	1606	1558			1595	1592	1597	1546	1602	1598	1590	1543	1570	1608	1610	1565	1578
2274.485	1562	1582	1568	1569	1559	1548	1599	1557	1572	1607	1602	1610	1608	1553	1580	1562	1593	1617	1541	1594	1562	1594	1599	1579	1621	1622	1604	1574
2276.494	1549		1611	1597	1565	1566	1595	1531	1595	1610	1600	1600	1598	1614	1577	1587	1574	1557	1600	1591	1550	1571	1610	1584	1604	1534	1590	1581
2276.510	1552	1599	1611	1594	1565	1571	1593	1532	1597	1609	1589	1593	1583	1607	1566	1579	1581	1566	1600	1587	1556	1575	1603	1578	1615	1550	1593	1580
2277.572	1581	1575	1570	1571	1541	1553	1577	1585	1568	1610	1605	1576	1604	1587	1600	1583	1563	1526	1576	1560	1602	1565	1590	1604	1588	1561	1559	1602
2281.461	1562	1579	1592	1586	1581	1551	1589	1546	1572	1567	1572	1533	1594	1600	1568	1589	1602	1624	1532	1577		1598	1569	1573	1557	1621	1589	1586
2296.411	1562	1607	1564	1573	1548	1571	1593	1597	1569	1601	1593	1531	1565	1619	1580	1570	1588	1561	1572	1553	1604	1561	1598	1595	1598	1611	1598	1564
2298.379	1552	1602	1582	1581	1547	1546	1597	1589	1563	1575	1598	1593	1566	1591	1592	1584	1598	1599	1559	1604	1607	1586	1595	1591	1595	1563	1591	1609
2298.388	1553	1601	1586	1585	1543	1540	1598	1584	1563	1577	1601	1595	1567	1579	1591	1576	1594	1604	1559	1600	1599	1592	1594	1587	1592	1566	1595	1607
2306.468	1566	1601	1565	1592	1574	1560	1545	1565	1567	1595	1598	1607	1588		1570	1596	1599	1608	1602	1552	1598	1583	1606	1594	1600	1587	1584	1608
2307.444	1567	1570	1577	1565	1591	1584	1596	1561	1597	1612	1554	1572	1585	1613	1586	1573	1596	1572	1562	1588	1529	1557	1582	1592	1616	1566		1579
2309.432	1564	1574	1608	1569	1584	1539	1598	1542	1607	1602	1595	1607	1568	1618		1596	1583	1616	1545	1570	1557	1581	1584	1608	1624	1601	1600	1566
2338.337	1581	1611	1622	1584	1555	1596	1591	1587	1598	1612	1570	1562	1613	1593	1588	1555	1600	1571	1589	1580	1595	1600	1600	1612	1577	1607	1573	1608
2752.278	1571	1586	1611	1600	1573	1575	1565	1551	1602	1611	1586	1570	1592	1614		1566	1557	1615	1579	1541	1545	1566	1609	1610	1568	1611	1590	1593
2752.296	1569	1594	1603	1596	1570	1562	1543	1554	1595	1604	1589	1537	1596	1611		1568	1557	1614	1579	1550	1549	1567	1599	1613	1578	1611	1590	1589
3392.358	1575	1589	1548	1600	1589	1530	1587	1526	1578	1613	1534	1572	1566	1615	1547	1595	1601	1546	1580	1578	1602	1602	1580	1602	1610	1609	1546	
3393.367	1548	1601	1583	1578	1568	1563	1555	1587	1576	1619	1605	1519	1617	1614	1598	1539	1593	1617	1570	1583	1588	1578	1599	1574	1550	1623	1598	1598
3395.461	1555		1556	1600	1591	1585	1560	1573	1590	1619	1586	1616	1567	1532	1582	1604	1557	1605	1577	1564	1605	1554	1610	1597	1574	1574	1594	1606
3399.432	1529	1562	1618	1558	1583	1561	1581	1557	1611	1578	1542	1612	1609	1619	1595	1579	1578	1589	1522	1607	1552	1605	1606	1577	1553	1545	1591	1577
3399.482	1542	1571	1611	1565	1588	1579	1586	1517	1608	1593	1544	1609	1616	1571	1577	1579	1553	1595	1538	1608	1545	1578	1606		1564	1571	1587	1586
3401.368	1572	1559	1613	1554	1568	1577	1577	1588	1608	1569	1575	1564	1615	1569	1588	1592	1557	1623	1599	1584	1538	1551	1601	1566	1537	1611	1576	1585
3401.513	1548	1591	1579	1593	1587	1541	1598	1603	1564	1588	1599	1569	1572	1600	1563	1558	1601	1521	1527	1591	1574	1581	1601	1596	1576	1616	1601	1595
3459.304	1572	1563	1609	1576	1573	1554	1537	1588	1599	1606	1544	1602	1574	1592		1601	1605	1558	1535	1589	1593	1596	1600	1575	1594	1583	1551	1583
3459.321	1582	1567	1617	1570	1578	1554	1529	1592	1604	1611	1536	1611	1584	1598	1592	1605	1606	1527	1526	1574	1597	1602	1602	1577	1594	1588	1555	1583
3722.495	1548	1562	1583	1571		1536	1563	1589	1607	1617	1574	1606	1574	1616		1579	1579	1622	1583	1581	1600	1590	1560	1596	1607		1566	1606
3722.556	1559	1574	1563	1559	1576	1552	1576	1586	1576	1604	1530	1610	1590	1618		1586	1594	1601	1582	1588	1594	1593		1605	1578		1586	1592
3723.484		1608	1555	1594			1591	1528	1572	1603	1612	1569	1598	1572		1601		1617		1597	1562		1619	1592	1579			1567
3756.401	1587	1582	1564	1570		1593	1607	1539	1603	1593	1559	1607	1571	1623	1578	1596	1613	1512	1572	1589	1559	1582	1555	1613	1584	1606	1596	1594
3759.352	1549	1577	1596	1590	1550	1586	1576	1549	1565	1561	1553	1617	1613	1631	1576	1575	1609	1566	1589	1597	1601	1571	1601	1560	1606	1545	1561	1585
3761.336	1561	1564	1626	1565	1556	1545	1583	1591	1569	1609	1604	1529	1595	1528	1564	1572	1567	1624	1561	1571	1560	1607	1611	1578	1598	1617	1567	1578
3774.314	1581	1592	1572	1608	1580	1553		1533	1593	1615	1591	1618	1599	1588	1587	1566	1573	1594	1553	1584	1591	1607	1536	1581		1548	1570	1602
3775.280	1565	1584	1572	1571	1598	1575	1582	1579	1585	1586	1554	1582	1589	1584		1590	1579	1523	1574	1602	1559	1584	1599	1615	1598	1620	1571	1577
3775.336	1572	1563	1600	1591	1554	1548	1534	1591	1603	1611	1541	1595	1617	1529	1576	1605	1555	1555	1582	1608	1548	1604	1605	1605	1590	1620	1590	1577
3775.381	1577	1569	1618	1605	1520	1549	1545	1593	1614	1620	1562	1609	1620	1546	1598	1612	1569	1576	1591	1614	1564	1613	1611	1588	1591	1566	1603	1582
3775.438	1582	1583	1614	1596	1534	1563	1561	1594	1604	1598	1572	1611	1601	1570		1600	1577	1595	1591	1596	1575	1603	1604	1562	1598	1538	1600	1593
3775.47[illegible]	1598	1597	1615	[illegible]	1558	1580	1573	1597	1601	1567	1580	1624	1590	1589		1579	1593	1605	1594	1569		1587	1605	1564	1604	1552	1607	1601
4118.418	1594	1605	1604	1579	1544	1569	1605	1545	1596	1567	1615	1562	1618	1521		1595	1566	1622	1590	1552	1586	1596	1570	1606	1563	1618	1587	1602
4118.449	1594	1602	1613	1598	1551	1585	1553	1553	1606	1584	1616	1584	1617	1550	1595	1599	1558	1617	1595	1562	1593	1606	1579	1608	1567	1621	1600	1580
4144.342	1582	1572	1564	1581	1512	1563	1524	1570	1606	1610	1601	1573	1598	1600	1599	1584	1601	1598	1602	1543	1597	1604	1565	1575	1624	1622	1582	1577
4144.388	1591	1584	1585	1553	1537	1545	1542	1585	1609	1596	1602	1585	1608	1601	1592	1559	1604	1517	1556	1555	1596	1598	1579	1580	1585	1618	1587	1589
4144.424	1579		1587	1548	1538	1530	1543	1583	1611	1561	1603	1597	1605	1601	1557	1551	1599	1524	1528		1602	1572	1576	1584	1553	1617	1591	1592
4145.327	1527	1600	1589	1586	1588	1595	1600	1587	1562	1612	1567	1543	1570	1568	1562	1585	1570	1615	1567	1590	1579	1580	1613	1603	1582	1600	1590	1603
4156.270	1531	1573	1581	1576	1556	1574	1598	1538	1589	1599	1613	1524	1604	1577	1592	1599	1577	1617	1541	1598	1575	1577	1552	1607	1599	1604	1606	1596
4156.303	1540	1561	1588	1558	1524	1585	1606	1542	1600	1615	1621	1538	1593	1553	1608	1604	1562	1621	1529	1601	1580	1556	1564	1602	1600	1607	1599	1604
4156.344	1545	1566	1603	1559	1531	1596	1602	1550	1605	1616	1611	1555	1567	1559	1604	1598	1562	1630	1537	1608	1588	1564	1572	1588	1599	1616	1579	1610
4156.368	1549	1566	1607	1555	1541	1595	1607	1561	1613	1618	1614	1564	1564	1561	1592	1587	1563	1624	1547	1608	1588	1566	1573	1577	1596	1612	1572	1603
4156.405	1566	1581	1616	1568	1548	1595	1603	1561	1606	1596	1602	1575	1570	1570	1572	1575	1575	1537	1549		1597	1576	1577	1575	1612	1616	1570	1590
4156.432	1562	1584	1609	1574	1559	1596	1606	1571	1604	1563	1607	1586	1570	1575	1562	1575	1583	1507	1563	1576	1600	1580	1584	1575	1599	1615	1567	1584

2440000+																												
1981.275	1573	1606		1587	1574	1603	1536	1583	1608	1551		1517	1597			1588	1573	1527	1551	1534	1573	1569	1546	1598			1548	1602
2274.485	1547	1575	1560	1602	1589	1600	1563	1563	1564	1559	1605	1508	1614	1565	1593	1595	1571	1536	1567	1566	1576	1585	1598	1579	1595	1614	1575	1607
2276.494	1592	1599	1559	1572	1604	1583	1550	1620	1568	1559	1570	1483	1592	1557	1620	1592	1574	1589	1550	1551	1603	1585		1580	1595	1607	1563	1590
2276.510	1589	1599	1557	1567	1597	1569	1547	1614	1570	1566	1571	1489	1598	1553	1612	1591	1578	1582	1548	1550	1600	1582	1589	1591	1590	1611	1562	1578
2277.572	1562	1576	1591	1562	1586	1598	1600	1608	1581	1546	1566	1517	1571	1588	1616	1557	1551	1547	1548	1587	1589	1573	1561	1557	1560	1584	1572	1573
2281.461	1599	1589	1546	1584	1589	1562	1569	1587	1606	1569	1586	1525	1566	1574	1607	1590	1564	1553	1549	1554	1599	1588	1564	1588	1592	1564	1569	1611
2296.411	1572	1582	1533	1563	1594	1601	1565	1586	1594	1566	1586	1525	1565	1550	1602	1591	1561	1547	1547	1588	1571	1591	1600	1602	1564	1593	1561	1587
2298.379	1599	1591	1554	1591	1582	1571	1569	1585	1585	1548	1559	1524	1608	1542	1617	1570	1555	1538	1576	1582	1571	1584	1575	1605	1546	1590	1547	1610
2298.388	1594	1597	1558	1592	1579	1571	1564	1584	1584	1549	1563	1523	1611	1540	1611	1575	1556	1539	1567	1582	1580	1587	1580	1606	1555	1587	1550	
2306.468	1512	1599		1560	1598	1587	1575	1605	1586	1582	1583	1533	1592	1584	1612	1575	1587	1587	1548	1589	1597	1592	1599	1589	1591	1606	1579	1610
2307.444	1595	1566	1589	1605	1583	1573	1553	1604	1583	1553	1552	1492	1575	1561	1619	1573	1561	1543	1581	1558	1567	1585	1587	1591	1550	1593	1549	1581
2309.432	1597	1575	1579	1574	1575	1573	1548	1565		1576		1509	1605	1563	1552	1561	1562	1582	1576	1585	1591	1588	1603	1600	1545	1599		1608
2338.337	1586	1604	1562	1570	1584	1604	1570	1583	1581	1540	1607	1519	1614	1596	1590	1587	1561	1566	1550	1556	1606	1578	1577	1582	1585	1565	1582	1577
2752.278	1559	1594	1568	1560	1572	1598	1563	1608	1600	1569	1580	1503	1609	1578		1575	1547	1543	1556	1575	1593	1569	1604	1603	1538	1577	1564	1585
2752.296	1562	1599	1573	1555	1568	1589	1562	1611	1602	1568	1558	1505	1612	1574	1598	1576	1543	1535	1556	1574	1584	1569	1603	1598	1530	1585	1560	1590
3392.358	1595	1583	1530	1600		1560	1552	1614	1583	1564	1604		1555	1533	1597	1547	1542	1549	1522	1582	1561	1566	1545	1612	1552	1578	1568	1606
3393.367		1572	1586	1567	1591	1604	1545	1609	1598	1550	1585	1511	1610	1585	1551	1581	1589	1573	1536	1549	1588	1594	1595	1590	1589	1600	1555	1582
3395.461	1597	1593	1542	1584		1585	1559	1582	1610	1592	1557	1537	1613	1584	1622	1587	1567	1576	1554	1539	1580	1571	1602	1606	1589	1574	1588	1564
3399.432	1555	1614	1572	1600	1571	1586	1566	1588	1612	1563	1552	1504	1607	1584	1626	1563	1575	1583	1547	1589	1595	1576	1570	1602	1574	1602	1549	1619
3399.482	1568	1589	1575	1606	1577	1562	1574	1603	1580	1572	1555		1559	1564	1620		1549	1589	1565	1583	1570	1539	1549	1600	1577	1575	1539	1592
3401.368	1583	1608	1567	1603	1557	1567	1550	1623	1610	1577	1563	1541	1587	1582	1536	1590	1584	1547	1571	1562	1568	1591	1593	1588	1541	1602	1565	1562
3401.513	1598	1573	1592	1560	1601	1585	1581	1563	1567	1540	1605	1484	1610	1556	1582	1572	1552	1571	1550	1581	1575	1562	1571	1610	1573	1583	1579	1591
3459.304	1554	1606	1555	1556	1573	1604	1541	1615	1575	1510	1544	1509	1611	1590	1620	1600	1593	1566	1570	1544	1598	1583	1562	1601	1566	1594	1567	1586
3459.321	1551	1614	1570	1561	1576	1608	1554	1615	1570	1512	1552	1513	1613		1620	1601	1585	1579	1574	1540	1607	1592	1580	1609	1569	1595	1576	1595
3722.495	1559	1565	1545	1577	1583	1559	1531	1582	1603	1577	1544	1467	1616	1576	1619	1565	1559		1545	1568	1591	1568	1576	1604	1558	1582	1558	1560
3722.556	1502	1575		1591	1597	1570	1541	1597	1605	1553		1483	1573	1576	1557	1570	1571	1547	1559	1573	1599	1580	1589	1592	1567	1579	1560	1571
3723.484	1582	1610	1574	1554		1610	1564	1560		1563	1565	1511	1559		1627	1584	1561	1554		1583	1549	1588	1607	1577		1581	1559	1601
3756.401	1578	1591	1574	1604	1596	1579	1596	1603	1562	1599	1560	1537	1609	1562	1623	1578	1562	1590	1580	1599	1606	1561	1605	1579	1556	1593	1562	1567
3759.352	1594	1571	1523	1603	1568	1612	1555	1623	1610	1588	1562	1518	1596	1593	1630	1563	1597	1580	1584	1593	1608	1584	1609	1608	1565	1555	1573	1559
3761.336	1520	1578	1542	1601	1575	1562	1542	1571	1613	1519	1610	1503	1566	1574	1598	1575	1581	1534	1566	1587	1585	1565	1601	1615	1534	1567	1567	1607
3774.314	1591	1576	1565	1594	1601	1588	1565	1569	1584	1579	1555	1498	1615	1568	1625	1575	1558	1583	1585	1592	1571	1577	1590	1581	1591	1571	1574	1609
3775.280	1543	1598	1581	1556	1564	1569	1568		1606	1574	1600	1529	1609	1597	1621	1589	1580	1586	1572	1562	1603	1589	1604	1616	1547	1599	1575	1585
3775.336	1558	1617	1598	1570	1575	1563	1553	1569	1572	1581	1565	1528	1566	1601	1626	1607	1594	1583	1590	1553	1608	1561	1607	1582	1565	1572	1566	1613
3775.381	1564	1624	1597	1578	1584	1571	1544	1571	1564	1584	1560	1524	1573	1584	1630	1592	1596	1556	1593	1550	1584	1548		1567	1565	1549	1562	1618
3775.438	1576	1577	1588	1583	1582	1583	1551	1579	1568	1581	1573	1538	1594	1560	1613	1567	1584	1533	1564	1557	1564	1565	1560	1566	1573	1551	1555	1599
3775.472	1587	1577	1610	1609	1599	1606	1571	1598	1570	1584	1581	1539	1610	1567	1620	1567	1572	1548	1550	1575	1575	1577		1581	1584	1568	1562	1585
3776.286	1596	1570	1550	1602	1592	1599	1561	1611	1574	1551	1609	1504	1580	1566	1587	1561	1556	1546	1551	1582	1574	1582	1551	1587	1596	1580	1559	1565
3787.280	1557	1613	1580	1559	1593	1614	1565	1571	1558	1574	1596	1525	1559	1560	1607	1593	1578	1578	1573	1579	1571	1568	1562	1581	1566	1598	1571	1563
3787.443	1555	1574	1539	1584	1579	1569	1562	1624	1604	1577	1547	1498	1621	1561	1625	1573	1562	1525	1543	1591	1605	1594	1613	1602	1586	1568	1571	1597
3793.295		1592		1552		1620	1564	1597	1584	1582	1557		1590		1630		1584	1592	1534	1540	1555	1551	1593	1599	1538	1611	1574	
4118.377	1600	1576	1560	1576	1605	1569	1582	1596	1563	1590	1596	1493	1580	1554	1621	1563	1560	1549	1581	1590	1571	1606	1610	1587	1602	1599	1582	1567
4118.418	1577	1565	1577	1584	1606	1575	1592	1617	1581	1589	1567	1496	1567	1559	1631	1568	1571	1558	1563	1588	1572	1605	1602	1596	1602	1557	1584	1576
4118.449	1546	1570	1581	1604	1600	1592	1582	1625	1592	1595	1555	1512	1577	1559	1629	1573	1574	1567	1553	1595	1585	1590	1579	1609	1569	1551	1591	1585
4144.342		1605	1595	1591	1569	1556	1553	1610	1609	1538	1555	1535	1567	1580	1619	1585	1551	1586	1539	1597	1597	1579	1593	1592	1541	1612	1584	1596
4144.388	1593	1603	1591	1597	1582	1565	1550	1616	1587	1557	1559	1533	1577	1591	1612	1565	1560	1587	1562	1593	1600	1575	1606	1566	1558	1598	1575	1609
4144.424	1567	1592	1528	1599	1578	1565	1537	1616	1564	1556	1557	1467	1580	1579	1611	1546	1554	1562	1557	1556	1598	1565	1597	1564		1588	1561	1589
4145.327	1571	1571	1580	1559	1581	1615	1579	1581	1578	1586	1606	1511	1599	1578	1610	1560	1588	1548	1544	1555	1565	1575	1606	1592	1588	1564	1555	1580
4156.270	1589	1615	1586	1571	1571	1606	1573	1617	1580	1553	1610	1477	1561	1586	1609	1597	1562	1594	1569	1583	1575	1588	1617	1591	1568	1602	1584	1558
4156.303	1588	1612	1525	1580	1555	1610	1581	1617	1571	1556	1611	1486	1572	1598	1615	1602	1561	1591	1577	1586	1564	1596	1604	1586	1570	1596	1587	1558
4156.344	1598	1601	1522	1600	1553	1603	1582	1606	1562	1565	1585	1494	1592	1596	1616	1602	1566	1592	1586	1593	1568	1602	1568	1584	1578	1611	1584	1571
4156.368	1589	1584	1534	1601	1560	1583	1588	1581	1567	1569	1570	1503	1593	1602	1625	1597	1564	1593	1588	1587	1573	1603	1558	1585	1572	1603	1585	1572
4156.405	1592	1565	1551	1603	1569	1565	1590	1558	1569	1574	1554	1513	1609	1597	1620	1588	1576	1570	1591	1596	1581	1610	1566	1587	1586	1598	1588	1590
4156.432	1594	1561	1557	1607	1574	1566	1586	1565	1584	1577	1562	1525	1617	1597	1624	1568	1578	1559	1591	1593	1588	1604	1578	1604	1585	1563	1586	1589
4168.421	1594	1586	1586	1610	1555	1605	1572	1595	1605	1590	1554	1529	1609	1546	1616	1579	1572	1550	1540	1576	1573	1590	1613	1609	1593	1578	1577	1565

Table 4 – *continued*

B MAGNITUDE X 100

HEL.J.D. 2440000+	2	3	4	5	6	7	8	9	10	11	12	13	14	15	16	17	18	19	20	22	23	24	25	26	28	29	30	31
2274.506	1609	1617	1590	1598	1615	1579	1645	1602	1609	1642	1648	1635	1647	1552	1610	1601	1608	1661	1559	1638	1559	1614	1642	1602	1667	1677	1643	1614
2276.486	1587	1635	1637	1627	1599	1590	1645	1548	1625	1637	1651	1636	1631	1651	1614	1626	1605	1577	1649	1626	1581	1593	1646	1629	1657	1550	1624	1609
2276.502	1590	1641	1644	1630	1601	1592	1638	1550	1628		1641	1636	1620	1657	1602	1620	1606	1585	1648		1584	1599	1648	1609	1647	1560	1631	1613
2277.563	1636	1606	1614	1607	1591	1590	1621	1630	1601	1647	1658	1618	1655	1621	1631	1620	1597	1531	1623	1592	1644	1591	1638	1641	1625	1617	1587	1646
2281.447	1617	1611	1618	1610	1624	1597	1621	1583	1599	1585	1611	1550	1632	1654	1599	1621	1638	1662	1585	1625	1588	1643	1605	1594	1587	1672	1627	1623
2298.383	1575	1638	1608	1617	1561	1550	1636	1629	1582	1605	1640	1639	1595	1625	1628	1613	1620	1643	1584	1643	1655	1618	1649	1623	1637	1598	1617	1642
2305.476	1629	1588	1597	1614	1638	1574	1645	1634	1630	1587	1651	1647	1651	1552	1626	1626	1585	1665	1629	1643	1653	1643	1625	1615	1614	1666	1608	1615
2306.477	1577	1645	1581	1626	1606	1566	1572	1587	1595	1617	1643	1654	1633	1671	1587	1640	1627	1659	1641	1581	1645	1608	1663	1622	1644	1620	1618	1647
2309.379	1599	1587	1618	1578	1631	1608	1641	1555	1635	1614	1627	1656	1591	1665	1604	1637	1643	1653	1553	1594	1547	1589	1597	1651	1659	1633	1630	1648
2715.332	1598	1617	1584	1640	1585	1559	1647	1616	1592		1567	1651	1645	1644	1585		1638	1530	1621	1647	1638	1593	1625	1644	1584	1639	1599	1625
2715.342	1623	1612	1576	1630	1608	1589	1645	1635	1598	1583	1579	1662	1648	1650	1595	1576	1643	1527	1633	1636	1638	1605	1636	1633	1580	1638	1625	1627
2716.267	1613	1649	1587	1584	1624	1598	1597	1644	1652	1646	1653	1629	1599	1557	1626	1613	1591	1665	1637	1566	1617	1610	1651	1603	1641	1587	1621	1644
2752.269	1623	1615	1640	1637	1624	1621	1631	1581	1640	1645	1628	1638	1621	1660	1628	1593	1570	1658	1626	1558	1558	1592	1658	1653	1602	1656	1626	1538
3392.328	1633	1638	1590	1644	1645	1574	1633	1567	1616	1658	1584	1615	1616	1672		1635	1656	1658	1668	1655	1644	1647	1676	1646	1627	1665	1576	
3393.439	1600	1647	1640	1630	1619	1549	1570	1635	1594	1637	1636	1589	1634			1583	1639	1662	1618	1633	1647	1634	1652	1634	1608	1667	1601	1647
3394.376	1619	1594	1641	1596	1589		1624	1634	1637	1646	1630	1625	1617	1602	1567	1609	1585	1659		1645	1590		1598	1657	1649	1627	1603	1640
3399.324	1627	1641	1615	1649	1619	1576	1591	1637	1617	1583	1662	1642	1619	1675	1628	1625	1641	1572	1642	1654	1637	1634	1647	1585	1575	1632	1613	1608
3399.388	1575	1606	1645	1604	1623	1575	1610	1645	1641	1592	1626	1655	1635	1667	1639	1615	1637	1611	1552	1653	1636	1644	1656	1597	1576	1555	1617	1604
3399.466	1580	1595	1651	1594	1643	1624	1636	1569	1659	1630	1575	1671	1656	1637	1634	1619	1592	1643	1584	1647	1576	1633	1664	1628	1602	1609	1633	1615
3399.531	1597	1614	1595	1614	1634	1625	1658	1565	1615	1658	1599	1652	1649	1557	1589	1624	1591	1658	1599	1647	1581	1586	1644	1644	1607	1626	1614	1638
3401.340	1637	1596	1647	1589	1615	1618	1614	1632	1642	1628	1609	1659	1644	1582		1630	1582	1664	1638	1627	1587	1604	1642	1608	1586	1649	1602	1624
3401.408	1581	1593	1595	1592			1617	1623	1642	1581		1545	1649	1609		1629	1588	1663	1601	1635	1580		1652	1615	1583	1659	1598	
3756.438	1633	1643	1595	1600	1627	1620	1643	1564	1642	1630	1598	1657	1595	1667		1634	1640	1557	1605	1654	1607	1615	1593	1649	1634	1567	1618	1619
3761.319	1595	1609	1656	1602	1594	1556	1616	1630	1596	1648	1641	1540	1639	1536		1605	1581	1665		1617	1625		1644	1624		1643	1593	1617
3775.310	1595	1596	1608	1612	1613	1560	1576	1621	1626	1640	1552	1633	1646	1568		1639	1593	1577	1618	1624		1613	1654	1649	1635	1664	1593	1610
3775.358	1619	1606	1658	1654	1530	1551	1559	1625	1653		1583	1657		1565		1647	1584	1593	1627	1665	1593		1670	1635		1648	1625	1614
3775.413	1628	1608	1654	1637	1554	1579	1584	1636	1654	1637	1605	1650	1644	1584		1646	1601	1615	1633	1663	1611	1634	1666	1604	1634	1560	1635	1622
3775.454	1614	1610	1628	1627	1542	1595	1612	1643	1637	1606	1615	1657	1620	1608		1630	1625	1640	1634	1612	1623	1609	1648	1597	1658	1582	1617	1627
3788.265	1599	1615	1670	1588	1605	1546		1635	1608	1600	1652	1679	1641	1597	1636	1636	1584	1672	1571	1644	1644	1623	1576	1618	1631	1639	1600	1647
3789.285	1617		1601	1627	1610	1555	1646	1568	1630	1576	1658	1631		1614		1577	1576	1656		1551	1594	1589	1662	1642		1594	1601	1627
4117.345	1578	1645	1581	1640	1626	1604	1608	1633	1643	1577	1593	1621	1622	1611	1586	1584	1581	1655	1572	1638	1647	1640	543	1598	1656	1659	1584	1593
4118.409	1647	1642	1631	1606	1573	1601	1660	1580	1624	1586	1655	1590	1650		1651	1632	1600	1675	1644	1585	1626	1643	1601	1651	1608	1662	1626	1653
4118.444	1645	1648	1659	1628	1581	1612	1593	1577	1634	1601	1653	1596	1656	1570	1633	1639	1579	1664	1635	1593	1641	1647	1614	1650	1617	1675	1637	1629
4144.331	1644	1598	1584	1628	1543	1615	1546	1612	1634	1648	1650	1601	1647	1642	1633	1627	1628	1647	1648	1577	1621	1648	1597	1604	1671	1656	1618	1604
4144.377	1646	1616	1616	1596	1570	1581	1562	1626	1651	1638	1655	1626	1649	1654	1635	1594	1643	1533	1620	1592	1636	1645	1610	1614	1645	1660	1638	1622
4145.318	1561	1642	1618	1620		1639	1651	1633	1586	1650	1590	1594	1594	1594	1600	1606	1593	1651	1511	1628	1632	1615	1664	1643	1622	1642	1644	1648
4156.277		1602	1602	1601	1567	1602	1653	1553	1619	1635	1662	1546	1638	1612	1642	1635	1605	1658	1557	1645	1613	1599	1583	1648	1658	1648	1638	1638
4156.310	1574	1582	1620	1589	1536	1622	1651	1568	1643	1651	1668	1559	1630	1599	1645	1637	1581	1671	1559	1651	1614	1582	1595	1633		1658	1636	1639
4156.353	1576	1587	1631	1576	1546	1624	1647	1575	1646	1650	1656	1576	1595	1589	1633	1625	1581	1663	1568	1652	1628	1581	1615	1618	1662	1665	1600	1544
4156.375	1594	1597	1650	1592	1559	1616	1649	1584	1643	1638	1644	1594	1591	1600	1616	1606	1591	1646	1567	1670	1642	1594	1614	1609	1656	1657	1594	1639
4156.414	1596	1612	1654	1603	1573	1612	1647	1596	1640	1614	1660	1612	1604	1617	1591	1610	1601	1541	1585	1647	1647	1596	1626	1601	1667	1662	1580	1621
4156.441	1614	1620	1643	1596	1581	1610	1652	1609	1625	1581	1631	1615	1600	1613	1588	1607	1617	1510	1589	1594	1648	1605	1621	1616	1670	1666	1578	1627
4168.378	1632	1579	1636	1620	1568	1581	1592	1585	1638	1652	1554	1554	1640		1612	1615	1628	1663	1619	1640	1632	1636	1621	1625	1657	1653	1625	1592
4168.410	1637	1590	1589	1629	1592	1606	1606	1555	1633	1630	1573	1582	1645		1593	1617	1502	1582	1630	1642	1633	1638	1626	1601	1662	1654	1637	1602

HEL.J.D. 2440000+	32	35	36	38	39	40	41	42	43	44	48	49	50	51	52	53	54	55	57	65	66	67	74	96	97	101	102	103
2274.506	1589	1609	1569	1622	1637	1643	1596	1583	1594	1590	1641	1527	1647	1587	1649	1637	1624	1588	1619	1615	1612	1628	1639		1644	1654	1630	1629
2276.486	1634	1629	1583	1590	1643	1618	1583	1649	1594	1597	1585	1505	1614	1590	1660	1624	1604	1629	1568	1572	1643	1617	1611	1617	1632	1642	1605	1612
2276.502	1635	1636	1587	1594	1639	1605	1574	1652	1597	1598	1590	1500	1622	1579	1665	1628	1608	1632	1571	1576	1645	1626	1617	1621	1633	1645	1604	1616
2277.563	1593	1613	1643	1596	1626	1651	1624	1651	1621	1578	1586	1553	1620	1624	1671	1589	1580	1593	1586	1632	1631	1616	1594		1605	1603	1631	1604
2281.447	1646	1622	1566	1609	1613	1588	1612	1614	1646	1608	1625	1554	1596	1605	1648	1618	1603	1600	1587	1600	1636	1636	1572	1637	1635	1592	1616	1655
2298.383	1626	1627	1569	1623	1607	1597	1577	1616	1624	1564	1563	1543	1643		1659	1598	1561		1589	1603	1598	1611	1587	1642	1566	1619	1566	1647
2305.476	1608	1614	1639	1620	1595	1649	1583	1586	1618	1584	1640	1527	1647	1595	1615	1616	1586	1620	1566	1618	1593	1566	1601	1646	1611	1593	1619	1596
2306.477	1513	1634	1580	1577	1635	1625	1604	1644	1620	1605	1615	1544	1608	1613	1640	1587	1613	1621	1558	1629	1632	1621	1634	1612	1627	1636	1616	1648
2309.379	1628	1591	1635	1636	1584	1579	1589	1615	1587	1612	1603	1520	1647	1628		1588	1621	1628	1594	1638	1606	1630	1623	1618	1613	1653	1619	1644
2715.332	1585	1595	1600	1638	1595	1607	1566	1582	1606	1588	1637	1534	1650	1611	1596	1569	1616			1569	1606	1594	1627	1655	1607	1647	1577	1591
2715.342	1608	1609	1611	1636	1605	1600	1582	1591	1612	1612	1651	1543	1650	1629	1617	1582	1635	1597	1622	1581	1623	1604	1622	1655	1608	1621	1589	1576
2716.267	1635	1656	1633	1593	1622	1628	1610	1656	1650	1629	1582	1523	1643	1606	1662	1607	1561	1580	1575	1604	1607	1594	1575	1624	1598	1587	1604	1637
2752.269	1603	1630	1621	1592	1604	1635	1600	1648	1631	1619	1615		1643	1615	1641	1610	1584	1591	1590		1639	1604	1632	1650	1584	1608	1619	1610
3392.328	1643	1614	1612	1646	1595	1593	1605	1666	1641	1630		1507	1590	1585	1633	1595	1590	1618	1586	1646	1597	1609	1617	1662	1588	1588	1637	1634
3393.439	1600	1598	1626	1632	1616	1590	1562	1651	1652	1595	1638	1539	1650	1618	1616	1626	1606	1607	1559	1605	1582	1560	1636	1630	1630	1632	1572	1634
3394.376	1610	1650	1570	1588		1636		1610	1604	1534	1573	1520	1624		1665	1613	1548			1607	1622	1585	1614	1655	1550	1607		1596
3399.324	1551	1647		1593	1630		1586	1591	1632	1605	1650	1564	1637	1638	1661		1631	1646	1579	1646		1643	1646	1609	1599	1644		1643
3399.388	1575	1671	1609	1617	1611	1652	1595	1603	1652	1600	1598	1548	1657	1628	1681	1613	1628	1625	1560	1627	1648	1632	1646	1630	1609	1654	1602	1667
3399.466	1612	1639	1627	1650	1618	1600	1634	1641	1635	1630	158[illegible]	1502	1600	1609	1679	1595	1595	1653	1611	1634	1610	1587	1582	1660	1627	1614	1599	1639
3399.531	1634	1597	1633	1654	1627	1597	1629	1654	1586	1631	1609	1504	1597	1597	1663	1603	1577	1624	1624	1637	1595	1578	1607	1658	1631	1588	1595	1598
3401.340	1624	1649	1612	1639	1585	1605	1588	1652	1642	1617	1586	1566	1607	1629	1617	1634	1629	1597	1618	1608	1618	1634	1616	1626	1576	1637	1616	1608
3401.408		1618		1627		1588		1640	1648	1595	1588	1549			1570						1565	1603		1632		1647		1586
3756.438	1515	1634	1609	1641	1631	1589	1615	1650	1589	1624	1568	1566	1648	1577	1658	1608	1588	1613	1606		1605	1605	1581	1602	1567		1577	1613
3761.319	1530	1612	1551	1631	1592	1591		1589	1637	1514		1523	1582		1626	1598	1586			1597	1622	1565		1646	1533	1615		1644
3775.310	1574	1652	1634	1581	1593	1590	1579	1604	1638	1618	1607	1561	1610	1617	1676	1633	1605	1628	1606	1588	1644	1590	1633	1646	1576	1608	1606	1626
3775.358	1580	1658	1643	1604	1613	1600	1568	1591	1591	1612	1567	1550	1587	1607	1684	1653	1612	1585	1616	1581	1634	1569	1608	1599	1603	1591	1589	1668
3775.413	1610	1635	1633	1608	1603	1605	1576	1601	1586	1614	1581	1560	1620	1593	1672	1604	1627	1567	1608	1581	1600	1578	1576	1599	1602	1564	1577	1661
3775.454	1609	1603	1626	1625	1614	1627	1583	1624	1612	1615	1602	1567	1631	1588	1664	1584	1606	1571	1573	1582	1586	1583	1591	1612	1602	1586	1590	1619
3788.265	1631	1628	1610		1613	1617	1556	1604	1626		1612	1531	1627	1594	1585	1591	1598	1563	1619	1578	1635	1609	1628	1641	1632	1588	1593	1660
3789.285	1586		1581			1575		1657	1587	1556	1583	1523	1650	1592	1658		1599			1613	1613	1599	1575	1594		1672		
4117.345	1574	1612	1640	1640	1594	1635	1570	1652		1621	1577	1556	1636	1602	1658	1642	1627	1632	1591	1602	1619	1611	1594	1646	1622	1604	1603	1605
4118.409	1630	1591	1610	1614	1638	1614	1634	1648	1601	1640	1593	1523	1586	1585	1676	1601	1600	1606	1594	1640	1597	1649	1640	1634	1655	1600	1638	1591
4118.444	1582	1592	1620	1641	1643	1619	1613	1656	1613	1642	1580	1518	1588	1575	1675	1604	1598	1601	1575	1646	1605	1637	1602	1650	1619	1583	1632	1619
4144.331	1633	1648	1646	1630	1599	1594	1593	1642	1637	1569	1586	1561	1586	1617	1663	1630	1581	1640	1575	1632	1633	1620	1622	1623	1577	1656	1631	1647
4144.377	1630	1651	1638	1641	1618	1591	1580	1651	1622	1593	1582	1565	1591	1625	1661	1597	1592	1646	1595	1645	1645	1616	1636	1592	1595	1636	1622	1644
4145.318	1617	1602	1628	1581	1628	1639	1615	1610	1595	1632	1643	1547	1621	1631	1661	1604	1630		1572	1610	1597	1618	1646	1634	1634	1584	1596	1608
4156.277	1630	1648	1602	1600	1596	1646	1599	1658	1609	1585	1646	1495	1584	1621	1656	1638	1591	1637	1601	1625	1593	1625	1646		1605	1655	1634	1585
4156.310	1650	1654	1553	1622	1576	1650	1621	1662	1589	1593	1638	1513	1598	1639	1671	1648	1586	1634	1609	1639	1597	1648	1627		1609	1646	1630	1587
4156.353	1630	1626	1547	1625	1573	1632	1621	1627	1588	1600	1605	1517	1617	1631	1670	1640	1590	1633	1617	1625	1590	1630	1576	1619	1612	1663	1626	1600
4156.375	1626	1614	1567	1649	1588	1607	1614	1597	1591	1602	1585	1528	1633	1630	1671	1632	1591	1618	1620	1629	1609	1646	1571	1618	1622	1653	1622	1609
4156.414	1615	1596	1578	1642	1596	1597	1620	1589	1601	1601	1574	1536	1635	1621	1688	1605	1585	1594	1629	1624	1618	1630	1591	1627	1609	1634	1619	1623
4156.441	1621	1597	1589	1646	1610	1580	1605	1582	1599	1606	1568	1534	1653	1613	1663	1587	1604	1537	1616	1624	1621	1629	1604	1631	1630	1625	1617	1641
4168.378	1622	1600	1612	1636	1570	1642	1590	1609	1634	1622	1620	1553	1648	1583	1649	1621	1594	1612	1569	1609	1614	1616	1634	1646	1637	1650	1621	1614
4168.410	1641	1606	1625	1647	1581	1640	1607	1620	1640	1637	1595	1558	1648	1581	1664	1615	1606	1590	1572	1615	1595	1620	1642	1656	1636	1626	1627	1586

2.2 PERIODS AND LIGHT CURVES

The periods adopted for the 56 variables in the Bologna study were obtained both from analysing our observations alone with a period finding program based on Stellingwerf's (1978) method, and with hand computations based on the phase shifts between the various

Table 5. M15 RR Lyrae mean magnitudes and colours from Bologna observations.

Var.	Period Day	Epoch 2444156+	$\langle V\rangle$	$\langle B\rangle$	$\langle B\rangle-\langle V\rangle$	$\langle B-V\rangle$	$\langle V\rangle_c$	$[\langle B\rangle-\langle V\rangle]_c$	$\langle B-V\rangle_c$
2	0.684349	.303	15.650	16.071	0.421	0.430	15.650	0.426	0.435
3	0.3887407	.310	15.858	16.186	0.328	0.337	15.858	0.328	0.337
4	0.313570	.187	15.888	16.161	0.273	0.282	15.888	0.273	0.282
5	0.3842142	.325	15.810	16.127	0.317	0.321	15.810	0.317	0.321
6	0.6659671	.313	15.640	15.976	0.336	0.360	15.765	0.390	0.415
7	0.367577	.194	15.629	15.894	0.265	-	15.869	0.300	-
8	0.6462446	.620	15.770	16.140	0.370	0.400	15.804	0.399	0.430
9	0.7152819	.255	15.704	16.065	0.361	0.372	15.724	0.384	0.392
10	0.3863931	.169	15.853	16.180	0.327	0.330	15.883	0.346	0.348
11	0.343215	.466	15.860	16.140	0.280	0.292	15.860	0.284	0.300
12	0.5928520	.522	15.820	16.202	0.382	0.401	15.820	0.387	0.406
13	0.574923	.285	15.822	16.188	0.366	-	15.837	0.386	-
14	0.3820024	.392	15.889	16.236	0.347	0.353	15.889	0.347	0.353
15	0.583509	.349	15.871	16.254	0.383	0.402	15.871	0.388	0.407
16	0.399218	.478	15.772	16.107	0.335	0.341	15.772	0.343	0.353
17	0.4288924	.407	15.837	16.192	0.355	0.357	15.857	0.370	0.374
18	0.3677379	.323	15.816	16.110	0.294	0.298	15.843	0.312	0.316
19	0.5723030	.428	15.828	16.150	0.322	0.360	15.828	0.327	0.365
20	0.6969598	.296	15.681	16.085	0.404	0.420	15.801	0.457	0.475
22	0.7201510	.503	misses	maximum	-	-	-	-	-
23	0.6326959	.183	15.798	16.192	0.394	0.406	15.798	0.399	0.411
24	0.3696955	.323	15.793	16.107	0.314	0.316	15.853	0.338	0.338
25	0.6653286	.210	15.826	16.245	0.419	0.432	15.826	0.424	0.437
26	0.402277	.405	15.881	16.236	0.355	0.358	15.881	0.355	0.358
28	0.6706464	.527	15.824	16.240	0.416	0.427	15.824	0.421	0.432
29	0.5749761	.065	15.905	16.264	0.359	0.388	15.905	0.364	0.393
30	0.4059796	.400	15.792	16.089	0.297	0.298	15.792	0.305	0.310
31	0.4081781	.128	15.890	16.255	0.365	0.367	15.890	0.365	0.367
32	0.6054150	.624	15.652	15.955	0.303	0.326	15.699	0.336	0.361
35	0.3839986	.430	15.895	16.239	0.344	0.351	15.895	0.351	0.363
36	0.6241424	.337	15.700	16.070	0.370	0.386	15.810	0.422	0.441
38	0.3752769	.219	15.830	16.157	0.327	0.340	15.840	0.340	0.357
39	0.3895696	.335	15.811	16.130	0.319	0.324	15.839	0.338	0.342
40	0.3773302	.417	15.845	16.164	0.319	0.325	15.845	0.322	0.332
41	0.3917493	.160	15.608	15.950	0.342	0.347	15.768	0.374	0.377
42	0.3601745	.408	15.899	16.204	0.305	0.316	15.899	0.305	0.316
43	0.3960120	.353	15.846	16.160	0.314	0.312	15.846	0.314	0.312
44	0.595628	.210	15.634	15.960	0.326	0.334	15.734	0.374	0.384
48	0.3649762	.419	15.794	16.050	0.256	0.263	15.794	0.265	0.275
49	0.6552054	.243	15.110	15.363	0.253	-	-	-	-
50	0.2980583	.265	15.913	16.187	0.274	0.281	15.913	0.274	0.284
51	0.3969565	.119	15.730	16.040	0.310	0.314	15.845	0.340	0.339
52	0.5756132	.005	15.940	16.320	0.380	-	15.940	0.385	-
53	0.4141270	.487	15.791	16.112	0.321	0.327	15.801	0.335	0.344
54	0.3995683	.342	15.694	16.005	0.311	0.314	15.824	0.341	0.339
55	0.748596	.530	15.620	-	-	-	(15.790)	-	-
57	0.349264	.199	15.616	15.930	0.314	0.318	(15.716)	(0.342)	(0.342)
65	0.718196	.022	15.718	16.114	0.396	0.401	15.778	0.434	0.441
66	0.3793488	.322	15.829	16.143	0.314	0.318	15.853	0.331	0.335
67	0.404613	.153	15.787	16.086	0.299	0.303	15.937	0.331	0.331
74	0.296012	.377	15.831	16.099	0.268	0.275	15.941	0.298	0.300
96	0.3963520	.292	15.907	16.258	0.351	0.360	15.907	0.351	0.360
97	0.696333	.124	15.714	16.090	0.376	0.389	15.824	0.428	0.444
101	0.4003052	.097	15.836	16.181	0.345	0.356	15.836	0.345	0.356
102	0.759477	.713	15.690	16.093	0.403	0.406	15.830	0.459	0.463
103	0.3682424	.284	15.867	16.198	0.331	0.341	15.867	0.331	0.341

epochs of observation using periods published in SH. We adopted periods for the Bologna observations which are the same as SH for 34 variables and differ for 22 variables. Our finally adopted periods and epochs for Bologna observations are given in Table 5. Light curves for the variables are presented in Fig. 2.

In our re-reduction of SKS observations we used the same periods as published by SKS with the exceptions of V31, V50, V54, V61, V67 and V102 where the use of the period given by Cox *et al.* (1983) or Bologna slightly improved the light curve. SKS determined periods to satisfy their data after plotting preliminary periods from SH. We note that SKS

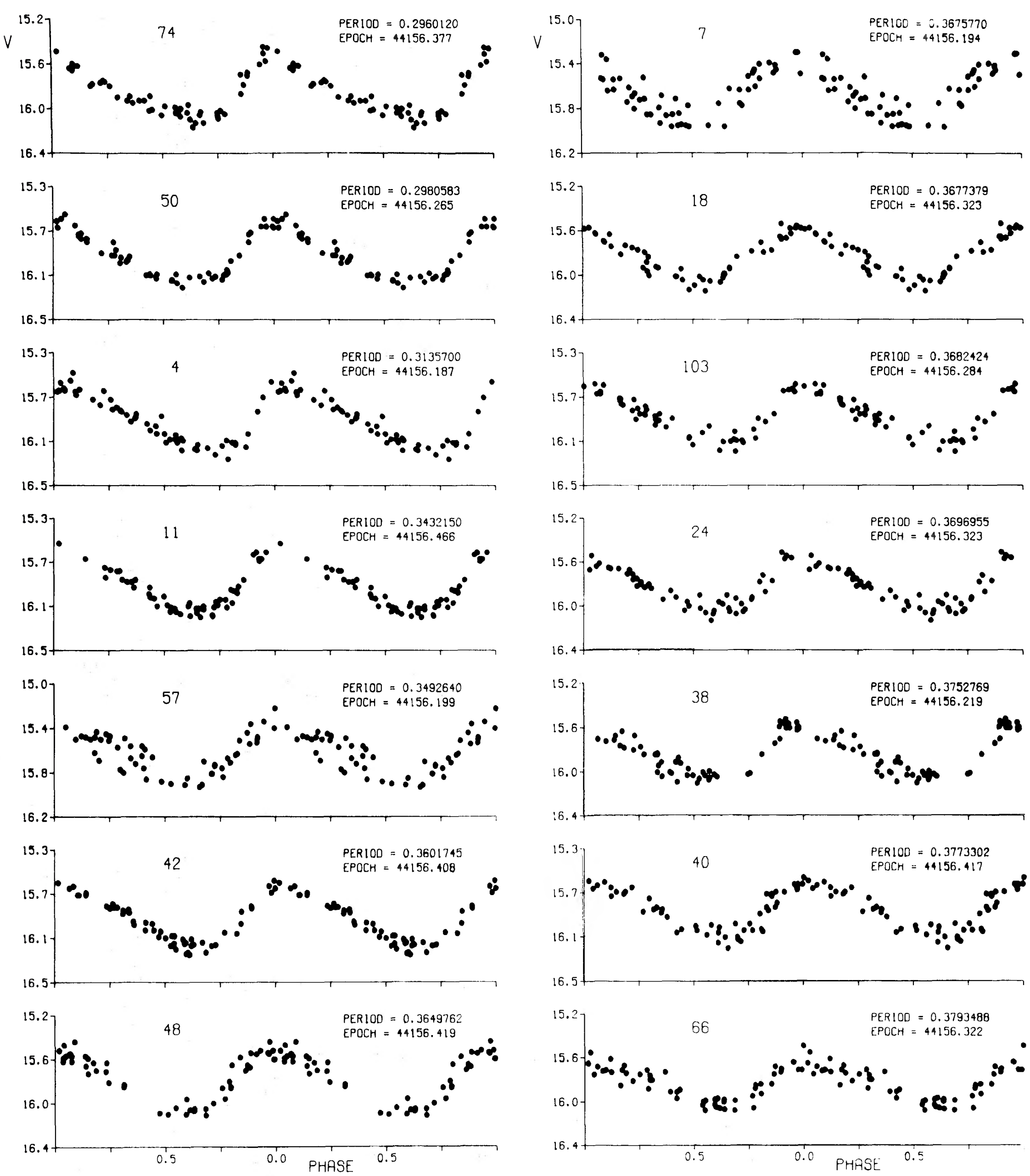

(a)

Figure 2. Light curves in V for 56 RR Lyraes measured on Loiano and Asiago plates (Bologna data). The variables are arranged in order of increasing period.

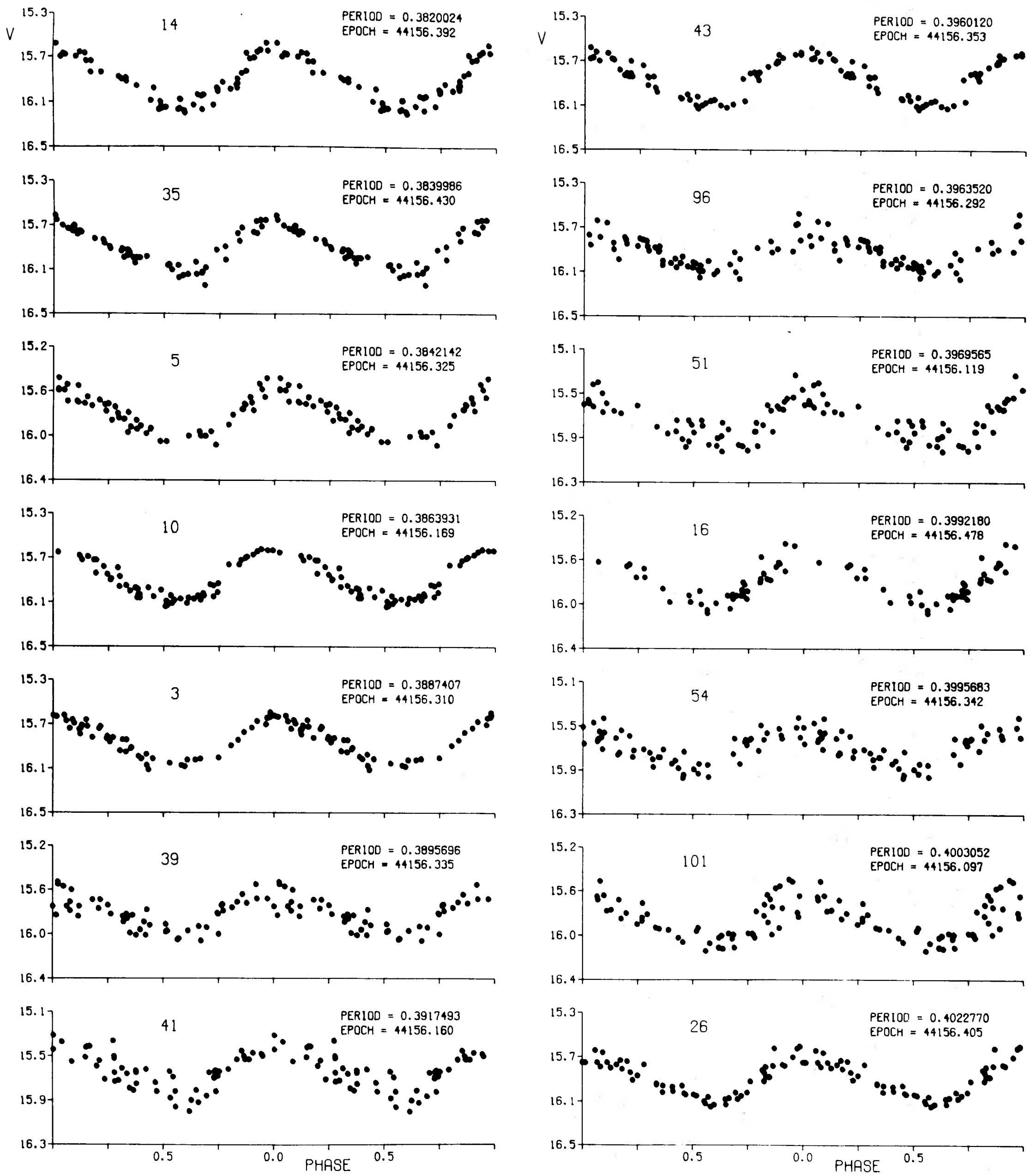

(b)

Figure 2 – *continued*

variables III-5 = V67, IV-41 = V74, II-26 = V97 and I-24 = V102. Adopted periods and epochs for SKS observations are given in Table 6.

We note that there may be real period changes for some of the variables. Smith & Sandage (1981) studied period changes for RR Lyraes in M15 and found abrupt or erratic period changes as well as linear ones from observations between 1896 and 1978. Most of this period behaviour has mean rates of change which are larger than can readily be explained by stellar evolution and the cause is not known. Period determinations for M15 variables at various epochs have been published by Wesselink (1974), Smith & Wesselink (1977), Filippenko & Simon (1981) and some double-mode pulsation periods discovered by Cox

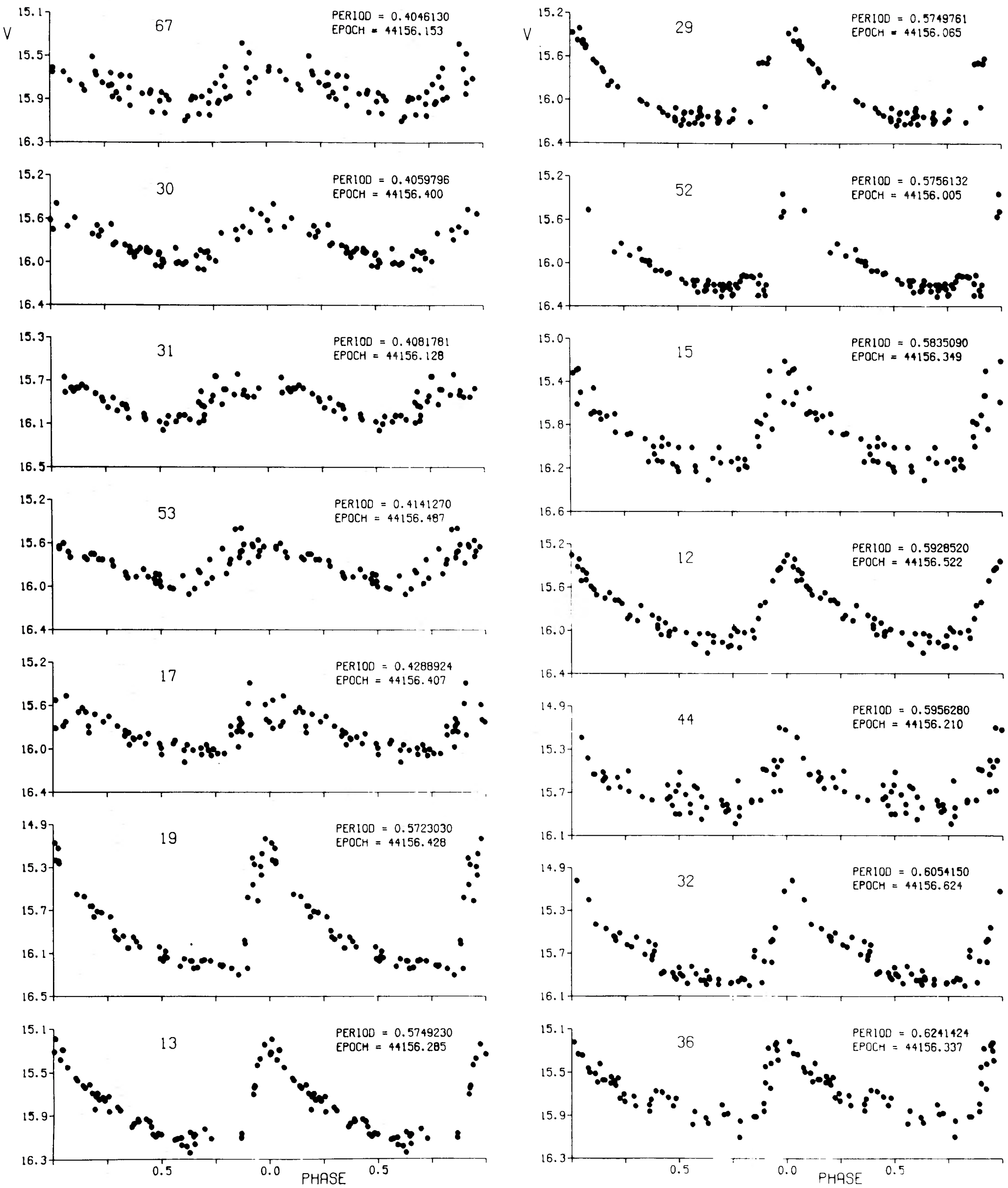

(c)

Figure 2 – *continued*

et al. (1983). The periods we adopt are used to derive mean light curve parameters from Bologna and Mount Wilson observations separately. These derivations will not be affected by small changes in adopted period, such as the difference between the period adopted in Tables 5 and 6 where for many of the variables the periods differ from the fifth decimal place.

It is not possible to combine the two series into one light curve for two reasons: the period does not fit adequately over the time interval involved of almost 20 years, and different photographic effects may be present in the two series of plates. Comments on individual variable stars are given in Table 7.

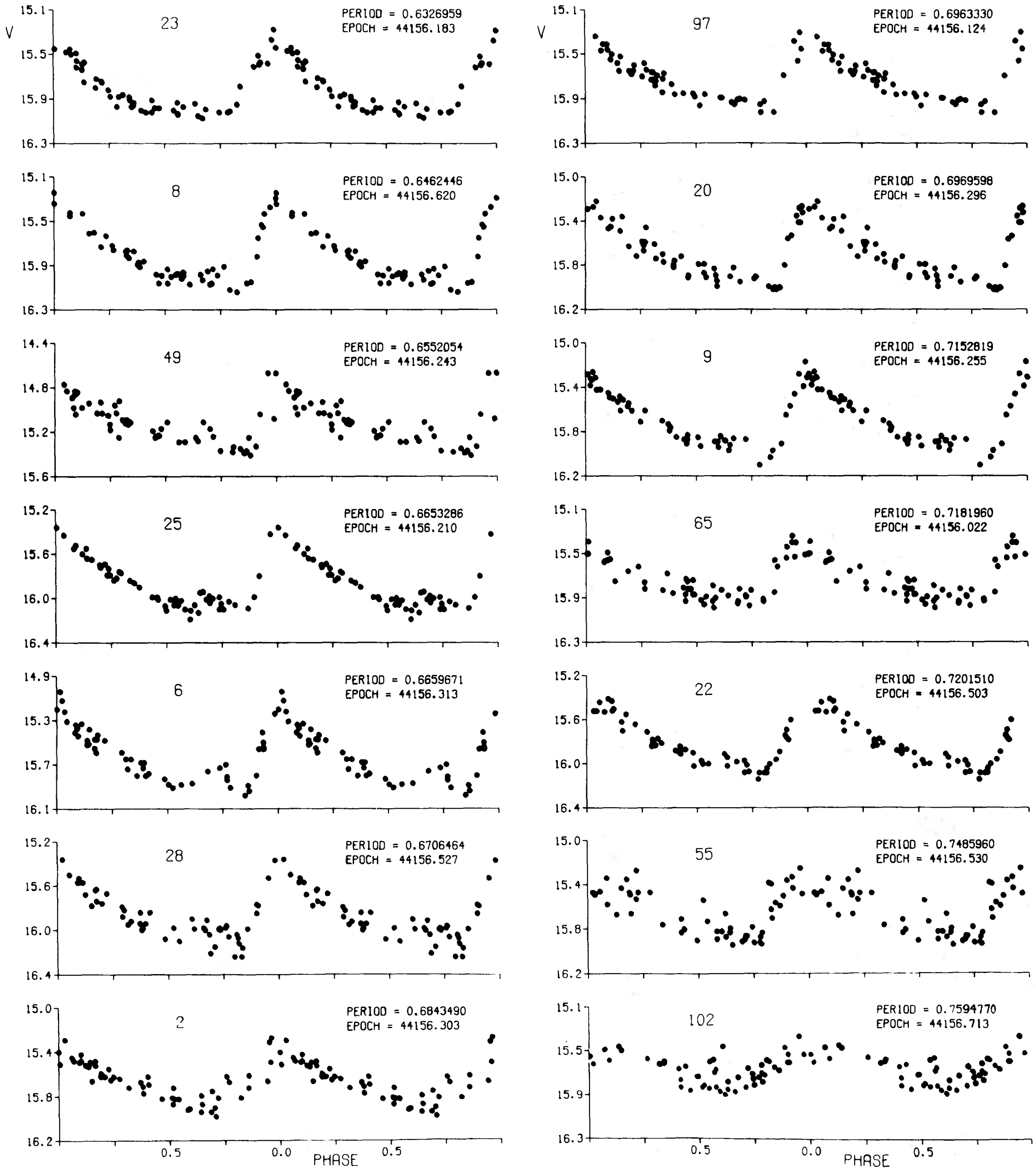

(d)

Figure 2 – *continued*

2.3 MEAN MAGNITUDES $\langle V \rangle$, $\langle B \rangle$ AND COLOURS $\langle B \rangle - \langle V \rangle$, $\langle B-V \rangle$

The observations in B and V were fitted by smooth light curves which were then converted to intensity units and averaged over a cycle to find the mean intensity. This procedure was carried out using a computer program on the STARLINK VAX 11/780 at RGO which obtains a light curve by spline fitting to the data. The fit can be varied by adjusting the weighting given to the points; for instance one can increase the weight of the brightest observations of an RR*ab*-type variable to define more accurately the rapid change in brightness on the rising branch. The light curve fits were checked visually and the best eye fit adopted for each variable. These mean intensities were then converted back to magnitude

1984MNRAS.209..765B

Table 6. M15 RR Lyrae mean magnitudes and colours re-reduced from SKS Mount Wilson observations.

Var.	Period Day	Epoch 2436488+	<V>	<B>	<B>−<V>	<B−V>	$<V>_c$	$[<B>-<V>]_c$	$<B-V>_c$
2	0.684270	.148	15.691	16.139	0.448	0.458	15.691	0.448	0.453
3	0.3887407	.319	15.796	16.135	0.339	0.350	15.796	0.339	0.350
4	0.313575	.027	15.876	16.136	0.260	0.269	15.876	0.260	0.269
5	0.3842086	.165	15.798	16.116	0.318	0.324	15.798	0.318	0.324
6	0.665971	.384	15.682	16.077	0.395	0.417	15.797	0.391	0.407
7	0.3675556	.324	15.714	16.048	0.334	0.344	15.874	0.319	0.334
8	0.646251	.270	15.755	16.170	0.415	0.438	15.783	0.415	0.428
9	0.7153076	.392	15.684	16.088	0.404	0.421	15.696	0.404	0.411
10	0.3864102	.231	15.824	16.185	0.361	0.367	15.854	0.347	0.357
11	0.3432499	.250	15.840	16.130	0.290	0.304	15.840	0.288	0.304
12	0.5929151	.437	15.830	16.221	0.391	0.416	15.830	0.391	0.411
13	0.574961	.438	15.836	16.230	0.394	0.420	15.844	0.394	0.410
14	0.381999	.083	15.908	16.240	0.332	0.341	15.908	0.332	0.341
15	0.5835668	.364	15.908	16.259	0.351	0.375	15.908	0.351	0.375
16	0.399234	.171	15.772	16.150	0.378	0.385	15.777	0.374	0.380
17	0.4288717	.214	15.796	16.184	0.388	0.392	15.816	0.378	0.382
18	0.3677382	.183	15.812	16.148	0.336	0.347	15.842	0.322	0.337
19	0.572293	.059	15.794	16.102	0.308	0.352	15.794	0.308	0.352
20	0.696932	.402	15.706	16.144	0.438	0.458	15.806	0.435	0.448
21	0.648800	.392	15.540	15.974	0.434	0.456	(15.700)	(0.428)	(0.446)
22	0.720222	.094	15.696	16.089	0.393	0.422	15.696	0.393	0.422
23	0.6327203	.544	15.809	16.226	0.417	0.435	15.809	0.417	0.435
24	0.369697	.189	15.794	16.136	0.342	0.350	15.849	0.327	0.340
25	0.665329	.298	15.827	16.265	0.438	0.450	15.827	0.438	0.450
26	0.4022426	.290	15.876	16.255	0.379	0.384	15.876	0.379	0.384
29	0.5749961	.189	15.890	16.283	0.393	0.410	15.890	0.393	0.410
30	0.405976	.261	15.802	16.167	0.365	0.367	15.807	0.361	0.362
31	0.4081781*	.058	15.837	16.215	0.378	0.381	15.837	0.378	0.381
32	0.605400	.532	15.688	16.046	0.358	0.386	15.728	0.358	0.376
35	0.383997	.309	15.870	16.216	0.346	0.354	15.875	0.343	0.349
36	0.6241230	.113	15.722	16.105	0.383	0.406	15.812	0.381	0.396
38	0.375274	.246	15.820	16.144	0.324	0.332	15.837	0.316	0.322
39	0.389568	.031	15.826	16.207	0.381	0.385	15.856	0.367	0.375
40	0.3773212	.213	15.850	16.178	0.328	0.336	15.850	0.327	0.336
41	0.391743	.097	15.660	16.032	0.372	0.378	15.780	0.357	0.368
42	0.3601746	.235	15.902	16.219	0.317	0.327	15.902	0.317	0.327
43	0.396009	.147	15.881	16.205	0.324	0.332	15.881	0.324	0.332
44	0.5956433	.233	15.693	16.080	0.387	0.406	15.773	0.386	0.396
46	0.691484	.535	15.590	15.988	0.398	0.424	(15.760)	(0.391)	(0.414)
48	0.364972	.294	15.802	16.128	0.326	0.338	15.810	0.321	0.333
49	0.655202	.587	15.207	15.461	0.254	0.270	–	–	–
50	0.2980583*	.103	15.922	16.188	0.266	0.275	15.922	0.266	0.275
51	0.396987	.062	15.763	16.125	0.362	0.368	15.863	0.347	0.358
52	0.575651	.054	15.910	16.312	0.402	0.433	15.910	0.402	0.433
53	0.4141614	.066	15.770	16.126	0.356	0.365	15.788	0.348	0.355
54	0.3995683*	.186	15.721	16.077	0.356	0.360	15.826	0.341	0.350
55	0.748590	.343	15.700	16.174	0.474	0.483	(15.850)	(0.468)	(0.473)
56	0.570353	.128	15.510	15.870	0.360	–	(15.740)	(0.352)	–
57	0.3496144	.302	15.708	16.062	0.354	0.359	(15.798)	(0.339)	(0.349)
58	0.407669	.077	15.654	16.029	0.375	0.379	(15.894)	(0.360)	(0.369)
61	0.400065*	.200	15.683	16.065	0.382	0.392	(15.823)	(0.367)	(0.382)
62	0.377318	.029	15.631	16.007	0.376	0.384	(15.761)	(0.361)	(0.374)
64	0.364191	.161	15.601	15.933	0.332	0.345	(15.861)	(0.317)	(0.335)
65	0.718199	.579	15.727	16.170	0.443	0.450	15.777	0.443	0.440
66	0.3793547	.226	15.845	16.195	0.350	0.355	15.873	0.337	0.345
67	0.404613*	.450	15.809	16.194	0.385	0.388	15.929	0.370	0.378
74	0.2960076	.211	15.858	16.127	0.269	0.279	15.948	0.254	0.269
97	0.696342	.132	15.710	16.158	0.448	0.460	15.800	0.446	0.450
102	0.759477*	.714	15.698	16.172	0.474	0.477	15.818	0.469	0.467

*Adopted periods and epochs are different from SKS

Table 7. Comments on M15 variables.

V	Comment
15	Irregular light curve
16	Close companion
17	Double-mode
21	Irregular light curve
23	Irregular light curve
26	Double-mode
30	Double-mode
31	Double-mode
32	Faint companion
33	R = 51", bad scatter in SKS observations, not used
39	Double-mode
41	Double-mode
44	Irregular light curve
49	Measures of unresolved double star
51	Double-mode
53	Double-mode
54	Double-mode
55	Bologna B bad scatter, not used
57	Faint companion. Period uncertain
58	Double-mode
61	Double-mode. Close companion
62	Close companions
64	Irregular light curve
67	Double-mode = SKS III-5
74	= SKS IV-41
96	Double mode
97	= SKS II-26
102	= SKS I-24. New period determined.

means, $\langle V\rangle$ and $\langle B\rangle$. The $\langle B\rangle$–$\langle V\rangle$ colour is the difference between $\langle B\rangle$ and $\langle V\rangle$. In addition, for each variable a colour curve was defined by the difference between the smoothed *B* and *V* light curves and a mean $\langle B-V\rangle$ colour derived from the mean intensity of the colour curve. The amplitudes in *B* and *V* were also obtained from the smooth light curves. The measurements of SKS were re-reduced in the same way. We used the observations from SKS Tables 1 and 2 which give individual *B* and *V* magnitudes, with Julian dates, from their Mount Wilson plates. The values obtained are given in Table 5 for our Bologna data and Table 6 for our treatment of the SKS Mount Wilson observations.

2.4 RADIAL CORRECTIONS AND FINAL LIGHT CURVE PARAMETERS

The positions of variables measured are shown in Fig. 3; the *x, y* coordinates are given in SH. Although no measurements were made in the central region of the cluster, plots of $\langle V\rangle$ or $\langle B\rangle$ against radial distance from the cluster centre still show a systematic increase in brightness at smaller radial distances. This is attributed to contamination from cluster background light. The effect is qualitatively similar in the data from the Mount Wilson, Loiano and Asiago plates. SKS made corrections for contamination in $\langle V\rangle$ and in $\langle B\rangle-\langle V\rangle$ depending on distance from the cluster centre, with all the variables grouped together. In the present work this method of correction has been improved by grouping the variable stars by RR Lyrae type *ab* or *c*. This is felt to be a more correct procedure because of the intrinsic differences between the mean magnitudes and colours of the different types, of about 0.06 mag. Furthermore the background effect depends on magnitude and the magnitude range of the two types is different.

Our $\langle V\rangle$ corrections are shown in Fig. 4(a) for Bologna data and in Fig. 4(e) for Mount Wilson data separately. The same zero points at large cluster distances were taken for both series, $\langle V\rangle=15.79$ for RR*ab* and $\langle V\rangle=15.85$ for RR*c*. The mean correction lines were drawn taking into account the non-uniform distribution of number of variables with period,

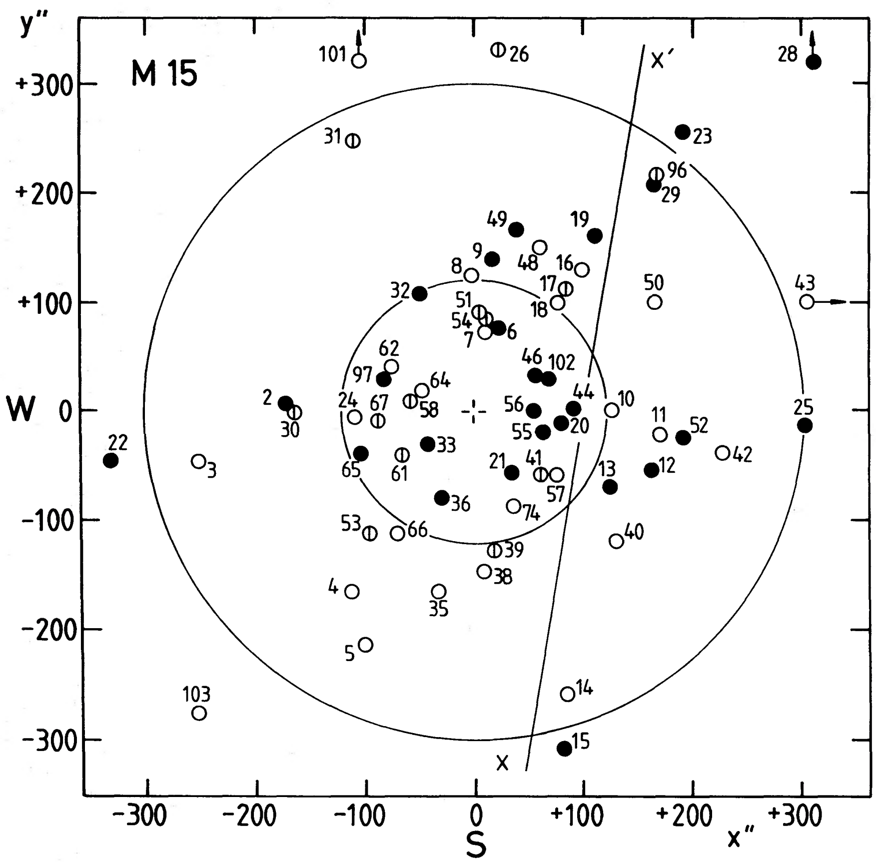

Figure 3. *X, Y* plot showing the positions of the RR Lyrae variables measured. The coordinates are taken from Sawyer-Hogg (1973). As in all relevant subsequent figures, the *c*-type variables are plotted as open circles or open circles with bar (multimode behaviour), *ab*-types as filled circles. The large circles enclose a region ($2 < r < 5$ arcmin) similar to that measured by Buonanno *et al.* for the colour–magnitude diagram (see 3.1.1). Variables east of the line XX′ tend to be fainter than average, and have shorter periods. This is thought to be due to chance.

and therefore with magnitude, and the fact that there is a positional effect east to west of the cluster with a fainter group on the east of the cluster having shorter periods. (These effects can be seen in the period-luminosity plot of Fig. 18.) The two series of data were corrected separately, the results of which are given in Tables 5 and 6. Fig. 5 shows that there is no resultant radial effect between corrected $\langle V \rangle$ magnitudes of each data set. Final $\langle V \rangle$ magnitudes were obtained by combining the corrected magnitudes with weighting factors assigned according to the quality of the light curves. The latter was assessed by the distribution in phase of the points and their scatter. In general the SKS light curves show similar scatter in V and B which is similar to the Bologna V light curves; the Bologna B light curves show increased scatter. The resulting mean $\langle V \rangle$ magnitudes are given in Table 8.

In order to correct their measured $\langle B \rangle - \langle V \rangle$ colours for contamination depending on distance from the cluster centre, SKS used a plot of colour against radius. However, the distribution of stars with colour depends on their distribution with period. The *ab*-types and *c*-types occupy different colour ranges; also they are distributed differently with radius, there being more *ab*-types at smaller radii. Therefore for our colour corrections as a function of radius we again treat *ab*- and *c*-types separately and use instead of $\langle B \rangle - \langle V \rangle$ itself, a colour residual $\Delta(B-V)$ derived from plots of log period against colour. The two colour indices $\langle B \rangle - \langle V \rangle$ and $\langle B-V \rangle$ have been corrected separately using corrections determined

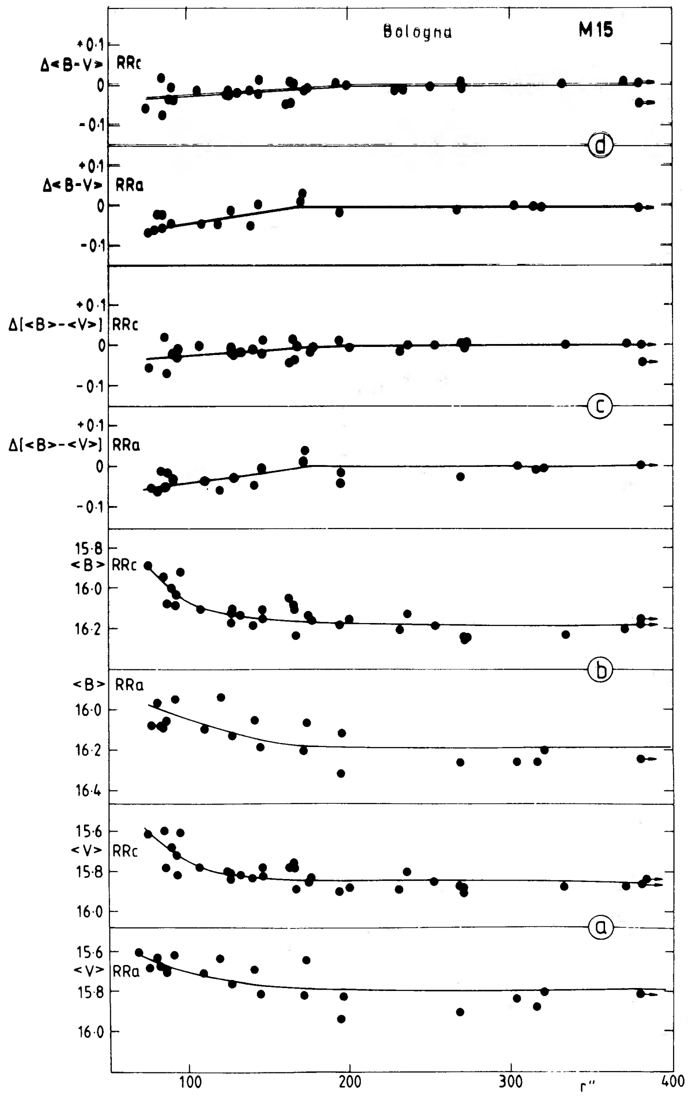

Figure 4. Adopted radial correction curves for Bologna data (a–d) and Mount Wilson data (e–h) in $\langle V\rangle$, $\langle B\rangle$, $\langle B\rangle-\langle V\rangle$ and $\langle B-V\rangle$. $\Delta[\langle B\rangle-\langle V\rangle]$ and $\Delta[\langle B-V\rangle]$ are colour residuals measured from their respective mean period–colour relations (see Fig. 6 and text); *ab*- and *c*-type variables are treated separately throughout. Corrections read from the mean lines shown are applied to the observed values of $\langle V\rangle$, $\langle B\rangle-\langle V\rangle$ and $\langle B-V\rangle$ to produce the corrected values, $\langle V\rangle_c$, $[\langle B\rangle-\langle V\rangle]_c$ and $\langle B-V\rangle_c$ given in Tables 5 (B) and 6 (SKS).

from $\Delta(B-V)$ as a function of radius. $\Delta(B-V)$ is measured from the mean relationships drawn in Fig. 6 of $\log P'$ against corrected $\langle B\rangle-\langle V\rangle$ or $\langle B-V\rangle$. We use $\log P'$ as defined by van Albada & Baker (1971)

$$\log P' = \log P + 0.336\,(\langle V\rangle_{\rm corr.} - \langle\bar{V}\rangle) \tag{1}$$

with $\langle\bar{V}\rangle = 15.833$, the average value of $\langle V\rangle_{\rm corr}$ for all variables (*ab*- and *c*-types). The use of $\log P'$ takes account of magnitude differences between the variables and reduces the scatter in the diagrams. The mean relationships were defined by lines of fixed (theoretical) slope = 1.35 fitted to observations at larger radial distances, $r > 160$ arcsec. The slope of 1.35 was derived as follows. From the pulsation equation (van Albada & Baker 1971)

$$\log P = -1.772 - 0.68\log(M/M_\odot) + 0.84\log(L/L_\odot) + 3.48\log(6500/T_e) \tag{2}$$

Since $\log L \sim -0.4\,V$ and $\log T_e = 3.929 - 0.388\,(B-V)$ for the RR Lyrae colour range and

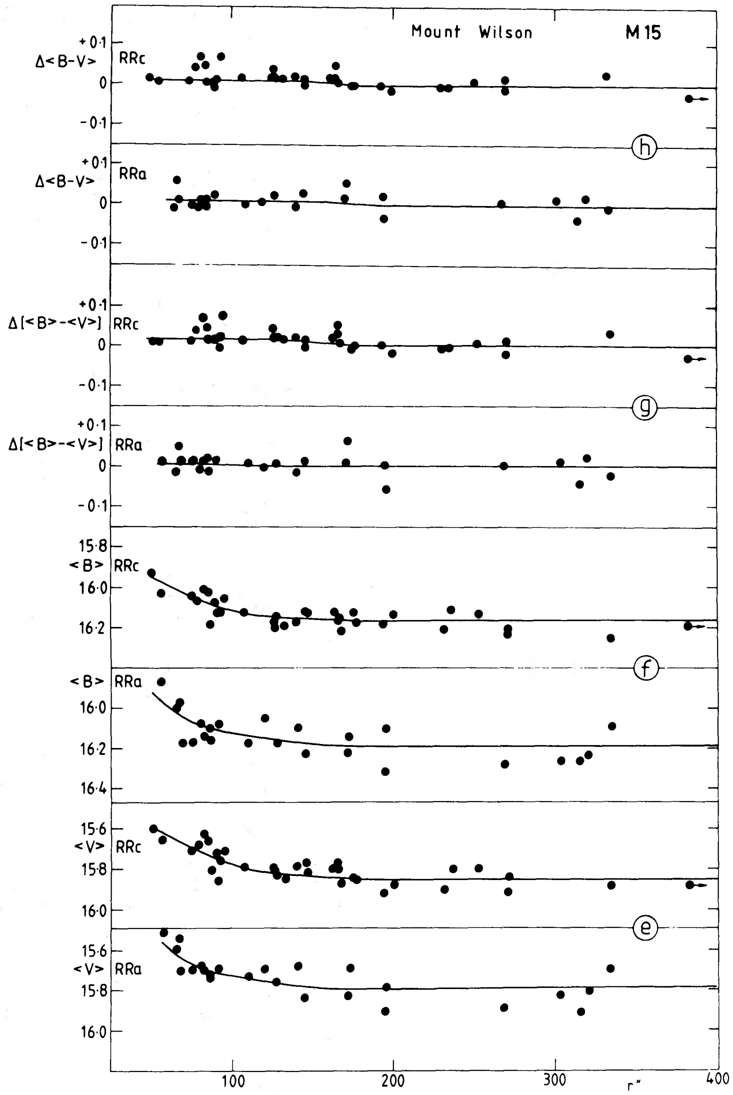

Figure 4 – *continued*

[Fe/H] = – 2.0 (using the colour–temperature relation in BDE from Bell models 1977, unpublished) we obtain

$$\log P + 0.336\ V = 1.35\ (B-V) - 0.68 \log M/M_\odot + \text{constant}. \qquad (3)$$

The lines were drawn with very slight bias to minimize as well as possible any systematic difference between Mount Wilson and Bologna. A residual difference of 0.005 mag remains, Mount Wilson being the redder. The colour residuals $\Delta(B-V)$ are plotted against distance

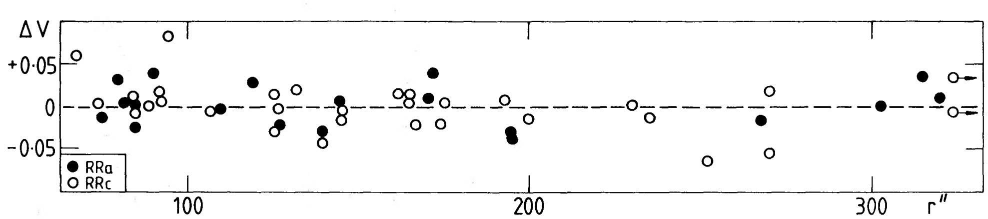

Figure 5. A comparison of the corrected $\langle V\rangle$ magnitudes between the two data sets, as a function of radius. $\Delta\langle V\rangle$ is defined as $\langle V\rangle_c$ Mount Wilson – $\langle V\rangle_c$ Bologna and shows no residual variation with radius.

Table 8. M15 RR Lyrae light curve parameters resulting from the combined observations from Bologna and SKS, corrected for background contamination depending on distance from cluster centre.

Var.	Type	P day	log P	log P'	<V>	<B>-<V>	<B-V>	A_B	A_V	r sec	pg.	$(B-V)_{eq}$	log Te_{eq}
2	ab	.6843	-.165	-.219	15.671	.440	.447	0.76	0.55	172	1	.445	3.812
3	c	.3887	-.410	-.412	15.827	.335	.346	0.61	0.45	252	1	.342	3.851
4	c	.3136	-.504	-.487	15.882	.266	.275	0.76	0.62	199	1	.272	3.875
5	c	.3842	-.415	-.425	15.804	.318	.323	0.60	0.50	235	1	.321	3.858
6	ab	.6660	-.177	-.194	15.781	.391	.410	1.12	0.77	80	2	.404	3.828
7	c	.3676	-.435	-.422	15.872	.312	.334	0.69	0.47	74	2	.327	3.856
8	ab	.6462	-.190	-.203	15.793	.409	.429	1.09	0.78	127	1	.422	3.821
9	ab	.7153	-.146	-.187	15.710	.397	.405	0.90	0.66	140	1	.402	3.829
10	c	.3864	-.413	-.401	15.868	.347	.353	0.58	0.45	126	1	.351	3.848
11	c	.3432	-.464	-.459	15.849	.286	.302	0.72	0.58	174	1	.297	3.867
12	ab	.5929	-.227	-.230	15.825	.389	.409	1.08	0.75	171	1	.402	3.829
13	ab	.5749	-.240	-.238	15.841	.391	.410	1.20	0.89	144	1	.404	3.828
14	c	.3820	-.418	-.396	15.898	.338	.346	0.63	0.56	270	1	.343	3.850
15	ab	.5835	-.234	-.215	15.890	.366	.388	1.05	0.79	315	1	.381	3.837
16	c	.3992	-.399	-.418	15.775	.361	.368	0.56	0.38	165	2	.366	3.842
17	c	.4289	-.368	-.367	15.836	.375	.379	0.43	0.33	139	1	.378	3.838
18	c	.3677	-.434	-.431	15.842	.318	.330	0.70	0.49	127	1	.326	3.856
19	ab	.5723	-.242	-.250	15.811	.316	.358	1.54	1.09	195	1	.344	3.850
20	ab	.6969	-.157	-.167	15.804	.444	.460	0.95	0.72	82	2	.455	3.809
21	ab	.6488	-.188	-.233	15.700	.428	.446	1.04	0.75	67	3	(.440)	(3.814)
22	ab	.7202	-.143	-.189	15.696	.393	.422	1.19	0.86	334	1	.412	3.825
23	ab	.6327	-.199	-.209	15.804	.411	.427	0.98	0.65	320	1	.422	3.821
24	c	.3697	-.432	-.426	15.851	.331	.339	0.62	0.48	107	2	.336	3.853
25	ab	.6653	-.177	-.179	15.827	.433	.446	1.00	0.67	303	1	.442	3.814
26	c	.4023	-.395	-.380	15.878	.367	.371	0.48	0.39	333	1	.370	3.841
28	ab	.6706	-.174	-.177	15.824	.421	.432	0.93	0.75	617	1	.428	3.819
29	ab	.5750	-.240	-.219	15.896	.383	.404	1.08	0.79	268	1	.397	3.831
30	c	.4060	-.391	-.403	15.800	.333	.345	0.40	0.35	165	1	.341	3.851
31	c	.4082	-.389	-.379	15.863	.372	.374	0.46	0.33	270	1	.373	3.840
32	ab	.6054	-.218	-.257	15.716	.350	.371	1.22	0.86	119	2	.364	3.843
35	c	.3840	-.416	-.398	15.885	.347	.356	0.60	0.45	167	1	.353	3.847
36	ab	.6241	-.205	-.212	15.811	.395	.411	1.02	0.73	86	2	.406	3.828
38	c	.3753	-.426	-.424	15.838	.328	.339	0.65	0.49	146	1	.335	3.853
39	c	.3896	-.409	-.405	15.847	.353	.359	0.52	0.37	126	1	.357	3.845
40	c	.3773	-.423	-.418	15.848	.325	.334	0.67	0.53	176	1	.331	3.855
41	c	.3917	-.407	-.427	15.774	.364	.372	0.55	0.44	84	2	.369	3.841
42	c	.3602	-.443	-.421	15.901	.311	.322	0.72	0.55	230	1	.318	3.859
43	c	.3960	-.402	-.392	15.864	.319	.322	0.64	0.50	430	1	.321	3.858
44	ab	.5956	-.225	-.252	15.754	.381	.392	0.98	0.63	91	2	.388	3.834
46	ab	.6915	-.160	-.185	15.760	.391	.414	1.20	0.81	65	3	(.406)	(3.828)
48	c	.3650	-.438	-.448	15.802	.302	.314	0.72	0.52	162	1	.310	3.862
50	c	.2981	-.526	-.497	15.918	.270	.279	0.67	0.51	193	1	.276	3.874
51	c	.3970	-.401	-.394	15.854	.344	.352	0.52	0.39	92	2	.349	3.848
52	ab	.5756	-.240	-.210	15.922	.396	.433	1.25	0.89	194	1	.421	3.822
53	c	.4141	-.383	-.396	15.795	.342	.350	0.52	0.37	145	1	.347	3.849
54	c	.3996	-.398	-.401	15.825	.341	.346	0.54	0.39	89	2	.344	3.850
55	ab	.7486	-.126	-.127	15.830	.468	.473	0.62	0.48	68	3	(.471)	(3.803)
56	ab	.5704	-.244	-.275	15.740	.352	–	0.90	0.75	57	3	(.352)	(3.847)
57	c	.3493	-.457	-.482	15.757	.340	.346	0.57	0.46	94	3	(.344)	(3.850)
58	c	.4077	-.390	-.369	15.894	.360	.369	0.60	0.40	56	3	(.366)	(3.842)
61	c	.4001	-.398	-.401	15.823	.367	.382	0.65	0.53	78	3	(.377)	(3.838)
62	c	.3773	-.423	-.448	15.761	.361	.374	0.66	0.49	82	3	(.370)	(3.841)
64	c	.3642	-.439	-.429	15.861	.317	.335	0.74	0.46	50	3	(.329)	(3.855)
65	ab	.7182	-.144	-.163	15.777	.440	.440	0.60	0.45	109	2	.440	3.814
66	c	.3794	-.421	-.411	15.863	.335	.341	0.56	0.41	132	1	.339	3.852
67	c	.4046	-.393	-.359	15.933	.354	.359	0.40	0.32	86	2	.357	3.845
74	c	.2960	-.529	-.491	15.945	.269	.280	0.74	0.62	93	2	.276	3.874
96	c	.3964	-.402	-.377	15.907	.351	.360	0.62	0.38	271	1	.357	3.845
97	ab	.6963	-.157	-.164	15.812	.440	.448	0.80	0.57	85	2	.445	3.812
101	c	.4003	-.398	-.397	15.836	.345	.356	0.70	0.50	550	1	.352	3.847
102	ab	.7595	-.119	-.122	15.824	.465	.466	0.40	0.26	76	2	.466	3.805
103	c	.3682	-.434	-.422	15.867	.331	.341	0.73	0.51	371	1	.338	3.852

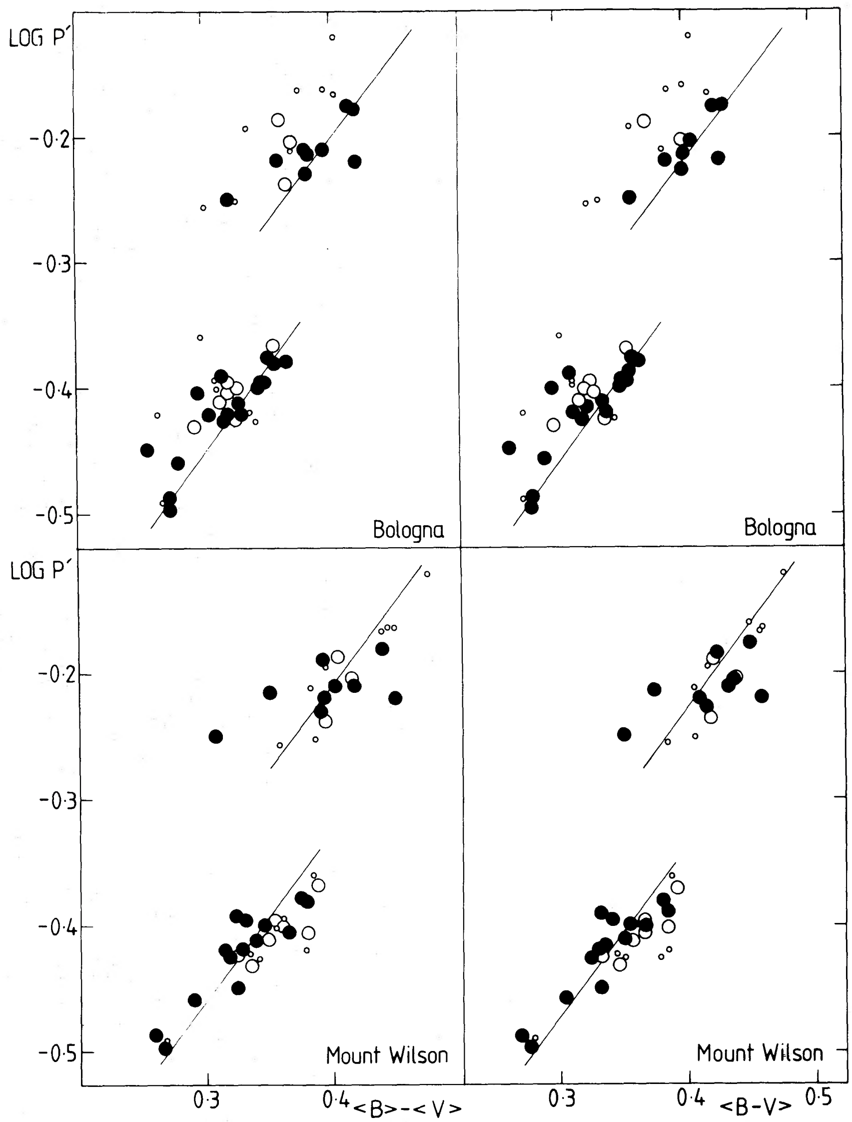

Figure 6. Period–colour relations for the uncorrected colours $\langle B\rangle - \langle V\rangle$ and $\langle B-V\rangle$ for Bologna and Mount Wilson data separately. Log $P' = \log P + 0.336\ (\langle V\rangle - \langle \bar{V}\rangle)$ is used to allow for the small luminosity differences amongst the variables. The fiducial lines are based only on variables for which there is essentially no radial correction to V and B, i.e. those with $r > 160$ arcsec represented by filled circles, and are used to derive the colour residuals plotted in Fig. 4 (c), (d), (g) and (h). Larger symbols are of higher weight.

from the cluster centre in Figs 4(c), (d), (g) and (h) and smooth correction lines drawn. These adopted colour corrections with radius were applied to the Mount Wilson and Bologna $\langle B\rangle - \langle V\rangle$ and $\langle B-V\rangle$ colour observations, as appropriate. These corrected colours are given in Tables 5 and 6. The final combined $\langle B\rangle - \langle V\rangle$ and $\langle B-V\rangle$ colour data were obtained from the Mount Wilson and Bologna corrected colours, by weighting the data according to the quality of the light and colour curves, and the resulting mean values are given in Table 8. The final $\langle B\rangle$ magnitudes given in Table 8 are obtained from $\langle B\rangle = \langle V\rangle + (\langle B\rangle - \langle V\rangle)$. Figs 4(b) and (f) show that a satisfactory fit is obtained to the uncorrected B observations with a smooth correction line derived from the combined radial corrections used for $\langle V\rangle$ and for $\langle B\rangle - \langle V\rangle$.

2.5 ANALYSIS OF PHOTOMETRIC ERRORS IN THE FINAL COMBINED DATA

We have compared photographic measures from each series of observations with photoelectric measures to test for any colour effect between the systems. The comparison, plotted in Figs 1(a), (b) and (c), show that in the range of RR Lyrae colour variation, any effect is small and not well enough determined to enable corrections to be applied (there are too few blue photoelectric standards). However, Fig. 1(d) suggests there may be a systematic colour difference in the colour range of the RR Lyraes of about 0.02 mag, Mount Wilson being the redder. Such a difference can indeed be seen in Fig. 7 which shows the differences between cor-

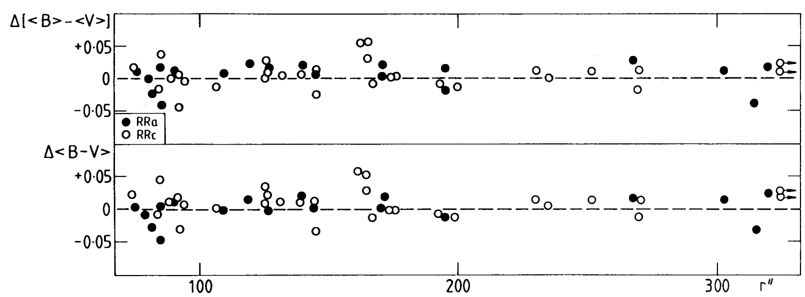

Figure 7. A comparison of the residual corrected colours, $\Delta[(\langle B\rangle - \langle V\rangle)_c]_{SKS-B}$ and $\Delta[\langle B-V\rangle_c]_{SKS-B}$ between Mount Wilson (SKS) and Bologna (b) data as a function of radius. There is a small systematic difference of 0.01 to 0.02 mag between the two sets, whose possible origin is discussed in the text and illustrated in subsequent figures.

rected Mount Wilson $\langle B\rangle-\langle V\rangle$ and $\langle B-V\rangle$ colours and corrected Bologna colours against cluster radius; on average Mount Wilson colours are about 0.02 mag redder. We have investigated whether these differences depend on position on the plate. Figs. 8(a) and 8(b) show on average a difference across the cluster in the north–south direction ~ 0.035 mag. This effect may also be present in the photographic photometry of non-variable blue horizontal branch stars, as shown in Fig. 8(c). A north–south difference of ~ 0.03 mag is not inconsistent with the residuals shown there. This positional effect could perhaps be caused by different photographic effects in the two plate series and related to distance from the photoelectric sequence which is offset north of the cluster. To see if there is any evidence for this we have examined the residuals in the individual data sets. Although now more marginal, we find that the effect appears partly in the Mount Wilson data and partly in the Bologna data in the opposite sense. In Fig. 9 we plot x, y positions of the colour residuals from the log P' against $\langle B\rangle-\langle V\rangle$ relationship drawn in Figs. 12(f), (g) (see next section) for the Mount Wilson and Bologna data separately. We see an average north–south effect across the plate of ~ + 0.01 mag in the Mount Wilson data and ~ − 0.02 mag in the Bologna data, resulting in a differential effect north–south, Mount Wilson–Bologna, of + 0.03 mag. We have further investigated whether the effect may arise in $\langle V\rangle$ or in $\langle B\rangle$, and show the $\langle V\rangle$ differences on an x, y plot in Fig. 10(a) and $\langle B\rangle$ differences in Fig. 10(b). These show an average difference in $\langle V\rangle$ north–south (Mount Wilson–Bologna) ~ − 0.03 mag and no difference in $\langle B\rangle$. This effect in $\langle V\rangle$ is consistent with the observed effect in $\langle B\rangle-\langle V\rangle$ and could well be the cause of it. The observations are consistent with there being no effect in $\langle B\rangle$ although the errors are larger. This analysis has indicated that there are small differences, depending on position between corrected $\langle V\rangle$ and $\langle B\rangle-\langle V\rangle$ obtained separately from the Mount Wilson and Bologna data. The effects are probably in opposite senses and can plausibly, but not conclusively be understood in terms of small plate errors over the field. In the combined data, Table 8, the net systematic error should be less than in either individual series. This is con-

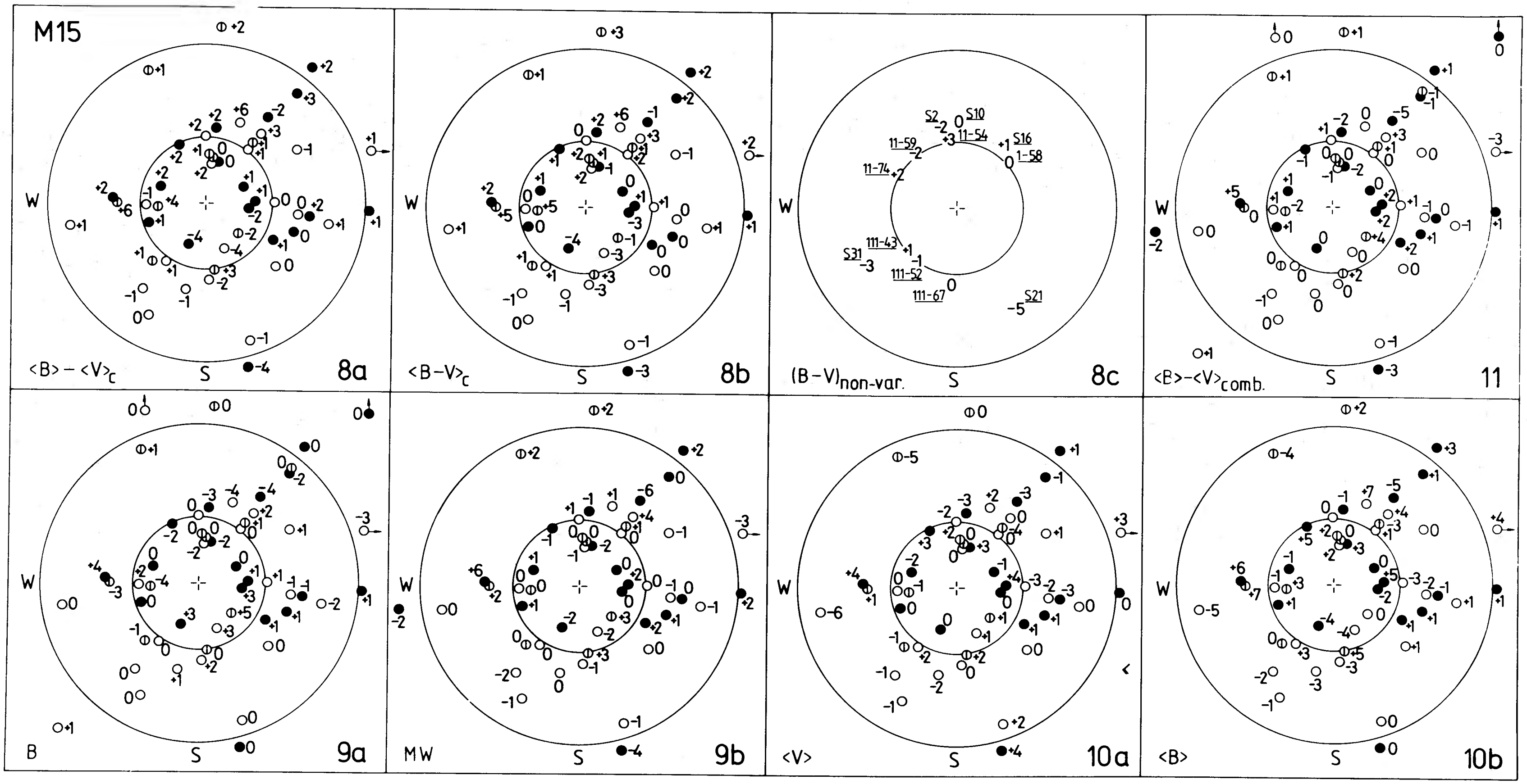

Figure 8. X, Y plots of the differences between corrected colours as defined in the caption to Fig. 7 for variable stars (8a, 8b) and for the non-variables in the same magnitude range measured in the same programme (8c). $\langle B-V \rangle$ is treated in the same way as $\langle B \rangle - \langle V \rangle$. There appears to be a systematic north–south effect ~ 0.03 mag, most noticeable for the variables but also present amongst the non-variables.

Figure 9. X, Y plots of the colour residuals $\Delta\{(\langle B \rangle - \langle V \rangle)_c\} \log P'$ obtained from the corrected period–colour relations for Bologna data (9a) and Mount Wilson data (9b). The north–south effect shown in Fig. 8 appears to arise partly from Bologna data (~ -0.02 mag) and partly from Mount Wilson data ($\sim +0.01$).

Figure 10. X, Y plots of the magnitude differences $\{\langle V \rangle_c\}_{SKS} - \{\langle V \rangle_c\}_B$ (10a) and $\{\langle B \rangle_c\}_{SKS} - \{\langle B \rangle_c\}_B$ (10b). A north–south effect ~ 0.03 mag in $\langle V \rangle_c$ can be seen, which is thought to be the cause of the north–south colour effect shown in Fig. 8.

Figure 11. X, Y plot of the colour residuals $\Delta\{(\langle B \rangle - \langle V \rangle)_{cc}\} \log P'$ from the period–colour relation of Fig. 12(h), using the final corrected and combined data from Table 8. No residual positional effects are now apparent.

firmed by Fig. 11, which is an x, y plot of the colour residuals from the log P' against final, combined $\langle B \rangle - \langle V \rangle$ plot (Fig. 12h). In summary, there appear to be small systematic calibration differences in $\langle V \rangle$ possibly combined with a small colour equation in SKS (Figs. 1c and d) which together give rise to the described effects and which tend to cancel out in the combined data.

The radial corrections in the preceding section took into account a small magnitude effect among the variables relating to plate position, with variables on the east of the cluster appearing fainter. This effect appears to be due to chance rather than to differential absorption because the periods are also affected. (See Fig. 18a.)

In Table 8, we assign a photometric quality (pg.) depending on cluster radius and on proximity of companion stars: quality 1 if $r > 120$ arcsec, quality 2 if $70 < r < 120$ arcsec, with these classifications downgraded if there is a close companion, and quality 3 if $r < 70$ arcsec. In the figures, the data of quality 1 and 2 are plotted with large and small symbols respectively and data of quality 3 are not plotted.

2.6 THE PERIOD–COLOUR RELATION AT VARIOUS STAGES IN THE REDUCTIONS

The period–colour relation is a fundamental tool for studying the properties of RR Lyraes in a globular cluster. Since one of the major aims of this investigation is to derive the best

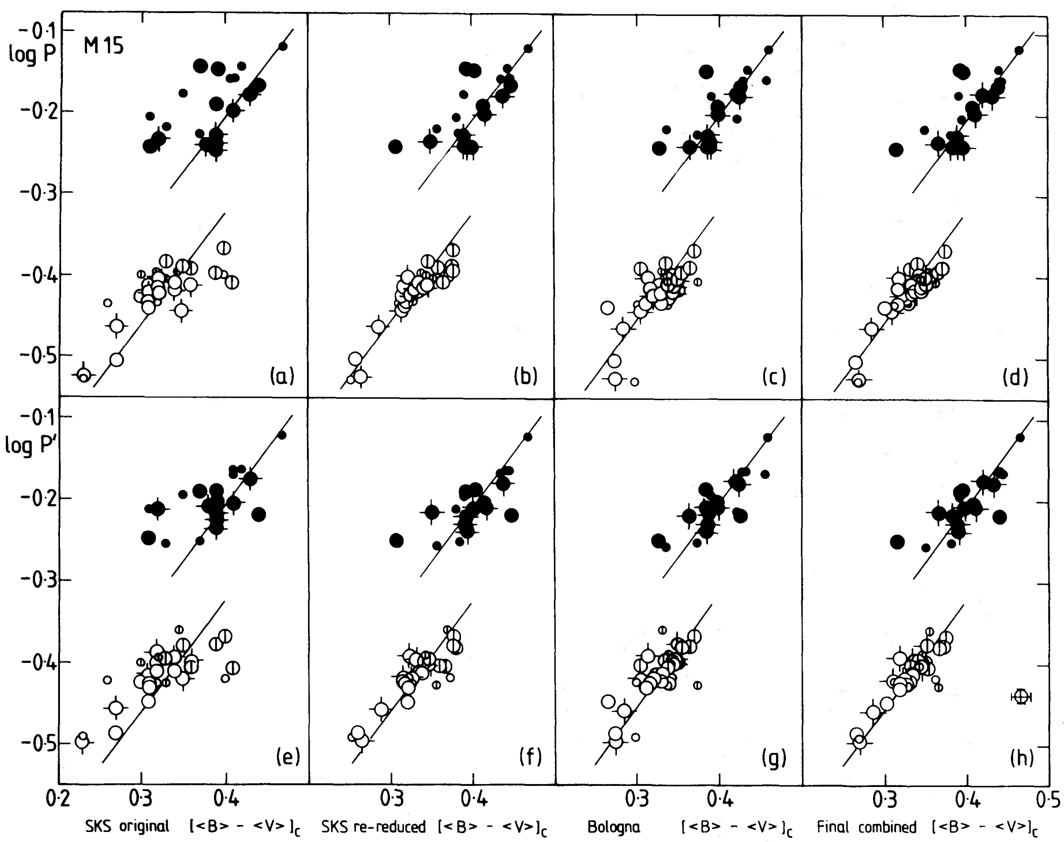

Figure 12. Period–colour relations at various stages in the reduction of the data. The variables lying east of the line XX′ in Fig. 3 are marked with ticks. In the top panels $\langle B \rangle - \langle V \rangle$ is plotted against log P, and in the lower panels against log P' to take account of the luminosity spread amongst the variables. The final radially corrected and combined data are plotted in panels (d) and (h). Note how the ab/c colour overlap is reduced, and that the multimode variables (open circles with bar) occupy a quite narrow colour range near the ab/c colour boundary. The (ticked) eastern variables also no longer appear anomalous (e.g. as in Figs. 12a, b). Representative error bars are indicated for higher weight observations, in Fig. 12(h).

possible relation it is of interest to see how it evolves through the various stages of reductions described earlier. Fig. 12 illustrates this development. The upper diagrams show plots of $\langle B \rangle - \langle V \rangle$ against $\log P$ and the lower ones use $\log P' = \log P + 0.336\ (\langle V \rangle - \langle \bar{V} \rangle)$. In all diagrams radial corrections to the colours have been applied. Fig. 12(a) shows the original SKS published data. Two obvious errors for V12 and V13 have been corrected, and variables V57, V61, V62 and variables within a cluster radius of 70 arcsec omitted because of excessive crowding. There is considerable scatter within both *ab*- and *c*- types, and considerable overlap in colour between them. The double-mode variables extend over a wide range in colour, an unexpected result in view of their extremely small range in period. In Fig. 12(b), we have taken the original measures published by SKS and completely re-reduced them, as discussed in the previous section. There is a significant change, with less scatter (particularly amongst the *c*-types), slightly less colour overlap and with the double-mode variables less spread out in colour. Fig. 12(c) shows the Bologna results similar to Fig. 12(b) except the *c*-types have a little more scatter. Fig. 12(d) shows the combined, final data. The relation is now better defined than in the first published data of Fig. 12(a) with just three or four *ab*-types standing off an otherwise tight correlation. A luminosity spread amongst the variables can be taken into account with the use of $\log P'$, which is used for plotting the diagrams below. The effect referred to earlier (see Section 2.4) that there are more faint *ab*-types on the eastern side of the cluster can be seen in all the upper diagrams, those variables lying east of XX′ in Fig. 3 being marked with ticks. The use of $\log P'$ removes the systematic bias they produce in the $\log P/\langle B \rangle - \langle V \rangle$ diagrams. The final combined data illustrated in Fig. 12(h) show very well-defined correlations with rather small scatter, and not much overlap in colour. In fact the use of the different mean colour $\langle B-V \rangle$ reduces the overlap still further (Fig. 13) the observed amount of 0.02 mag possibly arising from observational errors alone.

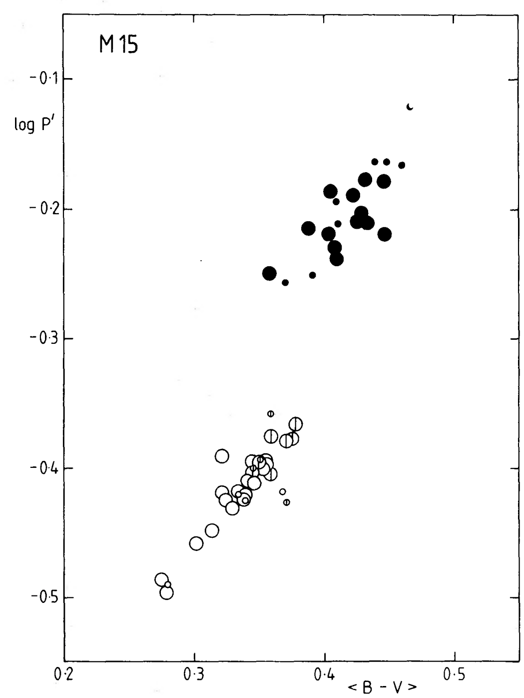

Figure 13. Period–colour relation using the colour index $\langle B-V \rangle$. Note how the overlap in colour is even further reduced from that in Fig. 12(h), mainly because the $\langle B-V \rangle$ colours of the larger amplitude *ab*-variables are significantly redder than $\langle B \rangle - \langle V \rangle$.

3 Analysis and discussion

3.1 CORRELATIONS BETWEEN LIGHT CURVE PARAMETERS

The parameters representing various properties of the light curves have been given in Table 8. In this section we shall confine ourselves to a presentation of the most interesting correlations. Comparison with other clusters and theory will be discussed later. Since our main aim here is to illustrate the observed properties, we shall use those quantities most well-determined from the observations, in particular the amplitude in blue light and the colour index ⟨*B*⟩–⟨*V*⟩ determined by differencing the separate intensity means of the *B* and *V* light curves. Later we shall need to consider how best to convert these parameters to those needed for comparison with theory.

3.1.1. *The colour–magnitude diagram*

Fig. 14 shows the positions of the RR Lyraes in the colour–magnitude diagram, together with non-variable horizontal branch (HB) stars taken from Sandage (1969, 1970) or measured in the RR Lyrae programme to assist in the delineation of the gap boundaries. The variable stars are plotted using ⟨*B*⟩ – ⟨*V*⟩ values from Table 8; the non-variable stars are plotted using either photoelectric measures by Sandage or photographic photometry from Sandage (1970), corrected for background contamination appropriate for RR Lyraes, and the values given in our Table 9. The bulk of the variables occupy a sloping region a little more than 0.1 mag deep and forming a continuous extension to the non-variable blue horizontal branch stars. There are a sprinkling of stars, mainly *ab*-type having ⟨*V*⟩ magnitudes a few hundredths brighter than average. These stars could well be in a slightly more advanced evolutionary state (to be discussed later). There is complete segregation of variable and non-variable stars at the blue edge of the instability strip, which is well defined at ⟨*B*⟩–⟨*V*⟩ = 0.255. There is also no overlap in colour at the red edge but the relative paucity of red horizontal branch stars and RR Lyraes and makes it difficult to define precisely the strip boundary here. Within the *ab*-types there is a tendency for the bluer variables to be fainter than average (excluding the probably more evolved stars). Only one *ab*-variable in our sample (V19) significantly

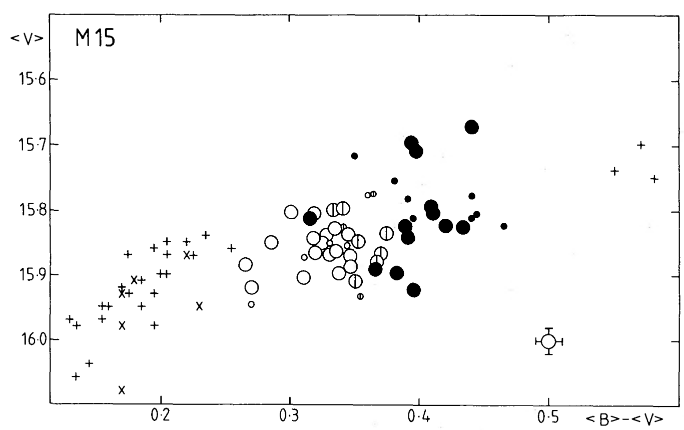

Figure 14. RR Lyrae variables in the colour–magnitude diagram. Non-variable stars, are also plotted, using photoelectric photometry from Sandage (1970) (crosses) and photographic photometry from Sandage (1970) corrected for background (+ signs). The bulk of the variables occupy a sloping region only about 0.1 mag in depth, with a sprinkling of brighter, probably more evolved stars. The blue edge of the instability region is clearly demarcated at ⟨*B*⟩ – ⟨*V*⟩ = 0.255, whereas the red edge is not well defined. Representative error bars are indicated.

Table 9. M15 photographic photometry of non-variable HB stars, corrected for background contamination (uncorrected data from Sandage 1970, table 8).

Star	r ″	V_{corr}	$B-V_{corr}$ *	Star	r ″	V_{corr}	$B-V_{corr}$ *
S2	162	15.87	0.175	II-54	139	15.85	0.22
S10	168	15.92	0.17	59	131	15.90	0.20
S16	150	15.97	0.13	73	116	15.93	0.175
I-4	86	15.98	0.195	74	120	15.98	0.135
7	88	15.74	0.55	III-15	89	15.97	0.155
9	88	16.04	0.145	28	97	15.75	0.58
11	104	15.95	0.155	43	120	15.86	0.195
51	103	15.86	0.255	52	124	15.85	0.205
54	115	15.90	0.205	67	140	15.95	0.16
58	124	15.91	0.185	IV- 2	93	15.93	0.195
II-11	79	15.95	0.185	44	109	15.84	0.235
23	94	15.87	0.205	66	86	16.06	0.135
24	90	15.70	0.57	68	90	15.87	0.225

* .005 arises from background correction

encroaches upon the territory occupied by the *c*-types, but it should be kept in mind that the use of $\langle B-V \rangle$ instead of $\langle B \rangle - \langle V \rangle$ would shift this star ~ 0.05 mag redwards. Thus there may be little real colour overlap in this sample. Note also that those *c*-types occurring closest to the transition colour are mostly (perhaps entirely) multimode variables, exhibiting a mixture of first harmonic and fundamental mode pulsation (Cox *et al.* 1983).

Fig. 15 shows a histogram of the distribution with colour over the whole HB using data for non-variables taken from Buonanno *et al.* (1983a). The RR Lyraes from the same region of study (between $r = 1.9$ arcmin and $r = 5.0$ arcmin) are shown hatched, using the present $\langle B \rangle - \langle V \rangle$ colours. The non-uniform distribution of stars is evident, the bulk of the stars lying to the blue of the instability strip. We shall return to a discussion of this distribution later.

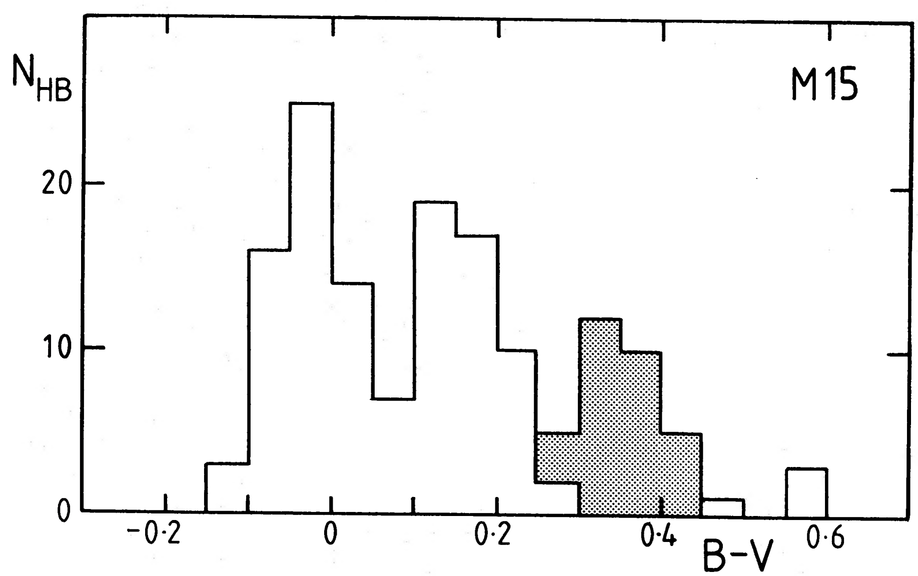

Figure 15. Histogram of the distribution with colour over the whole HB, using data for non-variables from Buonanno *et al.* and the present RR Lyrae photometry, both from the region ($1.9 < r < 5.0$ arcmin) (see Fig. 22). The RR Lyraes are represented by the shaded area. Note the distinctly non-uniform distribution along the HB.

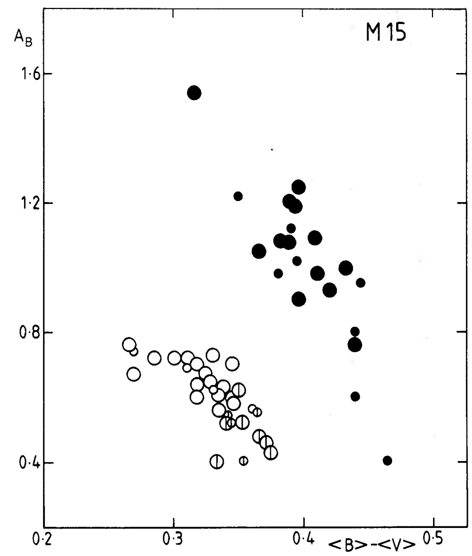

Figure 16. Correlation of amplitude in blue light, A_B, with $\langle B \rangle - \langle V \rangle$ colour. The strong decrease in amplitude with increasing colour shows that the *mean* amplitude depends sensitively on position within the instability strip. Note that the multimode variables have essentially the smallest amplitudes and are nearest to the transition point.

3.1.2 *The amplitude-colour relation*

Fig. 16 shows the correlation of blue amplitude, A_B, with mean colour. There is a strong dependence of amplitude on colour (and hence location within the instability strip in the colour–magnitude diagram) in both *ab*- and *c*-types, with amplitude decreasing with increasing colour. The correlation of amplitude with period within each type is now better defined than in the original SKS data (SKS Fig. 8a), the scatter within each sequence being attributable to observational error alone. The multimode variables have the smallest amplitudes amongst the *c*-types, as might be expected from their mixed-mode behaviour, and occur right at the transition edge. (The amplitude used is derived from the mean of the points plotted with the dominant first harmonic period.) It thus seems highly likely that the mixed-mode behaviour is closely related to the transition phenomenon. The distribution of amplitude with colour amongst the *ab*-types is rather non-uniform, with the largest amplitude variable (V19) out on its own. Although the temperature overlap may not be as large as implied by the $\langle B \rangle - \langle V \rangle$ colours (see below), the diagram indicates that the majority of stars belong to a family exhibiting a well-defined colour at which mode switching occurs, from *ab*-amplitude of 1.2 mag to *c*-amplitude of 0.4 mag (or vice versa), with V19 set apart for some reason, perhaps with some essential property causing it to prefer fundamental pulsation, with a consequently larger amplitude appropriate to its bluer colour.

3.1.3 *The period–amplitude relation*

The variation of amplitude, A_B, with log P is shown in Fig. 17(a). The *c*-types show a roughly constant amplitude at the shorter periods before decreasing to a minimum in the region occupied almost exclusively by the multimode variables. The *ab*-types, in the mean, show a steep decrease in amplitude with period although there is considerable scatter, with a large range of amplitude possible at a given period. The use of log P' (Fig. 17b) reduces the scatter in the *ab*-types although the brightest variable, V2, appears significantly discrepant

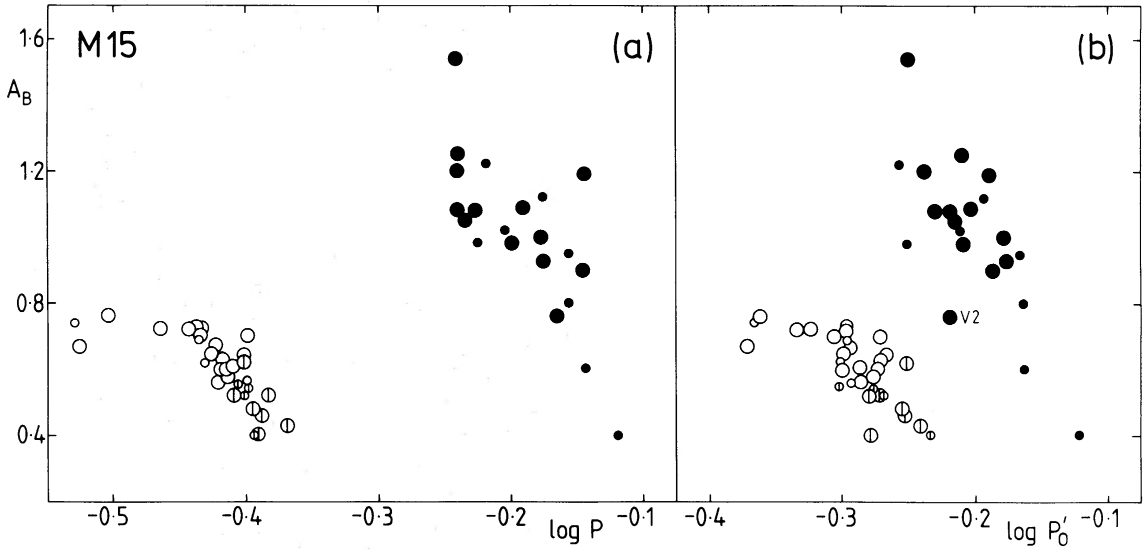

Figure 17. (a) Correlation of blue amplitude with log period. The *c*-types show a well-defined relation, with first constant and then sharply decreasing amplitude with increasing period but the *ab*-types show a large scatter in amplitude at a given period. The latter is somewhat reduced in (b), where the 'reduced' period P' is used, although the brightest variable, V2 now appears anomalous, perhaps due to its advanced evolutionary stage. Note that the fundamental period P_0 (given by $\log P_0 = \log P_1 + 0.125$ where P_1 is the first harmonic period) is used to better indicate the true contiguous transition between *c*- and *ab*- types at a well-defined fundamental period, $\log P_0' = -0.25$.

now. Note that in this diagram, we have 'fundamentalized' the *c*-types using the transformation $\log P_0' = \log P_1' + 0.125$ to illustrate better the sharply defined transition period.

3.1.4. *The period–luminosity relation*

The correlation of $\langle V \rangle$ with log P is shown in Fig. 18(a). Both types of variable exhibit a weak correlation, with the *ab*-types on average being slightly more luminous than the *c*-types. The variables marked with ticks lie east of the line XX′ in Fig. 3, showing the bias in

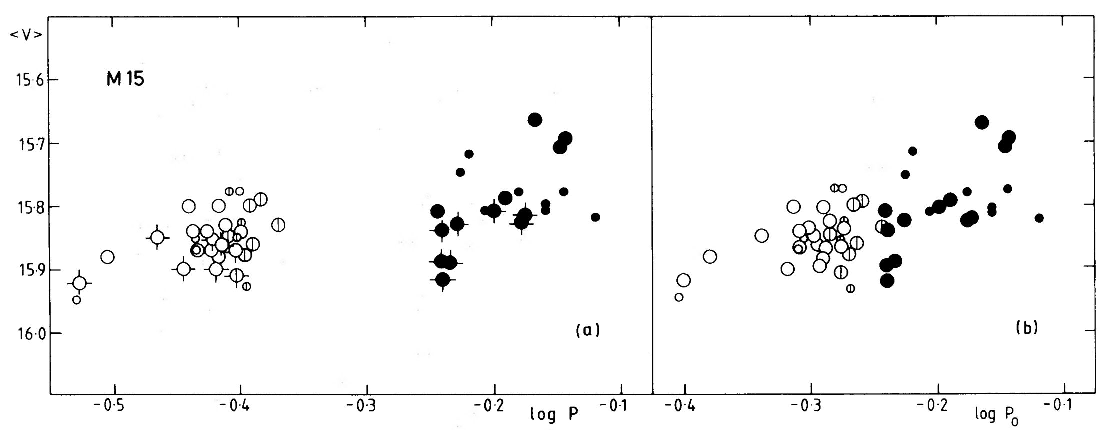

Figure 18. Period–luminosity relations. Panel (a) reveals the weak correlation of period with luminosity within each Bailey type. The variables east of the line XX′ (Fig. 3) are marked with ticks, and show the positional bias towards fainter magnitudes and shorter periods. Panel (b) uses the fundamentalized period to indicate the overall period-luminosity effect, which is important in the analysis of the period-colour diagram (see Fig. 19).

the distribution of periods and luminosities over the field. In Fig. 18(b), the *c*-types have been fundamentalized to illustrate better the overall period-luminosity dependence amongst all the variables.

3.1.5. *The period–colour relation*

The derivation of this relation has been discussed in the preceding section, leading to the plot of log P versus $\langle B\rangle - \langle V\rangle$ shown in panel (d) of Fig. 12. The main feature of the diagram, that of a well-defined sequence for each Bailey type, displaced in log P, is evident and forms the basis for the derivation of several physical parameters for the RR Lyraes. The shift of ~ 0.12 in log P is readily understood theoretically in terms of the different mode of pulsation of each type, as shown many years ago in the cluster M3 by Schwarzschild (1940). Before moving on to discuss the derivation of astrophysical parameters, we note that as in the period–amplitude diagram, the scatter in this diagram is somewhat reduced when allowance for the magnitude spread amongst the variables through the use of P' is made. This is illustrated in Fig. 12(h). However, the brightest variable, V2, is also discrepant in this diagram. The stars east of the line XX′ (Fig. 3) now mingle in with the others and no residual systematic affects are apparent. Note how the colour overlap is reduced when $\langle B-V\rangle$ rather than $\langle B\rangle - \langle V\rangle$ is used as abcissa, as illustrated in Fig. 13.

3.2 DERIVATION OF PHYSICAL PARAMETERS

The derivation of physical parameters, and the comparison with other cluster RR Lyraes and theory, requires various transformations to the observations to give astrophysically relevant quantities. The main requirements may be simply illustrated using linear pulsation theory as follows. The periods of fundamental and first harmonic pulsators may be accurately calculated using appropriate stellar models. From van Albada & Baker (1971) after slight reduction, we have the following expressions for the fundamental and first overtone periods, P_0 and P_1 respectively

$$\log P_0 = 11.50 - 0.68 \log M + 0.84 \log L - 3.48 \log T_e \tag{4}$$

$$\log P_0/P_1 = 0.438 - 0.032 \log M + 0.014 \log L - 0.09 \log T_e \tag{5}$$

where M is the mass of the star in solar units, L the bolometric luminosity and T_e the effective temperature, which for a pulsating star refer to its equilibrium values. The precision of the coefficients of log M, log L and log T_e, are quoted as approximately ± 0.02, ± 0.02 and ± 0.07 in equation (4) and about half as large in equation (5).

It is immediately evident that an observed correlation between log P and colour (and hence effective temperature) provides a means of determining an average mass-to-light ratio, M/L, for a group of variables having a small spread in these quantities, such as those within a cluster. Period–colour relations have been used by several authors in the past (e.g. Roberts & Sandage 1955; Dickens & Saunders 1965, van Albada & Baker 1971). However, there are a number of steps required before an observed correlation can be used in this way and we believe the precision of our data, the usefulness of the parameters sought and the importance of a detailed comparison with an Oosterhoff I cluster warrant a rather careful discussion of these steps as follows. We begin by considering the conversion of colour to effective temperature.

3.2.1 Interstellar reddening

An accurate reddening determination is the first requirement. Various methods have been applied to M15, yielding values of $E(B-V)$ between 0.08 and 0.12. We discuss these in turn, followed by a new application of Sturch's method (1966) to the M15 RR Lyraes.

Sandage (1969) derived $E(B-V) = 0.12$ from *UBV* photometry of individual stars, but SKS have used $E(B-V) = 0.08$, arguing that the *UBV* data are also consistent with this value. However, we have re-analysed the *UBV* data and come to the conclusion that the reddening of M15 is not well determined by this method, since most of the blue HB stars crucial to the determination have unreliable photometry, mainly due to crowding. A similar conclusion was reached by Buonanno *et al.* (1983a) from extensive photographic photometry based on the same photoelectric standards.

A second method based on integrated light measurements has been applied by Zinn (1980) to many globular clusters. He finds $E(B-V) = 0.08$ for M15 (the value adopted by SKS).

A third method using far ultraviolet photometry (van Albada, de Boer & Dickens 1981), again of the integrated cluster light yields $E(B-V) = 0.10 \pm 0.02$ for M15. Since this method gives values for globular clusters in excellent agreement with other well-established methods, notably those by Burstein and collaborators (e.g. Burstein & McDonald 1975; Kron & Guetter 1976; Burstein & Heiles 1978) it should be given high weight in our current determination.

A fourth method, using integrated DDO photometry has been applied by Bica & Pastoriza (1983) to yield $E(B-V) = 0.05 \pm 0.05$ (typical error of the method).

Finally, we have applied Sturch's method (1966) to a sample of M15 RR Lyraes as follows. The method uses a blanketing-free colour index at minimum light, defined as $(B-V)_c = (B-V)_\phi - 0.75\,\delta(U-B)$, where $(B-V)_\phi$ is the observed mean value of $(B-V)$ over the phase interval 0.5 to 0.8, and the ultraviolet excess parameter, $\delta(U-B)$, is related to the cluster metal abundance by $[\mathrm{Fe/H}] = 13.51\,\delta(U-B) - 2.47$ (Butler 1975). The colour excess for an individual variable is then given by $E(B-V) = (B-V)_c - 0.24P - 0.21 + E(B-V)_{\mathrm{pole}}$, where $E(B-V)_{\mathrm{pole}}$ is the colour excess in the direction of the north galactic pole, which we will assume to be zero.

Table 10 gives values of $(B-V)_\phi$ for 12 *ab*-type variables with radii greater than $r = 120$ arcsec (to avoid contamination) and using SKS data alone (the individual light curves are less well delineated in the Bologna data). Since the range of [Fe/H] is small ($\sigma[\mathrm{Fe/H}] \approx 0.08$, Buonanno, Corsi & Fusi Pecci 1984; $\sigma[\mathrm{Fe/H}] \approx 0.04$, Sandage & Katem 1977) a constant correction to $(B-V)_\phi$ to yield $(B-V)_c$ of -0.026 is derived, using $[\mathrm{Fe/H}] = -2.0$. Individual values of $E(B-V)$ for the 12 variables are given in Table 10, from which we derive a mean value of $E(B-V) = 0.11$. If, as discussed earlier, the Mount Wilson observations are subject to a small colour equation, then Fig. 1(c) suggests a further correction of -0.01 or -0.02 might be applicable to correct to the (true) photoelectric system.

We adopt finally a value $E(B-V) = 0.100 \pm 0.015$.

3.2.2 Mean colour index and effective temperature

The aim is to derive a temperature from the observed colour closest to the value the star would have were it not pulsating; i.e. an 'equilibrium' value. A number of discussions of this problem have appeared in the literature (Preston 1961; van Albada & de Boer 1975; Lub 1977, Davis & Cox 1980). The problem is by no means unimportant as we have seen that

Table 10. $B-V$ colours at minimum light for M15 RR*ab* variables to derive individual values of colour excess $E(B-V)$ using Sturch's method.

Var.	Period	$(B-V)_\phi$	E(B-V)
2	0.684	0.513	0.113
8	0.646	0.513	0.122
9	0.715	0.510	0.102
12	0.593	0.494	0.116
13	0.575	0.517	0.143
15	0.584	0.460	0.084
19	0.572	0.467	0.094
22	0.720	0.493	0.084
23	0.633	0.483	0.095
25	0.665	0.534	0.143
29	0.575	0.486	0.112
52	0.576	0.533	0.159
		mean	0.114
		median	0.112

different colour indices for larger amplitude variables in M15 may differ by 0.05 mag, which corresponds to nearly 0.02 in log T_e. Similar effects are found in other clusters (e.g. Dickens 1970) and in the field (Lub 1977). Equation (4) indicates the sensitivity of M/L to log T_e (e.g. at a given period) and, as we shall see later, the temperature of the blue edge is also needed to high accuracy to have a first estimate of the helium content, Y. Even for *c*-types, there can be a significant systematic difference in these mean colour indices (~ 0.02 mag).

A single hydrodynamically pulsating model was studied by Davis & Cox (1980) where they found the mean colour closest to that of the non-pulsating model to be given by $\langle B\rangle - \langle V\rangle$. Other mean colour indices such as $\langle B-V\rangle$ gave extremely poor agreement, in fact so poor that it is probably premature to attempt to base a choice on a single calculation. The ultimate solution to the problem will require accurate full amplitude non-linear pulsation calculations over a range of stellar parameters. We believe a practical approach here to be to follow van Albada & de Boer (1975) (a similar approach was taken by Preston) and define equilibrium quantities $L_{\mathrm{eq}} = \langle L\rangle$ and $R_{\mathrm{eq}} = \langle R\rangle$ where the brackets indicate averages over the pulsation cycle. The definition of L_{eq} is exact, and that for R_{eq} probably reasonably precise in view of the relatively small change in radius over the cycle. These lead to a definition of the equilibrium temperature

$$T_{\mathrm{eq}} = \langle (L/\langle L\rangle)^{1/2}\, T_e^{-2}\rangle^{-1/2} \tag{6}$$

This formula thus requires the calculation of the average value of $L^{1/2}\, T_e^{-2}$ over the cycle, which could be carried out for photometric observations of RR Lyraes if their light and colour curves are well defined, as in Lub's (1977) study of field RR Lyraes. For our photographic data, the colour curves are inadequate for the purpose. However, Lub has found extremely accurate correlations between equilibrium temperature and the different kinds of colour index in the Walraven photometric system, which lead, after transformation to the *UBV* system and slight simplification, to the following expression for the appropriate mean colour index

$$(B-V)_{\rm eq} = (2/3)\langle B-V\rangle + (1/3)(\langle B\rangle - \langle V\rangle) \quad (7)$$

where the averages are intensity means over the light cycle. Values of $(B-V)_{\rm eq}$ for the M15 variables have been thus obtained and are given in Table 8.

Equilibrium effective temperatures are then obtained using $(B-V)$ colours computed from model atmospheres and synthetic spectra. Models by Bell (Butler *et al.* 1978, BDE) and Buser & Kurucz (1978, BK) are closely similar in the temperature and gravity range of RR Lyraes and we adopt the BDE values here. The resulting equilibrium temperatures, log $(T_e)_{\rm eq}$ are given in Table 8.

3.2.3 Bolometric corrections

The observed visual magnitudes and amplitudes need to be converted to bolometric quantities for comparison with theory. The models cited above also provide these relations. However, there is a zero-point difference in the two relations, due primarily to a difference in the adopted bolometric correction for the Sun of 0.12 mag, but further, the BDE values run in the opposite sense to those of BK for reasons not currently understood. Further calculations are in hand to investigate this. A mean value of -0.05 is representative of the colour ranges of the RR Lyraes, being close to that obtained after adjusting the BK values to a bolometric correction for the Sun of -0.07 (as adopted by Bell & Gustafsson 1978). It should be noted that the mean visual magnitude of the RR Lyraes varies through the instability strip by ~ 0.1 mag, an amount comparable to the change in either set of bolometric corrections over the same temperature range. (This is over and above the spread in luminosity at a given T_e or P which is corrected for with the use of P'.) A resolution of this ambiguity with the bolometric corrections is thus highly desirable. There is also a significant increase, up to 15 or 20 per cent in the visual amplitude A_V of an RR Lyrae, which must be allowed for in comparisons with non-linear calculations of amplitudes. The blue amplitude, A_B, being observationally better defined than A_V is used here.

3.2.4 The periods

Equation (5) indicates that the fundamental-to-first overtone period ratio is rather insensitive to the stellar parameters and for the range of M, L of interest varies across the strip from $\Delta \log P = 0.120$ (blue edge of the *c*-types) to $\Delta \log P = 0.123$ (red edge of the *c*-types). Cox *et al.* (1983) find $\Delta \log P = 0.125$ (blue edge) and $\Delta \log P = 0.128$ (red edge) for the same parameters ($M = 0.65\,M_\odot$, log $L/L_\odot = 1.77$). Thus we can convert the *c*-type periods to the equivalent fundamental period with very little error by adding 0.125 to the log of the first harmonic period. This is appropriate for the discussion of the physical parameters of the stars rather than the details of their pulsational behaviour. Fundamental periods so derived are denoted P_0, with the same notation being used for periods of the true fundamental pulsators of type *ab*.

3.2.5 Evolutionary considerations

The distribution of stars on the horizontal branch (HB) is governed by their initial location on the zero-age line (ZAHB) combined with the effects of evolution. Rood (1973) and others have demonstrated that a spread in mass can account for the observed distribution of stars on the HB, although there could well be alternative candidates such as a spread in core mass. Rood also found that the calculated appearance of the HB is largely dictated by the initial ZAHB distribution rather than the effects of evolution. Although this may not in all circumstances be true, and could change with later revision of the evolutionary tracks, it is clear that the initial ZAHB distribution is likely to remain a strong influence. A study of the Sweigart–Gross (1976, SG) grid reveals that $\partial \log T_e/\partial \log M$ varies strongly with metal abundance and in the range of interest to the present discussion, implies a significant mass difference between ZAHB stars on each side of the instability strip. Thus a variation in mass across the instability strip as well as the difference in luminosity mentioned earlier must be allowed for in attempting to derive a mean mass from the slope of the period–colour relation.

3.2.6 The theoretical period–colour relation

The above considerations affect the theoretical relation in two ways. The variation in mean properties (M, L) across the strip gives rise to a change in the slope of the relation and a spread in these quantities (at a given T_e) gives rise to a scatter in the relation. Equation (4) indicates that

$$\partial \log P_0 = -0.68\ \partial \log M$$

$$\partial \log P_0 = 0.84\ \partial \log L$$

$$\partial \log P_0 = -3.48\ \partial \log T_e.$$

ZAHB models (SG) indicate that for $Z = 0.001$, $\partial \log T_e/\partial M = -4.4$ and for $Z = 0.0001$, $\partial \log T_e/\partial M = -1.4$. For M15, $Z = 0.0002$ so we adopt $\partial \log T_e/\partial M = -2.2$. Thus, across

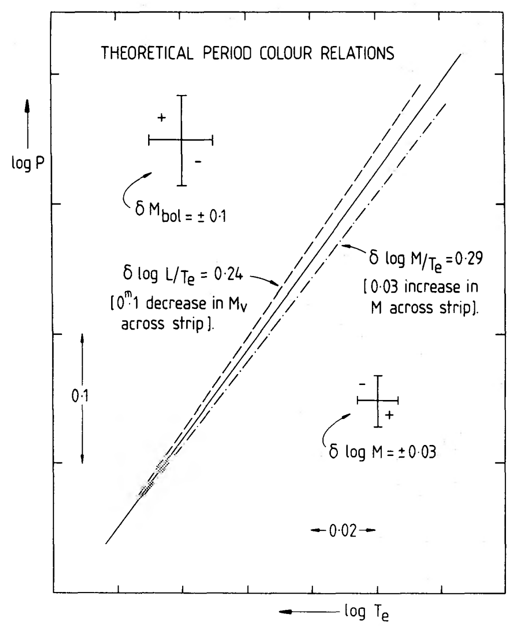

Figure 19. A schematic theoretical period–colour diagram in which the effects of variations in mass and luminosity within and across the strip are illustrated. The 'error bars' indicate the effects of intrinsic spread in mass and luminosity on the overall scatter expected, whereas the broken lines show the effect of systematic trends in these quantities across the instability strip. The solid line is that predicted by the van Albada & Baker relation (equation 4) for constant mass and luminosity.

the instability strip, $\partial \log T_e = -0.07$ (Fig. 19) implying an expected mass range of $\partial M \sim 0.03$ or $\partial \log M \sim 0.02$. This has the effect of increasing the expected (constant mass) theoretical slope of -3.48, as indicated in Fig. 19. The mean luminosity varies by ~ 0.1 mag in M_v across the strip (Fig. 14) or by ~ 0.1 mag over the range of period observed (Fig. 18). (Note that if the bolometric correction changes across the strip according to the BDE relation this would reduce to $\Delta M_{\text{bol}} = -0.042$ or $\Delta \log L = +0.017$.) This would decrease the (constant luminosity) theoretical slope of the period–colour relation, as illustrated in Fig. 19. Thus for reasonable parameters for M15, these effects work in opposite directions and indicate that the constant M/L slope is a reasonable relation to adopt. It must be kept in mind, however, that if the RR Lyraes are significantly evolved, the mass effect would be reduced and we should use a somewhat more negative slope than -3.48.

These considerations also indicate the spread at a given T_e (or $\log P$) expected for a spread in L or M. The luminosity effect can be removed empirically with the use of $\log P'$, leaving the residual scatter in the relation caused by a spread in mass coupled with observational error. The sizes of these effects for reasonable values appropriate to M15 are indicated by the error bars given in Fig. 19. Note that the few extremely luminous stars (e.g. V2, V9, V22, V32) may be in a different evolutionary state and/or may represent the extreme of the mass distribution present.

3.2.7 The observed log P/log T_e relation

Fig. 20 shows our final plot of $\log P'_0$ against $\log T_e$, where the latter has been computed from the $(B-V)_{\text{eq}}$ colours. The solid line indicates the best eye fit to the points of a line with the theoretical slope of -3.48 from equation (4). Using this equation, the intercept in Fig. 20 leads to the mass-to-light ratio

$$\log \{M^{0.81}/L\} = -1.92$$

which is our best estimate of this quantity for the M15 variables. We now discuss the uncer-

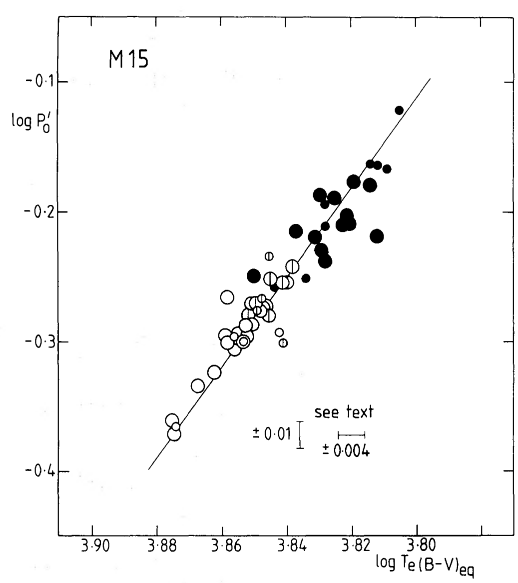

Figure 20. Observational data plotted in the theoretical period–colour framework, where the quantity $(\log T_e)\,(B-V)_{\text{eq}}$ represents our best estimates of the true equilibrium temperatures (see text) and P'_0 the fundamental period corrected for luminosity dispersion amongst the variables. The solid line is the best eye fit to the data, and leads to the derivation of $\log \{M^{0.81}/L\} = -1.92 \pm 0.03$ for the M15 variables.

tainties in this result, together with the sources of scatter in the diagram and will return later to consider other physical parameters that may be derived.

3.2.7.1 Uncertainty in the derived M/L due to systematic effects

These are of two kinds, an uncertainty in the zero point of the adopted temperature scale, through reddening, model and averaging uncertainties and the use of an incorrect slope for reasons discussed earlier. It is difficult to make a precise estimate of the zero point error. We believe the reddening to be uncertain by ± 0.015 mag ($\sim \pm 0.005$ in $\log T_e$), the temperature scale uncertain by $\sim \pm 0.004$ in $\log T_e$ from a comparison between BDE and BK and averaging uncertainty to be $\sim \pm 0.003$ in $\log T_e$. Taken together it is unlikely that $\log T_e$ is in error by more than ± 0.01 and an optimist would hope that it is somewhat smaller than this. We therefore adopt an uncertainty of ± 0.008 as our best estimate of the error in zero point of $\log T_e$. (Note that an error of this size implies that there could be very little real colour overlap between *ab*- and *c*-types.). This uncertainty leads to an uncertainty in $\log \{M^{0.81}/L\}$ of about ± 0.03 in the sense that a lower T_e gives a higher value of M/L. Error in the slope of the relation turns out to be of less importance in the derivation of M/L. This can be illustrated by considering the effect of the increase in mean M_V across the strip which, as discussed earlier, gives rise to a larger slope to the mean relation (but is likely to be counteracted almost exactly by the increase in mean mass across the strip). The observed change of 0.1 mag in M_V requires an increased slope of 3.68 which only changes $\log \{M^{0.81}/L\}$ by 0.01. Thus the range of slope indicated in Fig. 19 would lead to an error of ± 0.01 in $\log \{M^{0.81}/L\}$.

3.2.7.2 Scatter in the $\log P'_0/\log T_e$ diagram

A good estimation of the observational part of the scatter in Fig. 20 can be made since we have in M15 two completely independent sets of measures of the variables; a similar estimate is obtainable from the measures of the non-variable stars. Zero-point uncertainties are common to both sets, being calibrated by the same photoelectric sequence but the internal scatter can be reasonably accurately estimated. It is of great interest to do so, since as we have seen earlier, any residual intrinsic scatter in the diagram can only be attributed to a spread in mass (the observed spread in L being removed with the use of P'_0).

Two independent sets of values of $\langle V\rangle$ and $\langle B\rangle - \langle V\rangle$, SKS and ours (B) are given in Tables 5 and 6.

It is easy to show that the mean standard error of an individual $B-V$ value is given by

$$\mu_c^2 = (1/2N) \sum_{\text{stars}} \{(\langle B\rangle - \langle V\rangle)_{\text{SKS}} - (\langle B\rangle - \langle V\rangle)_{\text{B}}\}^2$$

with a similar expression for errors in $\langle V\rangle$. Considering first the observational error in $\langle B\rangle - \langle V\rangle$ from the values given for 48 stars in common to both series with quality 1 and 2 photometry, we find $\mu_c = 0.0154$ mag so that the error in a combined $\langle B\rangle - \langle V\rangle$ colour is $\mu_{cc} = 0.0109$ mag. Since $\partial(\log T_e) = 0.388\, \partial(B-V)$, this corresponds to a standard error in $\log T_e \langle B\rangle - \langle V\rangle$ of $\mu_{T1} = \pm 0.00423$. Observational errors in $\langle V\rangle$ must also be considered, since they contribute a scatter $\mu_{\log P'} \sim +0.336 \mu_V$. For 48 stars, we find the error in a combined $\langle V\rangle$ value to be $\mu_V = \pm 0.0161$ mag giving rise to an error $\mu_{\log P'}$ of ± 0.00531. This corresponds to an error in $\log T_e$ given by $\mu_{T2} = \pm 0.00531/3.48 = \pm 0.00153$. Thus the combined observational uncertainty in $\log T_e$ (assuming these two parts are uncorrelated) is $\mu_T = \pm 0.00450$. (1σ values). An error bar of twice this length is shown as a horizontal line in Fig. 20. Fig. 21 shows the distribution of temperature residuals taken about the mean line.

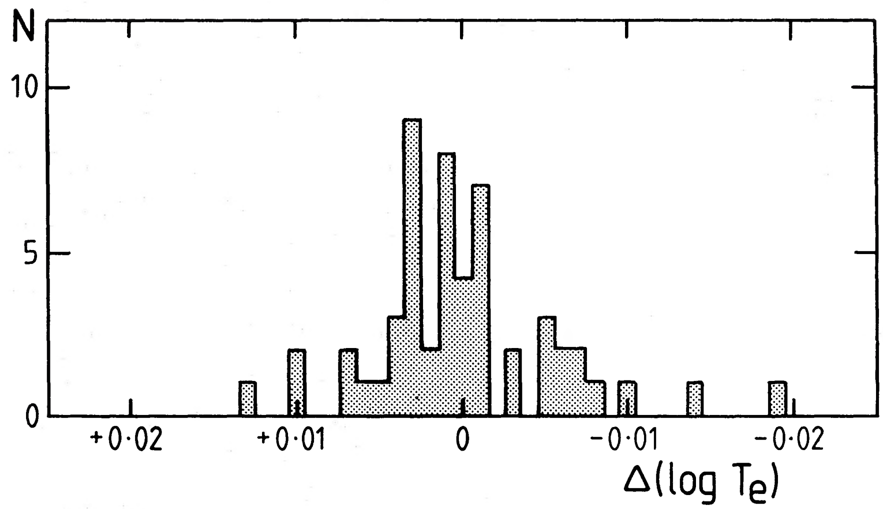

Figure 21. Histogram of the residuals Δ (log T_e) obtained from Fig. 20. Allowing for observational error, the distribution predicts a (1σ) dispersion in mass of ± 0.019 $M_\odot$ amongst the variables.

This distribution is characterized by a Gaussian width $\mu_0 = \pm\, 0.00590$. Since the errors in μ_T and μ_0 are ~ 10 per cent of the values, there appears to be a significant intrinsic spread in the data, characterized by a standard error of order $\mu_I = \pm\, 0.0038$. We believe this is caused by a spread in mass amongst the variables, and since $\partial(\log M) \sim 5.1\ \partial \log T_e$ (from equation 4), this is equivalent to a 'Gaussian' mass distribution with $\mu_{\log M} = \pm\, 0.019$. Thus the observations are consistent with a spread in total mass within the instability strip of a few hundredths of a solar mass, e.g. if the mean mass is given by 0.65 $M_\odot$ (see below) then most RR Lyraes would have masses between about 0.62 and 0.68 $M_\odot$, which is reasonable on the basis of stellar evolution theory (e.g. Rood 1973).

3.2.8 The helium abundance

Various methods can be employed to estimate Y using parameters deduced from the colour–magnitude diagram of the cluster and/or the properties of the RR Lyrae variables within the framework of pulsational and evolutionary theories. The different methods are often discrepant but such is the importance of the determination that a somewhat detailed discussion should be given here.

3.2.8.1 Pulsational properties

As is well known, the high temperature boundary of the instability strip is a sensitive function of Y. This boundary is delineated sharply by the blue edge of the *c*-type (first harmonic) variables. Similarly the high temperature boundary of the *ab*-types (fundamental pulsators) is also a sensitive function of Y. There is also a weak dependence on mass but as Tuggle & Iben (1972) have shown this dependence is very small in the range of interest for RR Lyraes. Fig. 20 indicates that $(\log T_e)_{\rm HBE} = 3.875$ and $(\log P'_1)_{\rm HBE} = -\,0.497$. The fundamental blue edge (FBE) is less well defined and has the additional uncertainty that if an either/or zone exists near the transition temperature (e.g. Stellingwerf 1975) we cannot be sure we are observing the true FBE. Nevertheless, as we shall see later it is most likely that the dominant evolution through the strip is bluewards, indicating that the bluest *ab*-types may indeed define correctly the FBE. On this assumption, Fig. 20 indicates the values $(\log T_e)_{\rm FBE} \sim 3.85$ and $(\log P'_0)_{\rm FBE} = -\,0.255$.

From graphical representations of the Tuggle & Iben relations we derive $Y_{HBE} = 0.29$ and $Y_{FBE} \sim 0.25$. Our estimate of the uncertainty in log T_e, due particularly to the uncertainty in the reddening indicates a formal error in $Y \sim \pm 0.04$. In addition to this, the location of the theoretical blue edges are sensitive, among other things, to the formulation of the opacities used in the models (e.g. see Tuggle & Iben 1971; Rood 1973).

Deupree (1977) has used the width of the instability strip to determine Y. However, the location of the true red edge in M15 is uncertain because of the scarcity of variables there and we have not applied this method here.

In the light of these comments, we derive a mean pulsational value of $Y = 0.27 \pm \epsilon(Y)$ where $\epsilon(Y)$ is formally $\sim \pm 0.04$ but may in practice be larger.

3.2.8.2 The R-method

The helium abundance can be estimated from the R-method (Iben 1968) where R is the ratio of the number of HB stars to the number of red giants brighter than the bolometric luminosity of the RR Lyrae variables in the cluster. This procedure has been recently applied by Buonanno *et al.* (1984) to the data derived from the photographic photometry of a complete sample of stars down to $B = 18.5$ in a ring between 1.9 and 5.0 arcmin from the centre of M15. Using a revised formula (Buzzoni *et al.* 1983) deduced from interpolation in the SG models, they obtained $Y = 0.23 \pm 0.03$, where the associated error is the formal error due only to the statistics of the stars considered. Applying this method to 15 well studied clusters, Buzzoni *et al.* (1983) deduced a mean value of $Y = 0.23 \pm 0.02$.

3.2.8.3 The A-parameter

Equation (4) can be written as $\log P_0 = 11.50 - 0.84A - 3.48 \log T_e$ where $A = -\log \{M^{0.81}/L\}$. Caputo & Castellani (1975) and Caputo, Castellani & Gregorio (1983) have shown on the basis of ZAHB models that A depends only on Y. We find a similar effect using the SG models, and find $A = 1.45 + 1.40\,Y$. For M15, with $A = 1.92 \pm 0.03$, we obtain $Y = 0.34 \pm 0.02$ (the error being that due solely to the error in A). Similarly high values for M15 and other clusters were obtained by Caputo and co-workers. The uncertainties in these values due to model deficiencies (as in 3.2.8.2. above) must again clearly be greater than the quoted values.

3.2.8.4. The Δ-method

Caputo & Cayrel de Strobel (1981) showed that the difference in luminosity, Δ, between the HB at the instability strip and the main sequence at $(B-V)_0 = 0.7$ depends somewhat on Z but changes mainly with Y. Therefore it allows the determination of Y whenever accurate colour–magnitude diagrams down to the main sequence are available. With $\Delta = 5.7$ mag and assuming $Z = 0.0001$ they derived a value of $Y = 0.23$.

3.2.8.5 Luminosity width of the horizontal branch

HB models indicate that the width in luminosity is a sensitive function of Y in the sense that an observed width can place upper limits on Y. This is caused mainly by the variation in track morphology with Y. Using the Sweigart–Gross grid, we find for $Y = 0.3$, the width in luminosity of the HB in the instability strip and redwards should be at least 0.2 mag whereas Fig. 18 indicates a value essentially less than 0.15 mag. Although a detailed comparison, which should include the effect of varying core mass, has not been made, the observed width suggests a value of Y closer to 0.2 than 0.3.

In discussing these results, we must distinguish between primordial helium, Y_p, and the present day helium abundance of HB stars, Y_{HB}, slightly enhanced at their surfaces through convective mixing during red giant evolution by an amount $\Delta Y = Y_{HB} - Y_p$. The R method gives an estimate of Y_p while Y deduced from pulsational properties is the current (enhanced) value. The best estimate for Y_p from external considerations is 0.23 ± 0.01 (e.g. see Pagel 1982). The R method applied to M15 also gives 0.23 but with the larger uncertainty of ± 0.03. Since ΔY is expected to be ~ 0.02 from stellar evolution calculations, the pulsational mean value for the M15 RR Lyraes of 0.27 ± 0.04 is consistent with that of 0.25 ± 0.03 expected for M15 HB stars from these considerations, and which we therefore adopt as a working value subsequently.

3.3 THE ABSOLUTE MAGNITUDE OF THE RR LYRAES USING PULSATIONAL DATA AND THE IMPLICATION OF THE RESULT FOR THE CLUSTER AGE

Knowledge of the intrinsic luminosity of RR Lyrae variables is central to the problem of determining cluster ages as illustrated in the Sandage series of papers on the Oosterhoff groups cited earlier. If the luminosity can be derived from methods insensitive to the properties of stellar models an important uncertainty is removed from this fundamental problem.

The determination of the periods and hence the theoretical period–colour relation should not be sensitive to details of the models and hence our derived mass-to-light ratio is only limited by observational constraints that have been discussed earlier. Furthermore, there is a method of mass determination for RR Lyraes that may also be essentially free of major defects in models and that results from the mixed mode behaviour found in some RR Lyraes whose period ratios are sensitive primarily to the stellar mass (see below). Thus a determination of the RR Lyrae luminosity is available that should be only minimally affected by model uncertainties.

As is well known, the age of a globular cluster is estimated using the luminosity of the turn-off point in the HR diagram. Again the derivation is model-dependent but the uncertainties in the luminosities of main sequence and turn-off models may be expected to be less severe than those of models in more advanced stages of evolution on the HB. We thus derive the mass and luminosity of the M15 RR Lyraes and hence the cluster age, where the relevant observational parameters are providing the main restriction on the precision of the results. This will therefore provide essentially a 'pulsational' age determination through independent calibration of the cluster's distance and which therefore gives useful input to the wider topic of globular cluster ages. However, a discussion of the overall age problem is outside the scope of this paper.

The method of mass determination was put forward by Jørgenson & Peterson (1967) and has been applied by Cox *et al.* (1983), using their own models, to the multimode RR Lyraes in M15. From 10 multimode variables in M15, Cox *et al.* (1983) gave a mean mass of $M = 0.65 \pm 0.05\, M_\odot$, where the uncertainty quoted embraces the range of M derived for the variables. Consideration of the various uncertainties involved in the derivation (Jørgenson, private communication to Cox) suggests that the above range is indicative of the true uncertainty in the derived mass, which could therefore be the same for all the multimode variables in the cluster. Thus with $\log\{M^{0.81}/L\} = -1.92 \pm 0.03$, we find a mean luminosity given by $\log L = 1.77 \pm 0.06$. Assuming a mean bolometric correction of -0.05, we derive an absolute visual magnitude $M_V = 0.39 \pm 0.15$ ($M_{\mathrm{bol}\odot} = 4.76$).

The luminosity of the turn-off point in the HR diagram can be obtained for M15 using the above RR Lyrae luminosity and the observed magnitude difference between HB and turn-off. For M15, Sandage (1982a) gives $\Delta M_v = 3.31$, based on Sandage (1970), with an estimated uncertainty of ±0.2 mag. Thus with an adopted bolometric correction at turn-off of −0.15 (BK adjusted to a bolometric correction for the Sun of −0.07) we find log $L_{TO} = 0.48 \pm 0.14$ (combined error). Using the interpolation formula for the age in units of 10^9 yr, t_9, given by Iben (1971), i.e.

$$\log t_9 = 1.42 - 1.1 \log L_{TO} - 0.59\,(Y - 0.3) - 0.14\,(3 + \log Z)$$

and with $Y_p = 0.23 \pm 0.01$, $\log Z_{M15} = -3.7 \pm 0.1$, we find $\log t_9 = 1.03 \pm 0.17$. A similar formula quoted by Sandage (1982a) gives $\log t_9 = 1.07 \pm 0.17$. Thus our derived age for M15 based on the RR Lyrae luminosity obtained from pulsation theory is close to 10 billion years with an estimated uncertainty of ±3 to 4 billion years. This age is substantially lower than that of 15 billion years derived by Sandage (1982a) and stems entirely from the brighter luminosity we derive for the RR Lyraes. Hansen (1979) also derives a brighter M15 RR Lyrae luminosity than Sandage by applying systematic corrections to the parallaxes of the calibrating subdwarf stars. A discussion of these results is, however, outside the scope of this paper.

The fainter value of $M_V = 0.64$ derived by Sandage would require a mass $\sim 0.5\,M_\odot$ to fit the observed M/L, which seems excluded on the current precepts and would lead to the impossibility of populating the instability strip with standard HB models (SG). However, other problems with the interpretation of multimode masses (e.g. in Cepheids, Cox 1982, and in M3, see later), together with the uncertain situation regarding bolometric corrections suggests caution in extending the discussion further at the present time. However, we note that non-standard values of [CNO/Fe] > 0, as has been found in the M15 planetary nebula (Peimbert 1973) could alleviate these problems, and restore a more conventional age for M15 through the Z_{CNO}-dependence of the age in the above equation. This would also significantly affect the colours of the HB models, and will be further discussed in the comparison with stellar evolution.

3.4 OOSTERHOFF I AND OOSTERHOFF II CLUSTERS

The Oosterhoff dichotomy has been the subject of a number of investigations as to its precise nature and underlying physical causes. Sandage (1959) proposed a luminosity difference between the groups, Stobie (1971) suggested that either a mass or a luminosity difference (or both) could be responsible and van Albada & Baker (1973) pointed out the possible importance of the direction of evolution through the instability strip, combined with hysteresis in the mode of pulsation, coupled with mass/luminosity differences between the groups. These, and other, investigations were hampered by the lack of accurate colours for the cluster RR Lyraes, particularly those of group II, which made it impossible to draw firm conclusions. The colours (and hence effective temperatures) are crucial to the interpretation since they enable physical parameters to be derived directly using pulsation theory (as discussed earlier in this paper) but furthermore, enable a tie-in with the evolutionary properties of horizontal branch stars via stellar structure models, thence allowing in principle all the physical parameters of interest to be derived.

The availability of new colour data for the two most populous group II clusters M15 (SKS) and ω Cen (BDE), and other clusters led Sandage and his collaborators (SKS, Sandage 1981b) to propose, using pulsation and evolution theory that the dominant, and probably sole property responsible directly for the Oosterhoff effect amongst clusters is indeed the luminosity of the RR Lyraes. Sandage (1982a) further showed that, rather than being a discrete effect, the clusters of each group possess a range in luminosity (giving rise to the observed range in the period shift) that is essentially continuous in nature, although with a paucity of clusters at intermediate period shifts (between the Oosterhoff groups) that gives rise to the observed dichotomy in mean period. Although there is still no clear understanding of this paucity, Rood (1973) showed that such apparently discrete effects can be produced with pseudo HR diagrams of cluster horizontal branches where the relevant physical parameters are varied continuously.

A further important effect discussed by Sandage concerns the correlation of the mean period shift with heavy element abundance amongst the clusters. Although it was earlier widely recognized that the Oosterhoff groups were related to abundance, since the clusters of group II were notably more metal-poor than those of group I, Sandage confirmed the existence and nature of a strong correlation amongst many clusters and more importantly, emphasized its fundamental significance in the study of the overall cluster properties, in particular in the derivation of cluster ages.

In view of the wide scope of Sandage's discussions of this problem we believe it appropriate here to concentrate on those aspects in which the new improved colour data presented here affect the conclusions drawn in his series of papers. These are essentially of two kinds, those which provide a more exact description of the behaviour of the M15 RR Lyraes (and how they differ from those in group I clusters) and the derivation of pulsational parameters, and those which concern the overall objectives of understanding the Oosterhoff effect in terms of observed cluster properties and pulsational and evolutionary theory.

In this section we concentrate on the first aspect and discuss the observed properties of the Oosterhoff groups, mainly as manifest by the most populous clusters of each group, M15 and M3. In the next section we consider the evolutionary aspects and conclude with a discussion of the Oosterhoff effect as far as it can be understood in the light of our discussion.

The Oosterhoff effect is illustrated schematically in Fig. 22 (taken from Dickens 1982, fig. 1) which compares the mean loci of the period–amplitude relations of M15 and M3 with

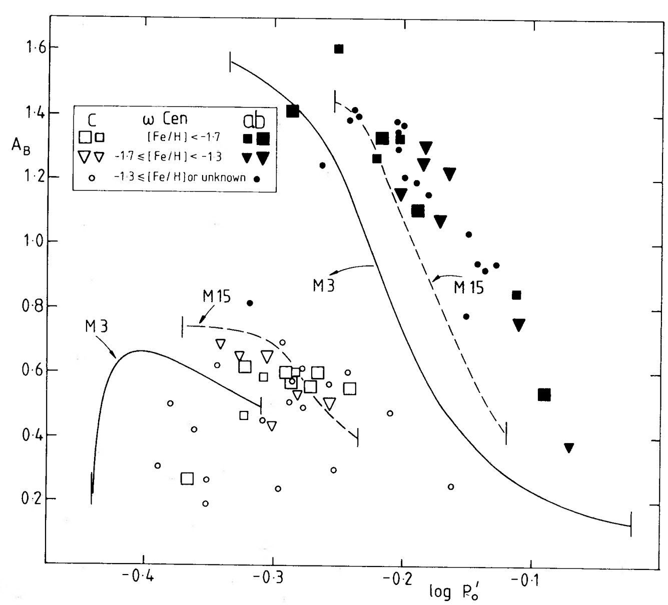

Figure 22. Correlation of blue amplitude, A_B, with log P'_0 for the clusters M15, M3 (schematic) and ω Cen (symbols). P'_0 is the fundamental period corrected for luminosity dispersion within each cluster. For *c*-type variables, the transformation $\log P'_0 = \log P'_1 + 0.125$ has been applied. The larger symbols have a higher weight.

individual data points for RR Lyraes in ω Cen (Dickens & Bingham, in preparation). Data for M3 are taken from Sandage (1981b); note that the log of the fundamental period log P'_0 defined earlier is used for all variables. The main feature giving rise to the mean period difference is seen to be a shift in log $P'_0 \sim 0.05$ (*ab*-types) or ~ 0.08 (*c*-types) between the two clusters. The distribution of the variables with period also affects the derived mean period and reference to the original diagrams will show that the large concentration of large amplitude *ab*-types in M3 (see Sandage 1981b, fig. 3), which are essentially absent in M15, contributes strongly in weighting the mean period towards the short period end of the distribution. Note also that the overall range of periods in M3 is much greater than in M15, having small amplitude, short period and long period tails to the distributions that are essentially absent in M15. This underlines the fact that the differences between clusters of each Oosterhoff group cannot be expressed simply as a period shift. The location of the ω Cen variables (Oosterhoff group II) is also not simply explained by a period shift since the loci are significantly different again from either cluster. Indeed ω Cen introduces a further complication in that the variables within it have a range in abundance larger than the difference in abundance between M3 and M15 yet do not define distinct period–amplitude relations. If, therefore, the abundance is an important factor in controlling the RR Lyrae periods, directly or indirectly, then yet another factor must be operating within ω Cen giving rise to a different behaviour, since the differences exhibited in this diagram are much larger than the observational errors in either parameter. A full treatment of the new ω Cen data will be given elsewhere (Dickens & Bingham, in preparation).

The behaviour of the amplitude as a function of temperature through the instability strip is illustrated in Fig. 23 in which log T_e as derived from the equilibrium colours $(B-V)_{eq}$ (see

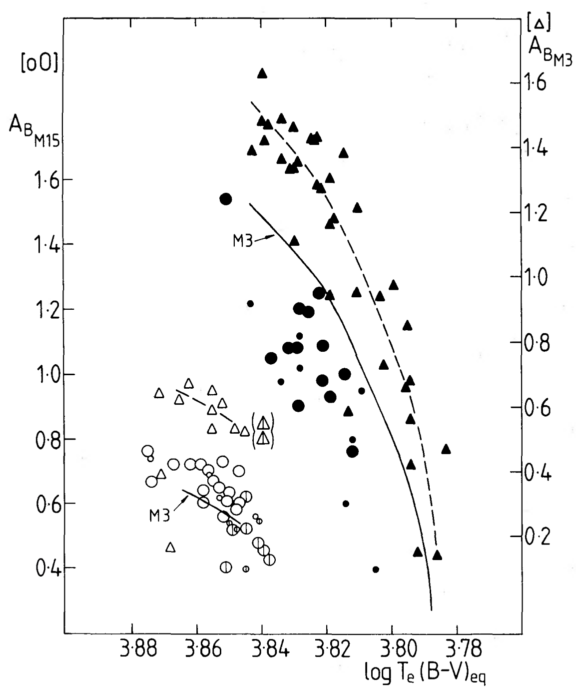

Figure 23. Blue amplitude as a function of log T_e for RR Lyraes in M15 (circles) and M3 (triangles). Open symbols denote *c*-type variables, those with vertical bars exhibiting multimode behaviour. Note that the M3 data points are plotted with respect to the ordinate scale on the right of the diagram, displaced from those of M15 (left ordinate) to show the two clusters separately. The solid line shows the position of the *mean* M3 relations referred to the left hand ordinate (i.e. directly comparable to the M15 data points). Effective temperatures are derived from the $(B-V)_{eq}$ colours using temperature scales from BDE and reddenings of $E(B-V) = 0.00$ (M3) and 0.10 (M15).

Section 3.2) is plotted against blue amplitude for the clusters M15 and M3. (Values of $(B-V)_{eq}$ for M3 have been calculated from the data given by Sandage, 1981b, table 2). The solid lines indicate the mean loci (dashed lines) of the M3 variables superimposed on the M15 points. Within each cluster there is a smooth change in mean amplitude across the instability strip, broken by the essentially sharp transition associated with the change in pulsation mode, which occurs close to log $T_e = 3.840$ in both clusters. The multimode variables in either cluster can be seen to occur precisely at, or very close to, this transition temperature suggesting very strongly that the multimode behaviour is intimately linked to whatever process is causing the mode-switching. Another important feature of the diagram concerns the uniqueness or otherwise of the amplitude/log T_e relation over all clusters. It is clear that uncertainties in the reddening or the transformations from $(B-V)$ to T_e cannot bring the relations into agreement, since an improve match in the *ab*- types would increase the difference in the loci of the *c*-types and vice versa. This is true whatever mean colour is used to determine the effective temperatures and is contrary to the conclusion of Sandage (1981a) that the amplitude/colour relation (plotted with colours corrected for differential blanketing and therefore equivalent to temperatures) does not change from cluster to cluster. This illustrates that amplitude should not be used as a fiducial parameter with which to compare cluster properties.

Finally, we compare the period–colour relations of M15 and M3 (in the theoretical frame) in Fig. 24 where the log of the corrected fundamental period, log P'_0 is plotted against

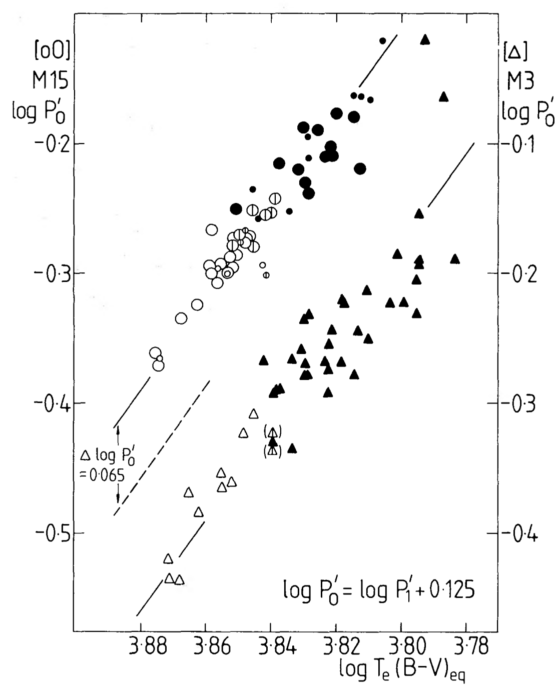

Figure 24. Comparison of the log P'_0/log $T_e(B-V)_{eq}$ relations of M15 and M3 (data from Roberts & Sandage). Note that the ordinate scales are different for the data points of the two clusters. Although the uncertainties in the absolute registration of the temperature scales ($\sim \pm 0.008$ in log T_e) must be kept in mind, the diagram represents the currently best estimate of the RR Lyrae temperatures. As such, it shows that the high temperature (and probably the low temperature) boundaries of the strip are very similar, the main difference between the clusters being the pulsational mode exhibited by the variables in the centre of the strip, close to the transition at about log $T_e = 3.840$, M15 is dominated by multimode variables, M3 by large amplitude *ab*-types. This property, coupled with the very different overall distributions of stars on the HB (Fig. 29) characterizes the main morphological difference between these clusters and, together with possible small mass and luminosity differences, provides the key to understanding the physical cause of the Oosterhoff phenomenon (see text).

log $T_e(B-V)_{eq}$. The mean location of the M3 variables in the M15 frame is indicated by the dashed line and shows that the principal difference between the clusters corresponds to a shift $\Delta \log P'_0 = 0.065$, i.e. comparable to that exhibited in the period–amplitude relations of Fig. 22. The uncertainty in the absolute registration of the temperature scales, as discussed earlier, renders $\Delta \log P'_0$ uncertain by $\sim \pm 0.03$. It can be seen that the high temperature boundaries and transition temperatures are essentially the same in both clusters, the variables in M3 extend to significantly cooler temperatures than those in M15. This might be expected on the basis of their HB morphologies (to be discussed) since M3 has a much greater population of RHB stars than M15 i.e. the M15 HB is becoming de-populated within the strip itself. The other principal difference between the clusters concerns the relative populations of each Bailey type in the neighbourhood of the transition zone, there being far more *c*-types in M15 than in M3, and far more *ab*-types (with the largest amplitudes) in M3 than in M15. There are also many more multimode variables in M15 than in M3, which may be related to this difference e.g. many of the multimode variables in M15 could be the counterparts of the large amplitude fundamental pulsators in M3, the preference for multimode behaviour arising by an unknown mechanism triggered by whatever physical parameter is causing the period shift between the clusters. Further reference to this will be made later in the comparison with stellar evolution.

In summary, the evidence provided in Figs 22–24, supported by the analysis of six clusters by Sandage (1981b) suggests that whilst complicating subtle effects are present, a principal difference between clusters of each Oosterhoff group is characterized by a systematic shift in period at a given temperature. In understanding the Oosterhoff phenomenon we must now consider how this period shift is related to other cluster properties and to what extent such relations can be understood qualitatively and quantitatively in terms of stellar models. The details of the distribution of period with temperature and amplitude may also play a useful role.

Sandage (1982a) has addressed this problem and, as mentioned earlier, has found a good correlation, taken over many clusters, between period shift and heavy element abundance [Fe/H]. In view of the current controversy over the abundance scale for clusters, we have reexamined this correlation using new abundances obtained by Pilachowski *et al.* (1983) and

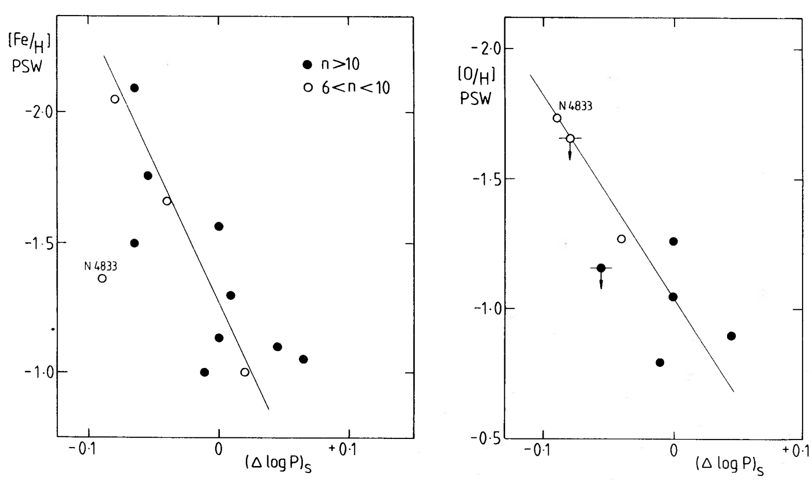

Figure 25. (a) Correlation of period shift determined by Sandage (1982) with metal abundance given by Pilachowski, Sneden & Wallerstein (1983 PSW) for RR Lyraes in clusters with more than 8 *ab*-type variables. (b) Correlation of period shift with the oxygen abundance determined by PSW. Note the better agreement of the oxygen deficient cluster NGC 4833. Arrows indicate lower limits. The straight lines are eye fits to the points.

used only clusters with sufficient variables for which a reliable period shift may be measured. The results are shown in Figs 25(a) and (b) in which [Fe/H] and [O/H] are plotted against $(\Delta \log P)_s$ as given by Sandage. Fig. 25(a), essentially confirms the correlation found by Sandage, i.e. $\Delta \log P \sim -0.1\, \Delta\, [\mathrm{Fe/H}]$ (solid line). A similar effect is found in field RR Lyraes (e.g. Lub 1977; Kemper 1982) and thus the evidence now very strongly supports the idea that the heavy element abundance plays a fundamental role in the Oosterhoff problem. Note also the good correlation of [O/H] with period shift, to be expected perhaps since oxygen is the dominant element of importance to HB stars (Rood & Seitzer 1981). [The oxygen depleted, Oosterhoff II cluster, NGC 4833 (Pilachowski *et al.* 1983) fits better in Fig. 25b than in Fig. 25a.]

Finally, the $\log P'_0/\log T_e(B-V)_{\mathrm{eq}}$ relation for M3 (Fig. 24) allows the determination of the mean mass-to-light ratio for the RR Lyraes in this cluster, which we then take as representative of that for Oosterhoff I clusters in later discussion. Using the same precepts as for M15, we find

$$\log \{M^{0.81}/L\}_{\mathrm{M3}} = -1.85 \pm 0.03$$

i.e.

$$\Delta \log \{M^{0.81}/L\}_{\mathrm{M3-M15}} = +0.07 \pm 0.04$$

Thus if the mean mass is constant between the clusters, the variables in M15 are 0.18 mag brighter (bolometrically), the solution favoured by Sandage. Clearly a smaller luminosity difference will require a greater mean mass for the M3 variables. Note however, that Cox *et al.* (1983) have derived a multimode mass of $\sim 0.55\, M_\odot$ for two variables in M3. Such a low mass would require $\{\log L\}_{\mathrm{M3}} = 1.64$, i.e. ~ 0.3 mag fainter than the RR Lyraes in M15. This point will be further discussed later.

3.5 COMPARISON WITH STELLAR EVOLUTION MODELS

Our objectives here are to address the following questions and to discuss the consequences.

(1) Are the pulsationally derived values of the mass and mass-to-light ratio understandable in terms of current horizontal branch models?

(2) Can the differences between M15 and M3 as regards their mean period shifts, pulsational masses and mass-to-light ratios be explained by current horizontal branch models?

(3) Can the morphology of the cluster horizontal branches, based on the considerations discussed in (1) and (2) above, be reconciled with current evolutionary tracks or tracks as they might be modified in a 'non-standard' framework?

3.5.1. The case of M15 alone

The tracks in Fig. 26 can be used to illustrate the overall situation. They have been taken, with interpolation, from Sweigart & Gross (1976, SG) and show the general morphology of tracks in the instability region for appropriate values of M and Y, and with an appropriate core mass of $M_c = 0.475\, M_\odot$. (Some hotter tracks are also shown, and will be referred to later.) Two values of the heavy element abundance are shown, corresponding approximately to those of M15 ($Z = 0.0002$) and M3 ($Z = 0.0005$).

To make comparisons with the clusters, it is convenient to make use of linearized interpolation formulae, based on evolutionary models, which denote the relevant parameters of ZAHB models within the instability strip. Renzini (1977) has given such relations which, after slight reduction, become (assuming a red giant mass of $0.8\, M_\odot$) for the core mass,

$$M_c = 0.4706 + 0.26\,(0.3 - Y) - 0.01\,(3 + \log Z) \qquad (8)$$

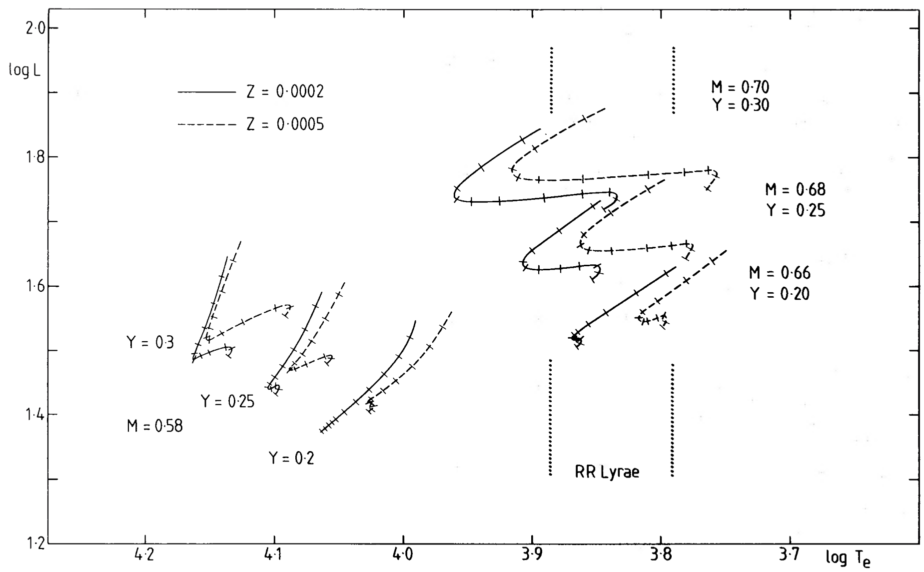

Figure 26. Evolutionary tracks, derived by interpolation in the Sweigart-Gross grid, for models covering the range in Z thought to be appropriate to M15 (solid) and M3 (dashed). The precise shapes and locations of the tracks may be slightly incorrect due to uncertainties in the method of interpolation but only very slight changes in the parameters would be needed to correctly register them. The tick marks correspond to the time intervals tabulated by Sweigart & Gross and generally occur at roughly equal time intervals. The location of the instability strip is shown schematically.

and, using this relationship to 'remove' the core mass dependence on the HB, a ZAHB model at log $T_e = 3.85$ (the centre of the instability strip) has

$$\log L_{3.85} = 1.70 + 1.168\,(Y - 0.3) - 0.072\,(3 + \log Z), \quad (9)$$

$$\log M_{3.85} = -\,0.209 - 0.230\,(Y - 0.3) - 0.072\,(3 + \log Z). \quad (10)$$

Equation (8) is based on Rood's (1972) models and equations (9) and (10) on the horizontal branch models of SG. The model mass-to-light ratio within the instability strip depends essentially only on Y, since from (9) and (10) we have

$$\log \{M/L\}_{3.85} = -\,1.91 - 1.40\,(Y - 0.3). \quad (11)$$

Log $\{M^{0.81}/L\}$ is of course a slowly varying function of log $\{M/L\}$ but for reasonable masses (see below), log $\{M^{0.81}/L\} = \log\{M/L\} + 0.04$. From here on, we drop the subscript 3.85, since the parameters given from the evolutionary models will always refer to values at log $T_e = 3.85$, and denote values obtained from the evolutionary models by the subscript 'evol'. Allowing a small evolutionary correction (Fig. 26) to log L for comparison with RR Lyrae values gives us finally

$$\log \{M^{0.81}/L\}_{\text{evol, RR}} = -\,1.40\,(Y - 0.3).$$

The following table gives values of log L_{evol} as a function of M and Y

Values of log L_{evol}

M	$Y = 0.25$	$Y = 0.30$
0.60	1.64	1.71
0.65	1.67	1.74
0.70	1.70	1.77

In comparison, the pulsational results from

$\log \{M^{0.81}/L\}_{\text{puls}} = -1.92 \pm 0.03 = A_{\text{puls}}$

(where A is the 'mass-to-light' parameter and is a function of P, T_e as defined earlier) require the following values of $\log L_{\text{puls}}$ as a function of A_{puls}

Values of $\log L_{\text{puls}}$

M	$A=-1.85$	$A=-1.89$	$A=-1.92$	$A=-1.95$
0.60	1.67	1.71	1.74	1.77
0.65	1.70	1.74	1.77	1.80
0.70	1.72	1.77	1.80	1.83

It can be seen that within the uncertainties of the pulsationally derived values of M and $\log L$, agreement with the evolutionary model values is possible, but only if $Y \gtrsim 0.3$. As shown earlier, such a value of Y is not inconsistent with those derived solely from pulsation theory. For $Y=0.3$, $M=0.7$ and $\log L=1.77$ the upper tracks in Fig. 26 should therefore be sufficiently representative of the M15 RR Lyraes to allow interpretation of their distribution in the HR diagram in terms of the models. Note, however,that a more plausible lower helium abundance, preferred from our previous analysis, of $Y \sim 0.25$ predicts a lower luminosity ($\Delta \log L \sim 0.1$) in the evolutionary models than required by the pulsational results.

Similar considerations have led Caputo *et al.* (CCG 1983) to propose a non-standard (denoted by them 'non-canonical') frame of evolutionary models in which the [CNO/Fe] abundance ratio and the core mass are allowed to vary within the frame, and are different from the 'canonical' values in the standard evolutionary frame (e.g. SG). There is some observational support for a variable [CNO/Fe] from observations that [O/Fe] in population II stars (Sneden, Lambert & Whitaker 1979; Barbuy 1981) and disc stars (Clegg, Lambert & Tomkin 1981) is enhanced and additional variations in core mass might be expected on theoretical grounds, for example through core rotation affecting the core mass at helium flash. CCG derive a linear approximation for the effects on the mass-luminosity parameter A which, after allowing a small evolutionary increase in $\log L$ as before, becomes

$$A = 1.52 + 1.2\,Y + 2.3\,DM_c + 0.03\ [\text{CNO/Fe}] \tag{12}$$

where DM_c is the difference in core mass from the standard value. Table 11 illustrates these effects on the evolutionary masses and luminosities in the range of interest. It can be seen that for $Y=0.25$ the pulsation results require at least an increase in core mass whereas for the $Y=0.30$ case, agreement can just be achieved within the extreme uncertainty of A_{puls} with $DM_c=0$ (no rotation) and [CNO/Fe] = 0 (no enhancement), i.e. the standard case, a

Table 11. Masses and luminosities of non-standard models according to equation (12).

Y	0.25	0.25	0.25	0.25	0.30	0.30	0.30	0.30
DM_c	0	0	0.03	0.03	0	0	0.03	0.03
[CNO/F_e]	0	1	0	1	0	1	0	1
A	1.82	1.85	1.89	1.92	1.88	1.91	1.95	1.98
$(\log L)_{M=0.60}$	1.64	1.67	1.71	1.74	1.70	1.73	1.77	1.80
$(\log L)_{M=0.65}$	1.67	1.70	1.74	1.77	1.73	1.76	1.80	1.83
$(\log L)_{M=0.70}$	1.70	1.73	1.77	1.80	1.76	1.79	1.83	1.86

result found earlier. However, for the most probable values of $M_{puls} = 0.65\,M_\odot$, log $L_{puls} = 1.77\,L_\odot$, departure from the standard models is required. We further remark that only a modest core rotation is needed to produce an increase in M_c of $0.03\,M_\odot$. We find $\Delta M_c = 138\,\Delta\omega$ (Renzini 1977, p. 182) where $\Delta\omega$ is the difference from zero angular velocity in rad s^{-1}. Thus for $\Delta\omega = 2.10^{-4}$, a typical main sequence value, $\Delta M_c = 0.028\,M_\odot$. This is all that is needed to ensure a precise match with the pulsation results, even for the lower limit of $Y = 0.23$.

In summary, the pulsation results for M15, at the limit of the estimated uncertainties can just be reconciled with predictions of current stellar evolution models, but only if $Y \sim 0.30$. If $Y \sim 0.25$ the models predict a lower luminosity than indicated by pulsation theory. Relaxing the standard frame, as demonstrated by CCG enables agreement (though again at the edge of the range of uncertainty allowed) with the expected behaviour of non-standard models having modest core rotation and $Y = 0.3$. The preferred pulsational values of $M = 0.65\,M_\odot$, log $L = 1.77\,L_\odot$ require both core rotation and [CNO/Fe] > 0 for agreement.

It is relevant here to point out a problem posed by the mass-to-light ratio obtained from the period–colour relation of M3 (Fig. 24), if the mean mass of the M3 RR Lyraes is indeed $0.55\,M_\odot$ as deduced from two multimode variables in M3 by Cox *et al.* (1983). Since $A_{M3} = -1.85 \pm 0.03$ (Fig. 24), $M_{M3} = 0.55\,M_\odot$ implies $(\log L)_{M3} = 1.64$ (~ 0.3 mag fainter than the M15 RR Lyraes). Although it would appear from Table 11 that consistency with the standard frame would be achievable with $Y \sim 0.27$, inspection of the SG grid reveals that models with any reasonable core mass are far too blue to reach the instability strip (except in a very rapid 'final' phase of HB evolution). Clearly, extrapolation of the above linear interpolation formulae is not appropriate here. Moving to the non-standard frame worsens the problem, therefore throwing into question the multimode mass determination for M3 and consequently adding a note of uncertainty to the M15 result. If the masses of the M3 variables are similar to those in M15, then the larger value of A for M3 enables consistency to be achieved within the standard frame at values of $Y < 0.3$ (see Table 11), i.e. values of Y less than those required to fit the M15 pulsational results into the standard frame.

3.5.2 *Comparison of M15 and M3: mean quantities*

Understanding the Oosterhoff problem centres on the interpretation of the differential period shifts from cluster to cluster, as typified by the comparison between M15 and M3 for which we have derived

$$\Delta\,\{\log P\}_{M15-M3} = 0.065 \pm 0.03 \text{ at constant } T_e, \text{ and}$$

$$\Delta\,\{\log M^{0.81}/L\}_{M15-M3} = -0.07 \pm 0.04.$$

The pulsation equation (2) may be used in conjunction with the linearized interpolation formulae (9), (10) for standard models given earlier to see if such a period shift would be predicted by the models. From (2) we have

$$\Delta \log P = -0.68\,\Delta \log M + 0.84\,\Delta \log L \quad (13)$$

Table 12 indicates values of the parameters needed to satisfy this equation. Substituting for $\Delta \log M$ and $\Delta \log L$ in (9) and (10) yields the prediction, for ZAHB models, that

$$\Delta \log P = 1.137\,\Delta Y - 0.011\,\Delta \log Z \quad (14)$$

Values of $\Delta \log P$ as a function of ΔY, $\Delta \log Z$ according to (14) are given in the following table:

Values of the predicted period shift, $\Delta \log P$, based on ZAHB models

$\Delta \log Z$	-0.25	-0.50	-1.00
$\Delta Y = 0$	0.003	0.006	0.011
$\Delta Y = 0.05$	0.060	0.063	0.068

Table 12. Mass and luminosity differences between M15 and M3 needed to satisfy the pulsation equation (13).

$(\Delta \log M)_{M15-M3}$	M_{M15}/M_{M3}	M_{M3} if $M_{M15} = 0.65\ M_\odot$	$(\Delta \log L)_{M15-M3}$	$(\Delta M_{bol})_{M15-M3}$
0.0	1.0	0.65	0.08	0.20
-0.047	0.90	0.72	0.04	0.10
-0.096	0.80	0.81	0.0	0.0

It can be seen that the models fail to predict a significant period shift between two clusters of differing metal abundance unless the helium abundance also differs. In the particular case of M15 versus M3, $-0.5 \lesssim \Delta \log Z \lesssim -0.2$ depending on whose abundances are used (e.g. see Pilachowski *et al.* 1983, PSW). Thus the observed period shift of $\Delta \log P = 0.065 \pm 0.03$ would require a difference in Y between the clusters ~ 0.05 in the sense that the more metal-poor cluster (M15) would have a higher Y. The same conclusion was reached by SKS following a somewhat different route. Generalizing the problem to many clusters, Sandage has derived the following correlation between period shift and metal abundance

$$\Delta \log P = -0.116\ \Delta\ [\mathrm{Fe/H}] \tag{15}$$

based on Zinn's (1980) abundances. As discussed earlier (Section 3.4), we find $\Delta \log P = (-0.094 \pm 0.018)\ \Delta\ [\mathrm{Fe/H}]$ essentially confirming Sandage's result. Thus the sensitivity of $\Delta \log P$ to [Fe/H] required by the observations is an order of magnitude higher than that predicted by standard ZAHB models, equation (14), unless Y is inversely correlated with Z according to $\Delta Y \sim -0.08\,\Delta \log Z$. Sandage (1982a) has again reached a similar conclusion. Thus one has either to accept such an anti-correlation (arising perhaps through additional Z-dependent envelope enrichment of helium during evolution) within the framework of existing HB models or search for another explanation which of necessity will require either a non-standard frame and/or some change in the physics of the models. Renzini (1983) has discussed this question and suggests that, since increasing [CNO/Fe] will not have a sufficiently large effect on $\Delta \log P/\Delta$ [Fe/H] (based on Rood & Seitzer 1981), one should seriously question the input physics. He suggests that there are grounds for increasing the sensitivity to metal abundance of the opacities in the HB models which, when coupled with the observed trend in [O/Fe] with [Fe/H] are likely to be able to increase $\Delta \log P/\Delta$ [Fe/H] to the observed value.

Alternatively, CCG have pointed out that the inverse correlation between Y and [Fe/H] is removed in a non-standard frame if DM_c and [CNO/Fe] increase with decreasing [Fe/H]. Indeed equation (12) and Table 11 indicate that a change in core mass is also required for any realistic value of [CNO/Fe], as was pointed out by Renzini. As discussed previously, an increase in core mass is produced by rotation which, to remove the Y/[Fe/H] anti-correlation, must increase with decreasing Z, for which there is no obvious physical justification at present. A further difficulty with this hypothesis is presented by the expected effects of rotation on the effective temperatures of the models, a higher rotation moving the models bluewards (Fusi Pecci & Renzini 1975). If the distribution in rotation is Gaussian-like giving rise to a similar distribution in core mass on the HB, then the HB morphologies of M15 and M3 (e.g. see Fig. 29) require that amongst the RR Lyraes, we would expect to find comparable or even higher rotations on average in M3 than in M15, the converse of what is needed if M15 is to have a higher luminosity than M3 as a result of rotation. Thus in a non-standard framework within which M_c needs to vary, other possible physical causes must be sought. In this connection, Renzini (1983) has pointed out that an underestimate of the electron conduction opacity coefficients in the partially relativistic regimes of the helium cores would lead to an underestimate of the core mass.

3.5.3 The horizontal branch morphology

We have seen in the previous sections that for values of $Y \leqslant 0.25$, currently thought to be most plausible, current HB models cannot explain (1) the luminosity of the RR Lyraes in M15 derived from pulsation theory alone, the predicted model luminosity being too faint in log L by ~ 0.1 and (2) the correlation of observed period shift with metal abundance between M15 and M3, or over a range of globular clusters, unless Y is anti-correlated with [Fe/H], through mixing or some other unknown mechanism.

Despite these difficulties, it may be useful to compare the observed distribution of RR Lyraes in the HR diagram with theoretical predictions. It is important to attempt such a comparison, since the availability of accurate colour data for many variables in the principal clusters of each Oosterhoff group might shed further light on the cause of the Oosterhoff effect, over and above the mean properties of the groups that have been discussed already. Two such aspects concern the appropriate direction of evolution through the instability strip and the nature of the transition zone, aspects that have provided an important stimulus through the van Albada & Baker (1973) interpretation of the Oosterhoff effect and subsequent work (Stellingwerf 1975). Comparison with standard evolutionary tracks should be a reasonable procedure since the track morphology is unlikely to change dramatically, except perhaps to have variation in the extent of the loops if the opacities are increased (Renzini 1983), and changes in [CNO/Fe] can be simulated within the standard grid by appropriate adjustments to Z (since CNO is the important abundance parameter on the HB).

Fig. 27 shows the HR diagram of horizontal branch stars in M15, including the RR Lyraes, within an annular region between radii $r = 1.9$ arcmin and $r = 5.0$ arcmin. The colours of the non-variable stars are taken from Buonanno *et al.* (1983a). Fig. 15 shows the histogram of the colour distribution along the HB discussed earlier. Fig. 28 shows the same stars plotted in a log L/log T_e diagram. For the non-variable BHB stars with $B-V > 0.07$, temperatures and bolometric corrections were obtained from the individual V, $B-V$ observations using BK. For the hotter group of BHB stars, the V, $U-V$ diagram for the individual stars was used to define a mean relation, for which temperatures and bolometric corrections are given as a function of $(U-V)$ from BK. Temperatures for individual stars were derived from their observed V magnitudes via the mean $V/U-V$ relation whereas bolometric corrections were obtained directly from $U-V$, again using BK models. This procedure reduces the large scatter produced by even small errors in the observed colours if they are used directly with the BK grid to derive temperatures, at the same time retaining some dispersion reflecting the (effectively) smaller errors in V. Thus whilst the distributions of these stars in the HR diagram of Fig. 28, and in the histogram of Fig. 29a may not be truly representative of the 'theoretical' stellar distributions at the blue end of the HB, their mean locations should be

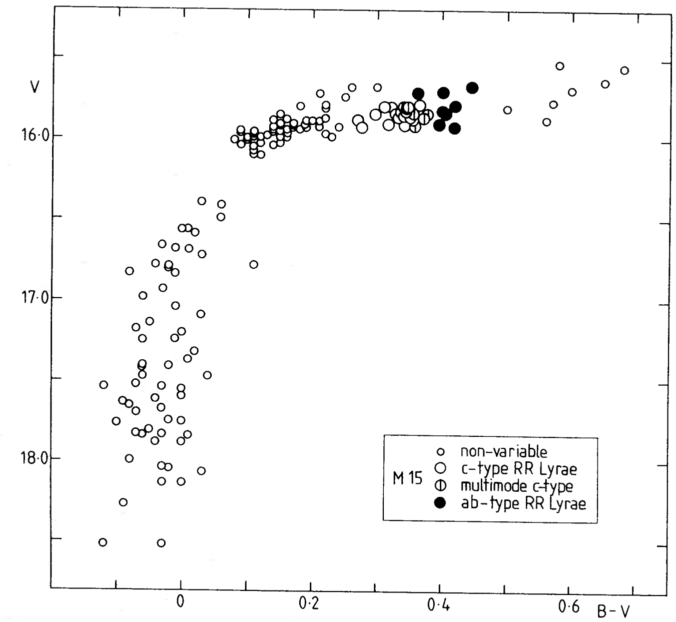

Figure 27. Colour–magnitude diagram of all horizontal branch stars within an annulus, defined by $1.9 < r < 5$ arcmin using present RR Lyrae data from Table 8 [$\langle V \rangle$ and $(B-V)_{eq}$] and that of Buonanno *et al.* for the non-variables. Note the obvious gaps or low density regions at $B-V = 0.07, 0.25$ (see Fig. 15) and the sprinkling of brighter stars away from the principal HB population including both non-variable and variable stars.

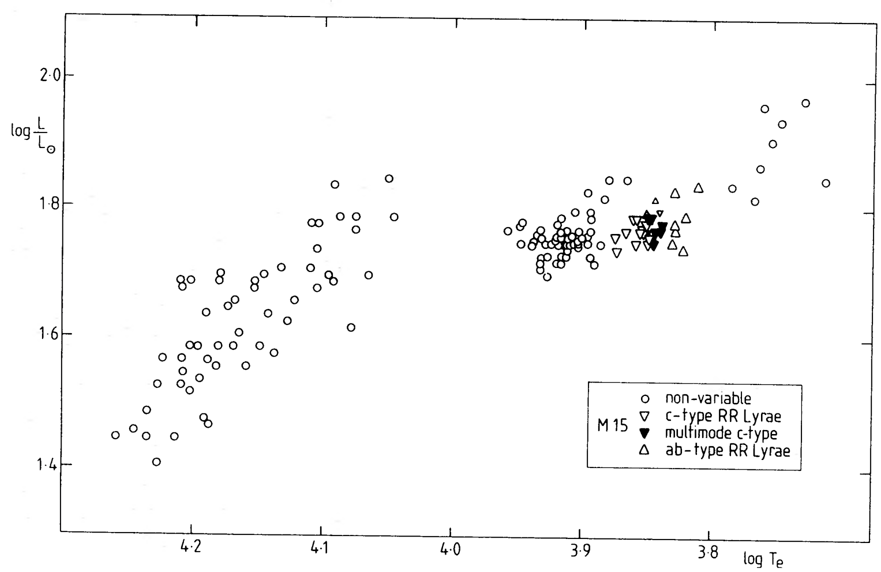

Figure 28. As Fig. 27, but plotted in the theoretical log L/log T_e framework. The precise location of the hot group of BHB stars is uncertain observationally for reasons discussed in the text, but they do indicate the general region of the theoretical HR diagram occupied by the stars, which extend to temperatures around 17 000 K. The precise locus of these stars is also very sensitive to the bolometric corrections used, which in this case were taken from Buser & Kurucz.

essentially correct, subject to the further uncertainties in the photometric calibration of the faint end of the HB, as discussed by Buonanno *et al.* (1983b), and the uncertainties in the models. The distribution with effective temperature remains clearly bimodal in M15, in strong contrast with that found in M3 (Fig. 29b), where the data are taken from diagrams published by Sandage & Katem (1982).

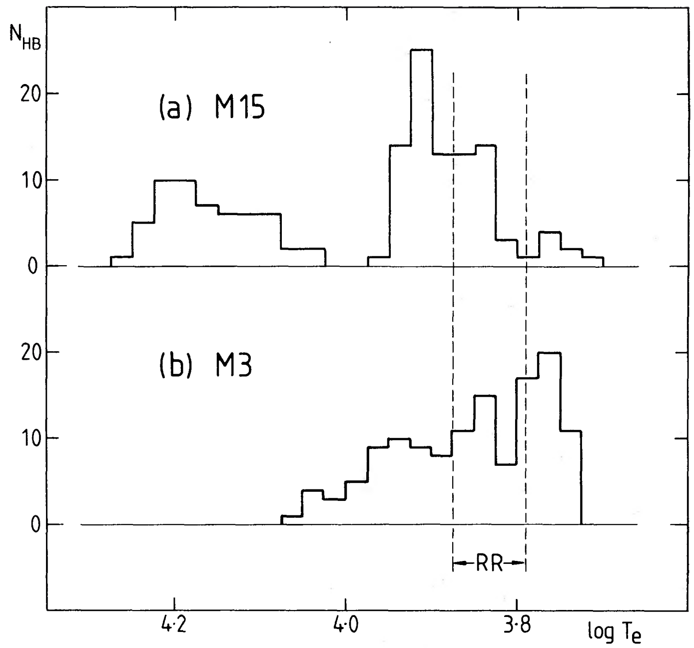

Figure 29. A comparison of the distribution with temperature of stars on the HB of M15 (a) and M3 (b). The latter is derived from diagrams published by Sandage & Katem. The distribution in M15 appears dichotomous with the peak of the main redder population occurring bluewards of the instability strip, whereas that in M3 is much more uniform, with the peak in the HB distribution to the red of the instability strip.

The uncertainty in Y and Z for M15 indicate, via equation 2.11 given by Renzini (1977), an uncertainty in possible core masses of (0.480) ± 0.012 (for $M_{\rm RG} = 0.8 M_\odot$). Since the expected spread is relatively small, it will be sufficient for our purposes to consider models with a core mass of $0.475 M_\odot$, and interpolate in the SG grid for values of Y and Z of interest. Fig. 26 shows the location of interpolated tracks for $Z = 0.0002$ (e.g. M15) and $Z = 0.0005$ (e.g. M3) for three values of the helium content and for masses chosen to represent the instability strip region ($\sim 0.7 M_\odot$) and the blue BHB region ($\sim 0.6 M_\odot$). It is evident that the track morphology is very similar until Y becomes quite close to 0.2. (Tick marks correspond to the time intervals along tracks given in the SG tables and mostly represent equal time intervals of 10^7 yr.) Since $\Delta \{\log L\}_{3.85} \sim 3.2 \, \Delta M_{\rm c}$ and $\Delta \{M\}_{3.85} \sim 1.72 \, \Delta M_{\rm c}$, an increase in core mass of $0.03 M_\odot$ would move the $M = 0.68$, $Y = 0.25$ model to approximately the position of the $Y = 0.30$ model, for which M would then be 0.73. The shape of the track should be quite similar to that shown. Similarly, if [CNO/Fe] = 1, this track would be appropriate for a model of mass $\sim 0.60 M_\odot$ with Y slightly higher than 0.30 (e.g. see SG, Rood & Seitzer 1981).

Considering first the M15 case, we show in Fig. 30 the tracks for $Y = 0.3$ superimposed upon the M15 $\log L/\log T_e$ diagram. (The higher Z tracks would be quite similar to lower Z tracks of a slightly higher mass.) The derived value of $\log L = 1.77$ has been used to set the ordinate scales. It can be seen that for $\log T_e < 4.0$ there is acceptable agreement with the evolutionary tracks in terms of the detailed characteristics of their evolutionary behaviour. We believe the errors in $\log L$ and T_e to be sufficiently small to make it unlikely that a single evolutionary track can account for the observed distribution. It is more likely that the clumpy distribution and observed spread of points is a natural consequence of the variable rates of evolution typical of these tracks, with some smearing of the distribution in tem-

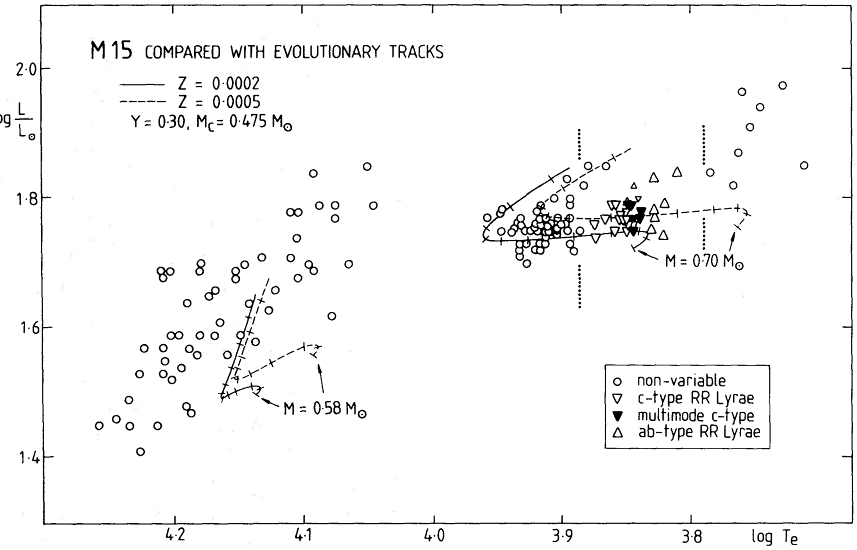

Figure 30. Evolutionary tracks for $Y = 0.3$ shown superimposed on the M15 HR diagram. Satisfactory representation of the main part of the M15 HB would be possible with a mass distribution characterized by a dispersion of a few hundredths of a solar mass and values of Y, Z, M and L within the formal uncertainties of those derived pulsationally (M, L, Y) or observed (Z) (see text). A clumpy low mass tail contributing to the non-uniform distribution displayed in Fig. 15 is also suggested. Note that the dashed track shown for $Z = 0.0005$ would be quite similar to a lower Z track of slightly higher mass.

perature expected for a spread in mass amongst the RR Lyraes. The few stars lying away from the main clumps occur at the brighter luminosity expected for a more advanced evolutionary stage. The location of the hot clump of BHB stars is less satisfactory, although it must be kept in mind that the luminosities and temperatures for these stars are rather uncertain, for reasons stated earlier. Indeed the sharp break in temperature around log $T_e = 4.0$ is impossible to explain with a theoretical HB for which the physical parameters vary continuously. It looks as though a clumpy low mass tail would be required to explain the distribution of the hotter BHB stars.

As is evident from the preceding discussion, the fits shown are not unique, in that small differences in the choice of total mass, core mass, Y and Z allow various combinations which could lead to consistency with the observations. Our main concern here is to show that the distributions of the RR Lyraes, and stars in neighbouring regions of the HB are broadly consistent with that expected from the evolutionary tracks of approximately the correct parameters.

The above considerations indicate that the bulk of the RR Lyraes in M15 are in an early stage of evolution from the ZAHB evolving through the instability strip from right to left, after the initial small excursion redward as they first leave their ZAHB location. As mentioned earlier, this pattern of evolution will only be significantly changed if Y becomes close to 0.2 where there are much smaller temperature excursions through most of the HB lifetime. It is important to consider whether such a low value of Y could also lead to acceptable agreement between pulsation and evolution parameters as regards the expected distribution of stars in the HR diagram appropriate to those parameters. Inspection of Fig. 26 shows that a fit of the $Y = 0.2$ track to M15 would require a luminosity of log $L \sim 1.55$ or less, as expected from considerations given earlier. Moving to a non-standard frame to match the evolutionary parameters with the pulsational results would require $DM_c > 0.03$ and

[CNO/Fe] > 1 to give $M \gtrsim 0.7$ and $\log L \sim 1.77$. These parameters and the retention of the $Y = 0.2$ track morphology could also probably satisfactorily account for the appearance of the HB, but would require a more clumpy initial mass distribution to produce the observed non-uniform distribution of stars between $\log T_e = 3.8$ and $\log T_e = 3.94$. Evolutionary effects would then be less important than the case with higher Y in determining the distribution along the HB. However, since we believe Y to be $\gtrsim 0.23$, this situation is rather extreme and therefore it is more likely that tracks of the kind shown in Fig. 30 are appropriate to the M15 variables.

Do these considerations also apply to M3? From the point of view of HB morphology, one obvious difference between the cluster horizontal branches, as indicated in the histograms in Fig. 29 is that the mean HB of M3 is shifted redwards from that of M15, giving rise to the significant population of RHB stars, the filling of the instability strip with RR Lyraes and the absence of the hotter BHB stars found in M15. The distributions in the redder parts of the HBs would be reasonable for a simple shift in the mean location of the ZAHB caused solely by the difference in Z between the clusters, as illustrated by the broken track in Fig. 30. However, this would not explain the larger shift in the blue HB or why the gap in the M15 BHB vanishes in such a transformation. We have seen earlier that if the only difference between M3 and M15 is one of abundance, the period shift would not be predicted within the standard frame. Clearly, similar considerations to those discussed above for M15 could equally well be applied to M3 in order to obtain the appropriate 'non-standard' values of M and L to match the dashed tracks in Fig. 30. We also note that consistency with the standard models can only be achieved from the pulsational mass-to-light ratio of M3 if $Y \gtrsim 0.3$ *and* we take the lower error limit to $\log \{M^{0.81}/L\} = -1.88$ *and* accept $M \gtrsim 0.77$ (i.e. ignoring the result from the multimode variables in M3). Note also that in M15 this was achieved by taking the upper limit to $\log \{M^{0.81}/L\} = -1.89$. This effectively minimizes the difference in the observed period–colour relations (and hence $\Delta \log P$) which we believe to be unrealistic and unlikely in view of the widespread nature of the correlation of period shift with [Fe/H] over many clusters.

It seems more likely, therefore, that the overall morphology of the evolutionary tracks in the instability strip is very similar for the horizontal branches of M3 and M15, the mean of the distribution being shifted to the red in M3 through a change in one or more of the parameters discussed. Since the overall pattern of evolution is therefore similar, this would appear at first sight to dispose of the interpretation of part of the Oosterhoff effect in terms of a difference in morphology (and hence dominant direction of evolution) of the evolutionary tracks appropriate to each Oosterhoff group, as put forward by van Albada & Baker (1973). Clearly the star-by-star shift in period at a given temperature, amplitude, or light curve shape is an important contributor. However, if the pattern of evolution within the horizontal branches of M15 and M3 is really the same, what is the explanation for the very different populations and distributions with period of *ab*- and *c*-types within these clusters? We discuss this point in more detail in the next section.

3.5.4 The Oosterhoff dichotomy within M15 and M3

A comparison of the properties of RR Lyraes in M3 (group I) and M15 (group II) typifies the Oosterhoff problem and is illustrated in Fig. 24, which shows the $\log P'_0/\log T_e$ relations of these two clusters and has been described earlier (Section 3.4). The mean period shift and different modal behaviour around the transition temperature combine to produce the difference in mean period of *ab*- and *c*-types between clusters of each Oosterhoff group.

We concentrate attention now on the principal difference between the distributions with temperature, which can be seen most clearly in the amplitude–colour relations of Fig. 23. Excluding (for an unknown reason!) the one large-amplitude *ab*-type in M15, the transition temperatures probably differ by less than 0.01 in log T_e and may in fact be identical in the two clusters at log $T_e = 3.84$. The essential difference between them can be seen to be in the larger amplitude and frequency of the *ab*-types in M3 on the cool side of, but near to the transition temperature, and the converse situation with the *c*-types on the hot side. Lying closest to the transition temperature are found the multimode variables in either cluster. Can these differences and similarities be understood in terms of the evolutionary tracks (Fig. 26) and current ideas on pulsation theory? If one allowed some residual uncertainty in the precise locations of the transition temperatures, such distributions would have been a natural consequence of a finite either/or region of width ~ 0.02 in log T_e in the middle of the strip, as found by Stellingwerf (1975), together with predominantly left-to-right evolution in M15 and right-to-left evolution in M3, as proposed by van Albada & Baker (1973). However, more recent theoretical work on pulsation (e.g. see report by Cox 1980) has essentially removed the second transition line at these luminosities and extended the either/or region over most of the instability strip, from the FBE to the red edge (RE). If dominant evolution were left-to-right, the first harmonic pulsators would populate the whole strip, whereas if it were right-to-left, a sharp transition would be observed at the FBE, as appears to be the case in both clusters. Furthermore, the preceding discussion favours a similar track morphology for both M15 and M3, the main difference being the higher Z for M3 (and/or 'non-standard' parameters) shifting the tracks redward from M15 and significantly populating the RHB, as illustrated by the upper right evolutionary track shown in Fig. 26. In fact even if the lower Y of ~ 0.2 were appropriate to M15, the lack of significant track excursion in temperature over most of the HB lifetime (see lower tracks in Fig. 26) would greatly diminish the effect of the rapid left-to-right evolutionary phase on the final HB distribution.

There may well be small differences in mass and luminosity between the two clusters, reflected in the observed period (and other) differences as has been discussed earlier and elsewhere (see Dickens 1982, for a recent assessment) but an outstanding question remains, what is the reason why, in the neighbourhood of the transition region, there are many more first harmonic pulsators in M15-like clusters (Oosterhoff II) than in M3-like clusters (Oosterhoff I)? A possibly important aspect of this problem concerns the multimode variables which occur only in this regime in clusters of both Oosterhoff groups. [The two cases in M3, V68 and V87 have log $T_e \sim 3.840$ based on photometry given by Roberts & Sandage (1955) although the photometry is of lower precision.] The time-scales for mode-switching are currently thought to be much too fast (Cox *et al.* 1983) to expect to see any caught in the act of switching. Therefore it seems more likely that multimode behaviour is a mode of pulsation stable over time-scales comparable to evolutionary time-scales within the instability strip. If the upper tracks of Fig. 26 or the tracks in Fig. 30 are representative of M15 (solid) and M3 (dashed), then the distributions of stars with log T_e given in Fig. 29 suggests that many M3 stars start their evolution on the RHB, or near the red edge of the strip whereas very few, if any, in M15 do.

Thus virtually all the RR Lyraes in M15 must begin their HB life within the strip whereas many RR Lyraes in M3 have evolved into the strip from cooler temperatures. Dominant evolution is eventually to the blue, with the region bluewards of the FBE (log $T_e \sim 3.84$) populated by first harmonic (1H) pulsators in both clusters. In M3, the RR Lyraes are well established in the fundamental mode and as they evolve to the blue, only switch mode when the growth rate of IH in F becomes positive close to the FBE. Because the HB does not extend very far redward in M15, this region of the instability strip is likely to be dominated by stars near the beginning of their HB life-times and inspection of Fig. 26 shows that they initially evolve redwards by ~ 0.01 in log T_e before changing their direction of evolution towards the blue. It seems plausible then on theoretical grounds that a significant fraction of stars found in this temperature regime in M15 are likely to be initially unstable to first harmonic or mixed-mode pulsation (being bluewards of the FBE), and will remain as dominantly 1H pulsators throughout their subsequent evolution within the strip (on the grounds of track morphology). The morphology of the tracks alone will tend to increase the density of stars in this temperature regime over those in M3 by perhaps a factor of 3 or so, which would then contribute significantly to the observed population difference between the clusters. In addition to these effects, the time-scales and direction of the evolutionary approach to the ZAHB could be relevant or even crucial, as has been discussed by Caputo, Castellani & Tornambé (1978).

It is interesting to speculate that since this intermediate region is dominated in M15 by variables exhibiting mixed-mode pulsation, that it is just in this region, in the neighbourhood of the transition edge that growth from zero amplitude develops into the stable mixed mode behaviour. Alternatively, it could be the preferred mode only at the transition edge, the much smaller number in M3 reflecting the relatively rapid evolution across the transition edge in that cluster.

Thus the very different frequency distributions with period, temperature and amplitude between RR Lyraes in clusters of each Oosterhoff group can plausibly be seen to arise naturally as a consequence of the likely morphology of the evolutionary tracks together with current ideas in pulsation theory. Inadequacies in the models are thought unlikely to significantly affect the track morphology, and therefore unlikely to effect these conclusions. However, non-standard parameters in the models, or improved physics may well be needed to reconcile the derived physical parameters and in particular the correlation of Oosterhoff period shift with metal abundance. Only when such improvements have been carried out can one attempt to tie down more precisely the parameters involved.

Acknowledgments

We thank L. Rosino for making available the Asiago plate material, Alvio Renzini for helpful discussions, Dave Pike for help with the light curve fitting programs, Monica Everest for tracing the diagrams and Joy Hamblyn, Barbara Herbert, Lise Karen-Alun and Hilary Saunders for their typing services. CC and FFP acknowledge the hospitality of the Royal Greenwich Observatory during the plate measurements, CC acknowledges support of a NATO fellowship. This research was supported in part by the National Group of Astronomy (GNA) of the National Research Council of Italy (CNR).

References

Andrews, P. J., 1980. *Star Clusters, IAU Symp. No. 85,* p. 425, ed Hesser, J. E., Reidel, Dordrecht, Holland.

Arp, H. C., 1955. *Astr. J.,* **60**, 317.

Aurière, M. & Cordoni, J.–P., 1981. *Astr. Astrophys.,* **100**, 307.

Baker, R. H. & Baker, H. V., 1956. *Astr. J.,* **61**, 283.

Barbuy, B., 1981. *Astrophysical Parameters for Globular Clusters, IAU Coll. No. 68,* p. 85, eds Davis Philip, A. G. and Hayes, D. S., Dudley Obs. Report No. 15, New York.

Bell, R. A. & Gustafsson, B., 1978. *Astr. Astrophys. Suppl.,* **34**, 229.

Bica, E. L. D. & Pastoriza, M. G., 1983. *Astrophys. Space Sci.,* **91**, 99.

Brown, B., 1951. *Astrophys. J.,* **113**, 344.

Buonanno, R., Buscema, G., Corsi, C. E., Iannicola, G. & Fusi Pecci, F., 1983a. *Astr. Astrophys. Suppl.,* **51**, 83.

Buonanno, R., Corsi, C. E. & Fusi Pecci, F., 1984. *Astr. Astrophys.*, in press.
Buser, R. & Kurucz, R. L., 1978. *Astr. Astrophys.*, **70**, 555.
Burstein, D. & Heiles, C., 1978. *Astrophys. J.*, **225**, 40.
Burstein, D. & McDonald, L. H., 1975. *Astr. J.*, **80**, 17.
Butler, D., 1975. *Astrophys. J.*, **200**, 68.
Butler, D., Dickens, R. J. & Epps, E. A., 1978. *Astrophys. J.*, **225**, 148.
Buzzoni, A., Fusi Pecci, F., Buonanno, R. & Corsi, C. E., 1983. *Astr. Astrophys.*, **128**, 94.
Cacciari, C., 1979. *Astr. J.*, **84**, 1542.
Cacciari, C., 1984. *Astr. J.*, 89, 231.
Caputo, F. & Castellani, V., 1975. *Astrophys. Space Sci.*, **38**, 39.
Caputo, F., Castellani, V. & Gregorio R. di, 1983. *Astr. Astrophys.*, **123**, 141.
Caputo, F., Castellani, V. & Tornambé, A., 1978. *Astr. Astrophys.*, **67**, 107.
Caputo, F. & Cayrel de Strobel, G., 1981. *Astrophysical Parameters for Globular Clusters, IAU Coll. No. 68,* p. 415, eds Davis Philip, A. G. & Hayes, D. S., Dudley Obs. Report No. 15, New York.
Clegg, R. E. S., Lambert, D. L. & Tomkin, J., 1981. *Astrophys. J.*, **250**, 262.
Cohen, J. G., 1978. *Astrophys. J.*, **223**, 487.
Cox, A. N., 1980. *Space Sci. Rev.*, **27**, 475.
Cox, A. N., 1982. *Pulsations in Classical and Cataclysmic Variable Stars,* p. 157, eds Cox, J. P. & Hansen, C. J., Boulder, Colorado.
Cox, A. N., Hodson, S. W. & Clancy, S. P., 1983. *Astrophys. J.*, **266**, 94.
Davis, C. G. & Cox, A. N., 1980. *Current Problems in Stellar Pulsation Instabilities, NASA Tech. Memo 80625,* p. 293, eds D. Fischel, L. R. Lesh & W. M. Sparks, Washington DC.
Demers, S. & Wehlau, A., 1977. *Astr. J.*, **82**, 620.
Deupree, R. G., 1977. *Astrophys. J.*, **214**, 502.
Dickens, R. J., 1970. *Astrophys. J. Suppl.*, **22**, 249.
Dickens, R. J., 1972. *Mon. Not. R. astr. Soc.*, **157**, 281.
Dickens, R. J., 1982. *Pulsations in Classical and Cataclysmic Variable Stars,* p. 182, eds Cox, J. P. & Hansen, C. J., Boulder, Colorado.
Dickens, R. J. & Flinn, R., 1972. *Mon. Not. R. astr. Soc.*, **158**, 99.
Dickens, R. J. & Saunders, J., 1965. *R. Obs. Bull.*, **101**.
Filippenko, A. V. & Simon, R. S., 1981. *Astr. J.*, **86**, 671.
Fusi Pecci, F. & Renzini, A., 1975. *Astr. Astrophys.*, **39**, 413.
Hansen, R. B., 1979. *Mon. Not. R. astr. Soc.*, **186**, 875.
Harris, H. C. & Canterna, R., 1977. *Astr. J.*, **82**, 798.
Hartwick, F. D. A., 1968. *Astrophys. J.*, **154**, 475.
Hesser, J. E., Hartwick, F. D. A. & McClure, R. D., 1977. *Astrophys. J. Suppl.*, **33**, 471.
Iben, I., 1968. *Nature,* **220**, 143.
Iben, I., 1971. *Publ. astr. Soc. Pacific,* **83**, 697.
Johnson, H. L. & Schwarzschild, M., 1951. *Astrophys. J.*, **113**, 630.
Jørgensen, H. E. & Peterson, J. O., 1967. *Zeitschrift fur Astrophys.*, **67**, 377.
Kemper, E., 1982. *Astr. J.*, **87**, 1395.
Kron, G. E. & Guetter, H. H., 1976. *Astrophys. J.*, **81**, 817.
Kukarkin, B. V., 1974. *The Globular Star Clusters Catalogue,* Nauka, Moscow.
Lub, J., 1977. The RR Lyrae Population of the Solar Neighbourhood, *PhD thesis,* University of Leiden.
Menzies, J., 1974. *Mon. Not. R. astr. Soc.*, **168**, 177.
Mosley, D. R. & White, R. E., 1975. *Bull. Am. astr. Soc.*, **7**, 535.
Oosterhoff, P. Th., 1939. *Observatory,* **62**, 104.
Oosterhoff, P. Th., 1944. *Bull. astr. Inst. Neth.*, **10**, 55.
Pagel, B. E. J., 1982. *Phil. Trans. R. Soc. Lond. A,* **307**, 19.
Peimbert, M., 1973. *Mem. Soc. R. Sci. Liege, Coll. 8, 6 Ser., Vol. 5,* 307.
Pike, C. D. & Meston, C. J., 1977. *Mon. Not. R. astr. Soc.*, **180**, 613.
Pilachowski, C. A., Sneden, C. & Wallerstein, G., 1983. *Astrophys. J. Suppl.*, **52**, 241.
Preston, G. W., 1961. *Astrophys. J.*, **133**, 29.
Renzini, A., 1977. *Advanced Stages of Stellar Evolution,* p. 184, eds Bouvier, P. & Maedier, A., Geneva Obs.
Renzini, A., 1983. The First Stellar Generations. *Mem. Soc. astr. Ital.*, 54.
Roberts, M. S. & Sandage, A., 1955. *Astr. J.*, **60**, 185.
Rood, R. T., 1972. *Astrophys. J.*, **177**, 681.
Rood, R. T., 1973. *Astrophys. J.*, **184**, 815.

Rood, R. T. & Seitzer, P. O., 1981. *Astrophysical Parameters for Globular Clusters, IAU Coll. No. 68,* p. 369, eds Davis Philip, A. G. & Hayes, D. S., Dudley Obs. Report No. 15, New York.
Sandage, A., 1959. *Astrophys. J.,* **129**, 596.
Sandage, A., 1969. *Astrophys. J.,* **157**, 515.
Sandage, A., 1970. *Astrophys. J.,* **162**, 841.
Sandage, A., 1981a. *Astrophys. J.,* **244**, L23.
Sandage, A., 1981b. *Astrophys. J.,* **248**, 161.
Sandage, A., 1982a. *Astrophys. J.,* **252**, 553.
Sandage, A., 1982b. *Astrophys. J.,* **252**, 574.
Sandage, A. & Katem, B., 1977. *Astrophys. J.,* **215**, 62.
Sandage, A. & Katem, B., 1982. *Astr. J.,* **97**, 537.
Sandage, A., Katem, B. & Kristian, J., 1968. *Astrophys. J.,* **153**, L129.
Sandage, A., Katem, B. & Sandage, M., 1981. *Astrophys. J. Suppl.,* **46**, 41.
Sandage, A. & Smith, L. L., 1966. *Astrophys. J.,* **144**, 886.
Sandage, A., Smith, L. L. & Norton, R. H., 1965. *Astrophys. J.,* **144**, 894.
Sandage, A. & Wallerstein, G., 1960. *Astrophys. J.,* **131**, 598.
Sawyer Hogg, H., 1973. *Publ. David Dunlap Obs.,* **3**, No. 6.
Schwarzschild, M., 1940. *Circ. Harward College Obs.,* **437**.
Searle, L. & Zinn, R., 1978. *Astrophys. J.,* **225**, 357.
Shapley, H. & Sawyer, H. B., 1935. *Harward Repr.,* **116**.
Smith, H. A. & Sandage, A., 1981. *Astr. J.,* **86**, 1870.
Smith, H. A. & Wesselink, A. J., 1977. *Astr. Astrophys.,* **56**, 135.
Sneden, C., Lambert, D. L. & Whitaker, R. W., 1979. *Astrophys. J.,* **234**, 964.
Stellingwerf, R. F., 1975. *Astrophys. J.,* **195**, 441.
Stellingwerf, R. F., 1978. *Astrophys. J.,* **224**, 953.
Stobie, R., 1971. *Astrophys. J.,* **168**, 381.
Sturch, C. R., 1966. *Astrophys. J.,* **143**, 774.
Sturch, C. R., 1977. *Publ. astr. Soc. Pacific,* **89**, 349.
Sweigart, A. V. & Gross, P. G., 1976. *Astrophys. J. Suppl.,* **32**, 367.
Tuggle, R. S. & Iben, I., 1972. *Astrophys. J.,* **178**, 455.
van Albada, T. S. & Baker, N., 1971. *Astrophys. J.,* **169**, 311.
van Albada, T. S. & Baker, N., 1973. *Astrophys. J.,* **185**, 477.
van Albada, T. S. & de Boer, K. S., 1975. *Astr. Astrophys.,* **39**, 83.
van Albada, T. S., de Boer, K. S. & Dickens, R. J., 1981. *Mon. Not. R. astr. Soc.,* **195**, 591.
Wehlau, A. & Potts, N., 1973. *Variable Stars in Globular Clusters and in Related Systems, IAU Coll. No. 21,* p. 95, ed Fernie, J., Reidel, Dordrecht, Holland.
Wesselink, A. J., 1974. *Astr. Astrophys.,* **36**, 163.
Zinn, R., 1980. *Astrophys. J. Suppl.,* **42**, 19.